INFORMATION TO USERS

This manuscript has been reproduced from the microfilm master. UMI films the text directly from the original or copy submitted. Thus, some thesis and dissertation copies are in typewriter face, while others may be from any type of computer printer.

The quality of this reproduction is dependent upon the quality of the copy submitted. Broken or indistinct print, colored or poor quality illustrations and photographs, print bleedthrough, substandard margins, and improper alignment can adversely affect reproduction.

In the unlikely event that the author did not send UMI a complete manuscript and there are missing pages, these will be noted. Also, if unauthorized copyright material had to be removed, a note will indicate the deletion.

Oversize materials (e.g., maps, drawings, charts) are reproduced by sectioning the original, beginning at the upper left-hand corner and continuing from left to right in equal sections with small overlaps.

Photographs included in the original manuscript have been reproduced xerographically in this copy. Higher quality 6" x 9" black and white photographic prints are available for any photographs or illustrations appearing in this copy for an additional charge. Contact UMI directly to order.

Bell & Howell Information and Learning
300 North Zeeb Road, Ann Arbor, MI 48106-1346 USA

UMI®
800-521-0600

THE INTERACTIONS
BETWEEN HUMAN ANTITHROMBIN AND HEPARIN

By

IRIS YE WU CHEN, M.B.

A Thesis

Submitted to the School of Graduate Studies

in Partial Fulfilment of the Requirements

for the Degree

DOCTOR OF PHILOSOPHY
SCIENCE

McMaster University

DOCTOR OF PHILOSOPHY (1997)
(Science)

McMaster University
Hamilton, Ontario

TITLE: THE INTERACTIONS BETWEEN HUMAN ANTITHROMBIN AND HEPARIN

AUTHER: Iris Ye Wu Chen, M.B. (Beijing Medical University)

SUPERVISOR: Dr. Morris A. Blajchman

NUMBER OF PAGES: xxi, 203

ABSTRACT

Antithrombin is a plasma serine proteinase inhibitor functioning physiologically as an anticoagulant. It inactivates thrombin and FXa by forming a 1:1 covalent complex between its P1 Arg and the catalytic serine of the proteinase. Antithrombin is a relatively inefficient inhibitor until it is activated by two specific glycosaminoglycans, heparin and heparan sulphate with the unique pentasaccharide sequence required for high affinity binding to antithrombin. Activation of antithrombin by the pentasaccharide and full-length heparin induces major conformational changes in the antithrombin molecule.

The pentasaccharide binding site of antithrombin has been mapped to the D-helix, the A-helix, and the N-terminus of the molecule. Arg47 is located where the base of the A-helix is in close proximity to the amino end of the D-helix. To characterize the role of Arg47 in antithrombin binding to and its activation by the pentasaccharide, antithrombin moieties with substitutions at Arg47 were created and expressed in transfected COS-1 cells. Our data suggest that a positively charged amino acid at position 47 is essential for heparin and the pentasaccharide to bind to AT with high affinity and the pentasaccharide- and heparin-accelerated inactivation of FXa. In addition, an Arg is preferred to Lys for activation by the pentasaccharide with respect to FXa inhibition.

Antithrombin interacts with target proteinases primarily through its P1-

P1' residues together with flanking binding subsites in the reactive centre loop. Heparin activates antithrombin through inducing a major conformational change in antithrombin which optimizes the presentation of the reactive centre loop to the target proteinases. While the pentasaccharide is sufficient for enhancing the rate of FXa inhibition, it has little effect on thrombin inactivation. Full-length heparin, on the other hand, enhances the rates of antithrombin inhibition of both FXa and thrombin. As demonstrated by the coincident 40% increase in endogenous Trp fluorescence with plasma antithrombin, the pentasaccharide and full-length heparin were reported to induce similar conformational changes in AT. The large rate enhancement of thrombin inhibition by full-length heparin was thus attributed solely to the ability of longer chains to accommodate AT and thrombin simultaneously. Based on the fact that substrate recognition of thrombin and FXa is different, it was hypothesized that the pentasaccharide and full-length heparin induce different reactive centre loop conformations. A Pro397Trp antithrombin moiety thus was generated in transfected CHO cells. We report here, for the first time, that the pentasaccharide and full-length heparin induce different conformational changes in the reactive centre loop. It thus appears that the pentasaccharide-induced reactive centre loop conformation represents a near optimal substrate to FXa, whereas the heparin-induced RCL conformation is apparently required for near optimal interaction with thrombin.

ACKNOWLEDGEMENTS

I am deeply endebted to my supervisor Dr. Morris A. Blajchman for taking me on as his student years ago when I just arrived in Canada with poor spoken English and little knowledge in molecular biology. I feel a deep sense of gratitude to Dr. Morris A. Blajchman for his wisdom and inspiration, for his generosity, and for his guidance, support, encouragement, and patience. I am very grateful for the additional members of my supervisory committee, Drs. Fred A. Ofosu, Bryan Clarke, and Daniel Yang for their efforts and invaluable input. I must express my profound appreciation to Dr. William Sheffield who has inspired and taught me so much. I also enjoy your humour and wit. A special thank you also goes to Dr. Mark W.C. Hatton for his encouragement.

I appreciate all the great people in the laboratory whom I have been blessed to know during my tenure. I owe my thanks to my many dear friends at McMaster University. Your friendship has strengthened me through the years. I acknowledge Mr. Myron Kulczycky, Dr. Xianjun Yang, and Dr. Ana for their technical help.

Finally, I would like to thank my parents and mother-in-law for their love and the sacrifice they have made to support me through these years. My deepest appreciation goes to my husband David, my companion, my inspiration, and my strength. You have been teaching me constantly that life is too short to

be little. Thank you for believe in me all the time, good or bad. I am also thankful for my two lovely daughters Ashley and Diana for their unconditional love and natural trust in me and for supporting my involvements outside the home.

TABLE OF CONTENTS

LIST OF FIGURES

LIST OF TABLES

LIST OF SYMBOLS AND ABBREVIATIONS

α	alpha
α_1-ACT	alpha$_1$-antichymotrypsin
α-AT	alpha-antithrombin
α-MEM	minimum essential medium alpha-medium
α_1-PI	α_1-proteinase inhibitor
Ala	alanine
AP	alkaline phosphatase
APS	ammonium persulphate
Arg	arginine
Asn	asparagine
Asp	aspartic acid
AT	antithrombin
AT-II	antithrombin-II
AT-III	antithrombin-III
ATP	adenosine 5'-triphosphate
ß	beta
ß-AT	beta-antithrombin
BCIP	5-bromo-4-chloro-3-indolyl phosphate
BIS	N,N'-methylene-bis-acrylamide

bp	base pair(s)
BSA	bovine serum albumin
cDNA	complementary deoxyribonucleic acid(s)
CHO	Chinese hamster ovary
CMV	cytomegalovirus
CNBr	cyanogen bromomide
COS	transformed African green monkey kidney cells
C-terminal	carboxyl terminal
Cys	cysteine
Da	Dalton(s)
dATP	deoxyadenosine 5'-triphosphate
°C	degrees Celsius
dd H_2O	deionized and distilled water
DEA	diethanolamine
D-MEM	Dulbecco's modified eagle medium
D-MEM-Gln$^-$Met$^-$Cys$^-$	Dulbecco's modified eagle medium-without L-Gln, L-Met, or L-Cys
DMSO	dimethyl sulphoxide
DNA	deoxyribonucleic acid(s)
1,5DNS-GGACK, 2HCl	1,5-dansyl-glu-gly-arg chloromethyl kekone, dihydrochloride

ds	double-stranded
DTT	dithiothreitol
E. Coli	*Escherichia Coli*
EDTA	ethylenediaminetetraacetic acid
ELISA	enzyme-linked immunosorbent assay
EtBr	ethidium bromide
FBS	fetal bovine serum
Fig.	figure
FIXa	activated factor IX
FXa	activated factor X
FXa-AT	activated factor X-antithrombin
FXIa	activated factor XI
FXIIa	activated factor XII
g	gram(s)
Gln	glutamine
Glu	glutamic acid
His	histidine
h	hour(s)
HC-II	heparin cofactor II
HCl	hydrochloric acid
I	ionic strength

IgG	immunoglobulin G
IgY	immunoglobulin Y
IPTG	ß-D-isopropyl-thiogalactopyranoside
kb	kilobase(s)
K_d	dissociation constant
kDa	kiloDalton(s)
L	litre(s)
LB	Lauria-Bertani broth
Leu	leucine
Lys	lysine
μCi	microcurie(s)
μg	microgram(s)
μl	microlitre(s)
μm	micrometre(s)
μM	micromolar
M	molar
Met	methionine
mg	milligram(s)
$MgCl_2$	magnesium chloride
min	minute(s)
ml	millilitre(s)

mM	millimolar
mm	millimetre(s)
Mr	molecular mass
mRNA	messenger ribonucleic acid(s)
MWCO	molecular weight cut-off
N_2	nitrogen
NaCl	sodium chloride
Na_2HPO_4	di-sodium hydrogen orthophosphate
NaN_3	sodium azide
NaOAc	sodium acetate
NaOH	sodium hydroxide
NBD	nitrobenzofuran
NBT	nitro blue tetrazolium
ng	nanogram(s)
nM	nanomolar
N-terminal	amino terminal
OD	optical density
ORF	open reading frame
PAGE	polyacrylamide gel electrophoresis
PAI-I	plasminogen activator inhibitor-I
PBS	phosphate buffered saline

PBS-T	phosphate buffered saline with Tween-20™
PCI	protein C inhibitor
PEG	polyethylene glycol
Phe	phenylalamine
PMSF	phenylmethylsulfonyl fluoride
PN-I	protease nexin I
PNPP	p-nitro-phenyl phosphate
Pro	proline
RFLP	restriction fragment length polymorphism
RNA	ribonucleic acid(s)
RNase	ribonuclease
RCL	reactive centre loop
RFLP	restriction fragment length polymorphisms
rpm	revolutions per minute
s	second(s)
SDS	sodium dodecyl sulphate
SDS-PAGE	sodium dodecyl sulphate polyacrylamide gel electrophoresis
Ser	serine
serpin	serine proteinase inhibitor
SV40	simian virus 40
T antigen	large tumor antigen

TAE	Tris-acetate-EDTA buffer
TBE	Tris-Boric acid-EDTA buffer
TBS	tris-buffered saline
TBS-T	tris-buffered saline with Tween-20™
TE	Tris-EDTA buffer
TEMED	N,N,N',N'-tetra-methylenediamine
TENS	Tris-EDTA-NaOH-SDS buffer
Thr	threonine
Tris	tris(hydroxymethyl)aminomethane
Trp	tryptophan
UV	ultraviolet
V	volt(s)
Val	valine
v/v	volume:volume ratio
W	watts
w/v	weight:volume ratio
X-gel	5-bromo-4-choloro-3-indolyl-ß-D-galactoside

1. INTRODUCTION

Hemostasis is a host defense mechanism called into play after a vascular injury to maintain the integrity of the circulatory system, while repair efforts by the body are undertaken. Blood coagulation plays an essential role in hemostatic plug formation through the generation of thrombin. Excessive and untimely activation of coagulation, however, can result in intravascular clot or thrombus formation, with potentially life-threatening consequences. Fortunately, under physiological conditions natural anticoagulants are capable of limiting coagulation to preserve the fluidity of circulating blood. The most abundant of these is a plasma glycoprotein, namely antithrombin (AT). For mainly historical reasons, AT has also been known as AT-III. The physiological importance of AT in the maintenance of the haemostatic balance has been shown by the well-established link between inherited AT deficiency and the increased risk of venous thromboembolism in affected individuals.

1.1. Historical Background

Based on the observation that thrombin activity is gradually lost when added to defibrinated plasma or serum, Morawitz (1905) first introduced the term AT to describe the ability of plasma or serum to neutralize thrombin. With the isolation of heparin and the discovery of its potent anticoagulant properties

(McLean, 1916), Brinkhous *et al.* (1939) demonstrated that heparin was effective as an anticoagulant only in the presence of an yet unidentified plasma component which they referred to as heparin cofactor. Historically, up to 6 AT activities have been described (Seegers *et al.*, 1954; Loeliger and Hers, 1957; Niewiarowski and Kowalski, 1958). Among these AT activities, only AT-II and AT-III turned out to be specific under physiological conditions. While AT-II represented the previously described heparin cofactor activity, AT-III became the term used for the progressive AT activity initially described by Morawitz. Subsequently, these two activities were found to reside in one and the same molecular species (Monkhouse, 1955; Waugh and Fitzgerald, 1956; Egeberg, 1965; Abildgaard, 1967; 1968; Rosenberg and Damus, 1973). Thus extensive investigations left AT-III as the only plasma constituent with AT activity under physiological conditions among those Roman numeral designated ATs. The term AT-III, however, continued to be used till recently when it was renamed AT by the Nomenclature Committee of the International Society of Thrombosis and Hemostasis. Unless otherwise indicated, AT will be used for the human species throughout this thesis.

1.2. Biochemistry of AT

1.2.1. Physicochemical Properties and Primary Structure of AT

AT is a single chain plasma glycoprotein with a molecular weight of 58 kDa and isoelectric point ranging from 4.9 to 5.3 (Nordenman *et al.*, 1977).

Plasma-derived AT comprises 432 amino acid residues (Bock *et al.*, 1982; Prochownik *et al.*, 1983a; Chandra *et al.*, 1883). Its six Cys residues are all linked in disulphide bonds located between residues 8 and 128, 21 and 95, and 247 and 430, respectively (Peterson *et al.*, 1979). Two forms of AT, termed α-AT and ß-AT, have been isolated from plasma (Peterson and Blackburn, 1985). As a result of full glycosylation at its four Asn-X-Ser/Thr consensus sequences, the predominant α-AT possesses four identical N-linked biantennary complex carbohydrate side-chains (Peterson *et al.*, 1979; Franzen *et al.*, 1980; Mizuochi *et al.*, 1980). These are coupled to Asn residues 96, 135, 155, and 192, respectively. The ß-AT, which constitutes approximately 10% of the total circulating plasma AT, differs structurally from α-AT only in that Asn 135 is not glycosylated (Brennan *et al.*, 1987). This incomplete glycosylation appears to be associated with a reduced efficiency of incorporating a carbohydrate chain at the consensus sequence Asn-X-Ser of residues 135-137 as compared to the Asn-X-Thr sequences constituting the other three glycosylation sites (Picard *et al.*, 1995). The carbohydrate side-chains thus comprise approximately 9-15% of the total molecular mass of AT (Miller-Andersson *et al.*, 1974; Kurachi *et al.*, 1976a).

1.2.2. Biosynthesis, Distribution, and *in vivo* Clearance of AT

As is found with many plasma proteins, AT levels are remarkably reduced in individuals with liver disorders (Lechner *et al.*, 1977; Ratnoff, 1982).

Thus, it has been inferred that liver is likely to be the major site of biosynthesis of AT. The perfused rat liver accordingly was shown to be able to synthesize and secrete AT (Koj *et al.*, 1978; Owens and Miller, 1980). Subsequently, the presence of AT in rat hepatocytes was demonstrated (Watada *et al.*, 1981; Leon *et al.*, 1982;) and localization of AT in the Golgi apparatus of hepatocytes was reported (Girot *et al.*, 1983). In addition, cultured rat hepatocytes were shown to actively synthesize AT (Leon *et al.*, 1983). A human hepatoma cell-line, Hep G2, was also shown to be capable of synthesizing biologically active AT (Fair and Bahnak, 1984). Moreover, AT biosynthesis occurs also in the kidney and endothelial cells (Lee, *et al.*, 1979; Chan and Chan, 1979; 1981).

AT is present normally in human plasma at a concentration of 150 to 200 mg/L, equivalent to 2 to 3 μM (Marciniak and Gora-Maslak, 1983). When the metabolism of AT was studied in the rabbit and the human, radioiodinated AT was found to distribute among three physiological pools (Carlson *et al.*, 1984; 1985). In human, the fractions of the total-body AT in the plasma, noncirculating vascular-associated, and extravascular pools were calculated to be 0.393 $\pm$ 0.015, 0.109 $\pm$ 0.016, and 0.496 $\pm$ 0.0014, respectively (Carlson *et al.*, 1985).

AT generally has a half life in the circulation of over 24 hr. It was reported to be 1.75 days in rabbits (Chandra *et al.*, 1976), 2.14 $\pm$ 0.09 days in male dogs and 1.97 $\pm$ 0.05 days in female dogs (Kobayashi and Takeda, 1977), and 2.83 $\pm$ 0.26 days in humans (Collen *et al.*, 1977). Once complexed with thrombin and

other serine proteinases, the proteinase-bound AT, however, is cleared more rapidly from the circulation than the native moiety. This has been demonstrated in humans and in animals including mice and dogs, where the half life of thrombin-AT complex was found to be a few min (Shifman and Pizzo, 1982; Fuchs *et al.*, 1982; Leonard *et al.*, 1983). The *in vivo* clearance of proteinase-AT complexes appears to occur on hepatocytes via a receptor-mediated process (Shifman and Pizzo, 1982; Fuchs *et al.*, 1984a). In this process, binding of the complexes to the receptor is followed by their internalization and subsequent degradation. The determinants for the binding of proteinase-AT complexes to their putative receptor and their subsequent rapid removal from the circulation are associated with the whole complex, rather than just the AT moiety or the proteinase with which AT is complexed (Shifman and Pizzo, 1982; Jordan *et al.*, 1989; Mast *et al.*, 1991). This has been suggested by the observation that neither the proteinase, the native AT, nor the cleaved but uncomplexed AT could compete for removal of the complex. This implies that, upon complex formation, a new determinant appears on the AT molecule, and that it is this new determinant that is recognized by the putative receptor.

1.3. Serpins and Insight into AT Structure and Function

1.3.1. The Serpin Superfamily of Proteins

Having noted a similarity of protein sequences among ovalbumin, α_1-

proteinase inhibitor (α_1-PI), and AT, Hunt and Dayhoff (1980) proposed that these three should be grouped in the same protein superfamily. Carrell and Travis (1985) named the superfamily SERPIN, an acronym for serine proteinase inhibitor, to describe the serine proteinase inhibitory properties of its most members. Today there are over 100 proteins in this superfamily widely distributed in nature. The best characterised members are the proteinase inhibitors of human plasma. These serpins generally participate in regulation of such crucial physiological processes as coagulation, fibrinolysis, inflammation, and the immune response, with consequent pathology associated with their deficiency states (Carrell and Travis, 1985).

Each inhibitory serpin has a reactive centre which can act as a pseudosubstrate for its cognate proteinase. The proteinase-sensitive scissile bond is denoted P1-P1' (Schechter and Berger, 1967). Residues N-terminal to the reactive centre scissile bond are designated successively P2, P3, etc., and C-terminal residues P2', P3', etc.. Based on the fact that the region P10 to P2' could be readily cleaved by nontarget proteinases (Kress and Catanese, 1981), it was proposed that the reactive centre and the analogous region of the non-inhibitory serpins lies within an exposed sequence, "the reactive centre loop" (RCL). When the crystallographic structural information became available, it became evident that the RCL is mobile in terms of its relationship with the main body of the serpin molecule (Carrell *et al.*, 1991; Carrell and Evans, 1992). Sequence

alignment of the serpins has shown some very interesting features in the RCL region. Whereas the reactive centre and flanking sequences, namely P8-P5', is highly variable, the "hinge region" from P15 to P9, where the RCL turns and joins the A ß-sheet as strand 5, is strongly conserved consisting of amino acids with short chains in all the inhibitory members of the family. The high variability of the reactive centre and flanking sequences presumably reflects the wide differences in target proteinase specificity. The conservation of the hinge region suggests a common structure-function relationship for this region. Actually, the hinge region is very important for the functioning of the mechanistically crucial loop-insertion process essential for formation of the serpin-proteinase complex. Accordingly, mutations in this region of the inhibitory serpins result in a loss of inhibitory activity. Major modifications are seen in this region in the non-inhibitory members of the family (Carrell and Evans, 1992; Gettins *et al.*, 1996).

1.3.2. Characteristic Properties of Serpins

Unlike most proteins the conformation of which is a thermodynamically-determined global energy minimum (Anfinsen *et al.*, 1973), native serpins fold in a kinetically-determined local energy minimum (Creighton, 1992; Baker and Agard, 1994). This kinetically-trapped metastable state appears to be linked to the need for subsequent conformational change upon serpin-proteinase interaction. In fact, inhibitory serpins undergo a major conformational

change as an essential part of their mechanism of inhibition (Engh *et al.*, 1990; Schulze *et al.*, 1990; Skriver *et al.*, 1991; Carrell *et al.*, 1991; Bjork *et al.*, 1993). For most serpins, cleavage at the P1-P1' peptide bond transforms them from a metastable state to a more thermostable form (Carrell and Owen 1985; Pemberton *et al.*, 1988). Thus, the general differences in folding state are manifested by the large energy difference between the native and cleaved forms of inhibitors (Fish *et al.*, 1979). Accordingly, the cleaved form of serpins is incapable of acting as inhibitors. Serpin-proteinase complexes, in almost all cases, are effectively irreversibly formed. Only cleaved form of serpins can be recovered from the complexes, as expected from slow continuation of the serpin-proteinase interaction where the serpins continue to function as a substrate (Longstaff and Gaffney, 1991; Hermans *et al.*, 1995). The molecular basis of this apparent irreversibility is the covalent nature of serpin-proteinase complexes, implied by their sodium dodecyl sulphate (SDS)-stable behaviour. Formation of such covalent complexes involves the P1 residue of the serpin and the catalytic serine of the proteinase. This covalent interaction contributes considerable binding energy to serpin-proteinase interaction and is essential for stable complex formation (Olsen, *et al.*, 1995a).

1.3.3. Three Dimensional Structure of Serpins

Three-dimensional X-ray crystallographic structural information is now

available for many serpins in either native or cleaved forms or both. The most striking feature is the almost invariant structure of the core domain. It is composed of three ß-sheets (designated A, B, C) and nine α-helices (designated A through I) packing around those three sheets. ß-sheet A, the dominant structural feature of the molecule, is composed of five strands of polypeptide; ß-sheet B, six strands; ß-sheet C, three strands. There are also remarkable differences in the core domains of various serpin structures, but they are all associated to the RCL conformation and its interaction with ß-sheets A and C. The structure of each serpin will be briefly discussed below, highlighting the characteristic flexibility of RCL in the intact form and the changes of RCL conformation upon cleavage at or close to the P1-P1' peptide bond.

Ovalbumin is a non-inhibitory serpin whose function is unknown. In the structure of cleaved form of ovalbumin, plakalbumin, the peptide loop analogous to the reactive centre of the inhibitory serpins is solvent exposed and protrudes from the main body of the molecule (Wright *et al.*, 1990). The distance between the terminal residues, P7 and P1', at the proteinase cleavage site, suggests little change in their positions upon cleavage. The RCL of cleaved α_1-PI, however, is fully inserted into ß-sheet A as an additional strand (Fig. 1.1.a) (Lobermann *et al.*, 1984). As a result of this extensive loop insertion, the native covalently linked P1-P1' residues are now located at opposite poles of the molecule, approximately 70 Å apart. An analogous insertion of the RCL into ß-

Fig. 1.1. Schematic pictures of serpins illustrating different conformations of serpin sequence equivalent to the RCL and strand s1C (light blue). The reactive centre is shown by the position of the P1 residue, and the proximal hinge of the loop, by residues P10-P14. The changes in tertiary structure involve the opening and closing of sheet A, due to the shift of a small fragment of the protein (pink) in relation to the rest of the structure (yellow). Panel (a) shows cleaved α_1-PI; (b), intact ovalbumin; and (c), intact AT, showing important heparin-binding residues (green). In the crystal structure, the RCL interacts with sheet C of another intact AT molecule, and which has a conformation similar to (d), latent PAI-1. Reprinted with permission from Stein and Carrell, 1995.

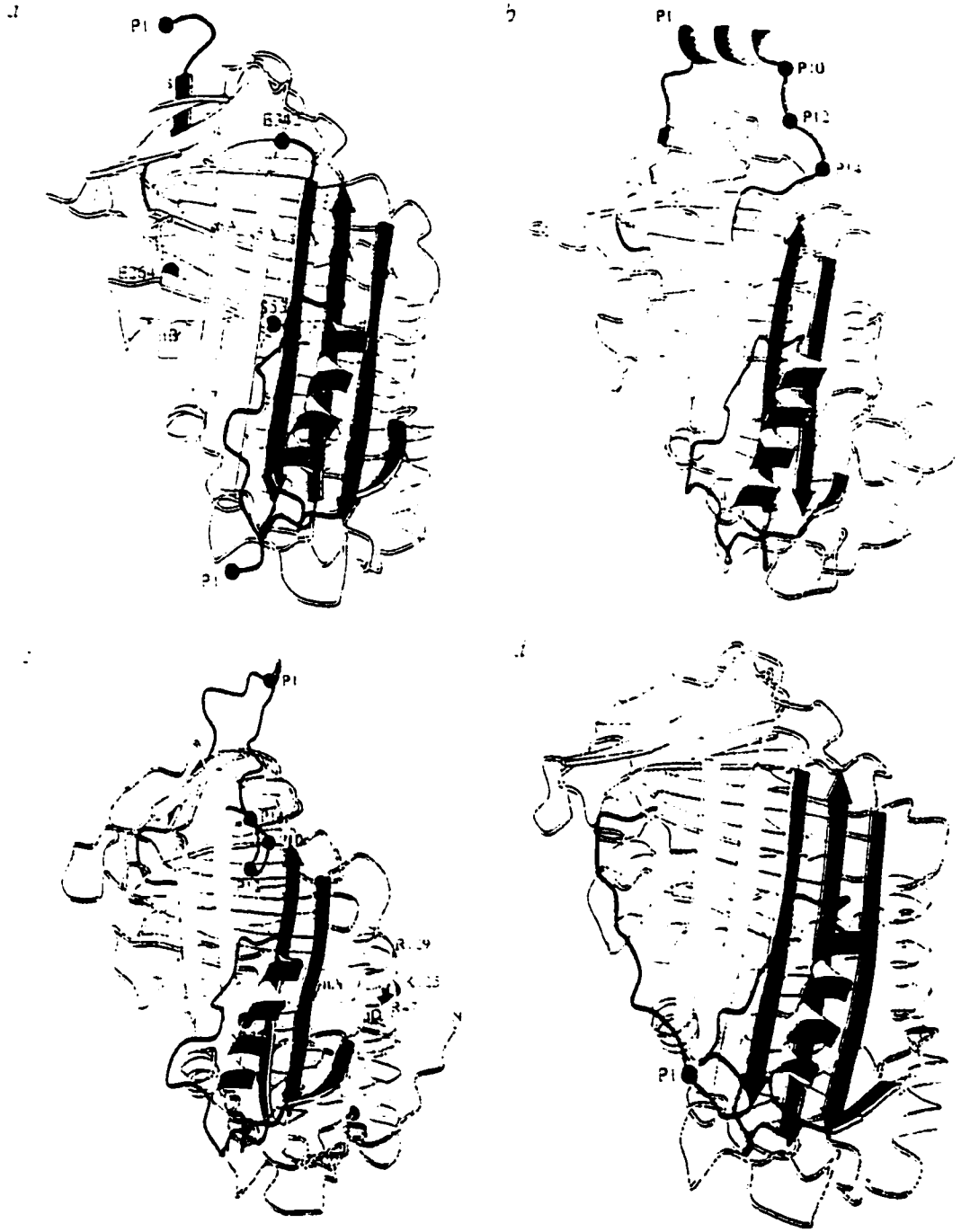
P1
P1
P1

sheet is also seen in the structures of other cleaved inhibitory serpins, including α_1-antichymotrypsin (α_1-ACT) (Baumann *et al.*, 1991), equine leukocyte elastase inhibitor (Baumann *et al.*, 1992), and bovine AT (Delarue *et al.*, 1990; Mourey *et al.*, 1990; 1993), as a consequence of proteolytic cleavage at or close to the P1-P1' peptide bond. Such insertion results in a large increase in the thermodynamic stability of the cleaved molecules in all these cases (Bruch *et al.*, 1988; Gettins and Harten, 1988).

Plasminogen activator inhibitor-I (PAI-I) spontaneously folds into a stable inactive state (Hekman and Loskutoff, 1985; Katagiri *et al.*, 1988). This state is termed "latent" because inhibitory activity can be restored through denaturation and renaturation. Latent PAI-I possesses a distinct type of loop-inserted structure (Fig. 1.1.d) (Mottonen *et al.*, 1992). Its RCL is fully inserted into ß-sheet A in a manner analogous to that of the cleaved RCL of α_1-PI, α_1-ACT, equine leukocyte elastase inhibitor, and bovine AT. Since the RCL of latent PAI-I remains intact, its P1 residue is translated over 70 Å, from one end of the molecule to the other. To permit such full incorporation, strand s1C, composed of residues P3'-P10', has been abstracted from ß-sheet C; its exposed extended conformation makes it long enough to connect the distal end of the inserted RCL to the "top" of the molecule (using the orientation of Fig. 1.1), ready to enter ß-sheet B. Extraction of s1C thus provide a return route for the now distal P1 residue back to the top of the molecule, as would be required by

transformation of PAI-I from its latent form to active form.

In intact ovalbumin, the peptide loop which forms the analogue to the RCL of the inhibitory serpins takes a α-helical conformation protruding from the main body of the molecule on two peptide stalks (Fig. 1.1.b) (Stein *et al.*, 1990). This is formed by a 19-residue segment extending from P15 to P5', with each stalk of about four residues and the P1-P1' exposed on the final turn of the three-turn helix.

In the intact and active inhibitory serpins such as α_1-ACT, α_1-PI, and human AT, the RCL adopts three distinct patterns of structure. The RCL, from P10 to P3', of a variant of α_1-ACT, constitutes a well defined but distorted helix that occupies a position similar to that of the α-helical RCL of ovalbumin (Wei *et al.*, 1994). Two structures have been determined for α_1-PI in the uncleaved and uncomplexed state. Based on incomplete low resolution data from a preliminary study, the RCL of α_1-PI takes a distorted helical conformation (Song *et al.*, 1995). In the structure of a mutant of α_1-PI (Phe51Leu), the RCL adopts a stable canonical-like conformation at its reactive centre P3'-P3, with extension as a ß-pleated strand conformation from P3 to P8 (Elliott *et al.*, 1996). The canonical conformation of the loop is stabilized by salt bridging of P5 Glu to a well defined pocket of 3 Lys and 1 Arg residues at the pole of the molecule beneath the s3A-s4C junction. The precision of docking of the reactive site with the active site of chymotrypsin, superimposably with that of a canonical inhibitor, strengthens the

conclusion that this novel conformation of RCL represents the loop in the optimal inhibitory conformation (Elliott *et al.*, 1996).

For AT, two independent structure determinations have been carried out; both happen to consist of a dimer of one active and one inactive molecule of AT. In one structure both AT molecules are intact (Carrell *et al.*, 1994). The inactive molecule adopts a structure analogous to that of latent PAI-I, with a totally inserted loop and a conformationally extended s1C (Fig. 1.1.d). The RCL of the active AT molecule is in a novel partial insertion conformation (Fig. 1.1.c). Part of the intact active loop, involving residues up to P14, is inserted into ß-sheet A, while residues P7-P3 of the same loop concomitantly interacts with ß-sheet C of the inactive molecule, essentially replacing the missing strand s1C of that molecule. In the other structure, one AT molecule is intact and the state of the other molecule is uncertain due to the absence of electron density corresponding to residues P4'-P11' (Schreuder *et al.*, 1994). Given the fact that these residues belong to strand s1C, strand s1C is either intact but disordered or it may have been excised by multiple proteolytic cuts. Full loop insertion into ß-sheet A is suggested for this cleaved or latent molecule by the clear visibility of electron density for residues P1'-P3' beyond the end of ß-sheet A. An equivalent novel partially loop-inserted conformation is seen for the RCL of the intact molecule, with residues P8-P2 again binding to the other molecule and replacing its strand s1C. Interestingly, the important P1 Arg393 residue of the active AT, in both

structures, points in towards the body of the molecule rather than being exposed on the surface, thereby rendering it ineffective for inhibitory function. In one structure, this inward position is due to a salt bridge with Glu237 of the other molecule (Schreuder *et al.*, 1994). In the other structure, the P1 Arg393 is positioned between Glu255 in the same molecule and Glu237 of the other molecule (Carrell *et al.*, 1994). It was thus postulated that an intramolecular salt bridge between Arg393 and Glu255 is formed in the monomer and that activation of AT involves the exteriorization of the P1 Arg393 through disruption of this salt bridge.

From the discussion above, it becomes very clear that the RCL of most serpins is capable of undergoing major structural transformations. These can vary from the exposed helical loop in ovalbumin, to the fully inserted loop, as a ß-strand in the A sheet, in the latent forms of PAI-1 and inactive AT. In between these two extremes are three structures of the active forms of the inhibitory serpins. In α_1-ACT the RCL is a distorted helix, in AT the RCL is partially inserted into the A-sheet with an obscured P1 reactive centre, and in α_1-PI the RCL adopts a canonical "perfect-fit" conformation that precisely matches the active site of the serine proteinase.

1.3.4. Mechanism of Action of Serpins as Suicide Inhibitors

The inhibitory serpins inactivate their cognate serine proteinases via

the formation of a 1:1 stoichiometric covalent complex apparently through their P1 residue and the catalytic serine of the cognate proteinases. The P1 residue of the serpin appears to confer primary proteinase specificity. The importance of the P1 residue in determining proteinase specificity is clearly manifested by the observation that amino acid substitutions at this position of many serpins, including AT (Howarth *et al.*, 1985; Erdjument *et al.*, 1987; 1989; Owen *et al.*, 1988; 1991; Lane *et al.*, 1989; Okajiman *et al.*, 1995), heparin cofactor II (HC-II) (Derechin *et al.*, 1990), α_1-PI (Owen *et al.*, 1983; Jallet *et al.*,, 1986; Schapira *et al.*, 1986; Scott *et al.*, 1986; Travis *et al.*, 1986; Patston *et al.*, 1990; Wachtfogel *et al.*, 1994), α_1-ACT (Rubin *et al.*, 1990; 1994; Schechter *et al.*, 1993), PAI-I (York *et al.*, 1991; Sherman *et al.*, 1992), C1-inhibitor (Aulak *et al.*, 1988; Eldering *et al.*, 1992), and protein C inhibitor (PCI) (Phillips *et al.*, 1994), can result in loss of inhibitory properties or a change in inhibitory specificity. The most significant is a α_1-PI variant, namely α_1-PI Pittsburgh. Replacement of the P1 Met with Arg in α_1-PI gave rise to a serpin with potent anti-thrombin activity but little antielastase ability (Owen *et al.*, 1983; Schapira *et al.*, 1986; Scott *et al.*, 1986; Wachtfogel *et al.*, 1994). The P1 residue, however, is not the sole determinant of inhibitory specificity (Johnson and Travis, 1979; Griffith *et al.*, 1985; Ragg and Preibisch, 1988). Accordingly, amino acid substitutions in the RCL beyond the P1 residue change the proteinase specificity (Theunissen *et al.*, 1993; Hopkins *et al.*, 1995; Olson *et al.*, 1995b; Djie *et al.*, 1996). It is worth mentioning that changing the P1'

Ser of AT dramatically affected the inhibition of thrombin, while having a relatively minor effect on the inhibition of FXa (Theunissen *et al.*, 1993). As a result, a FXa-specific AT moiety was generated.

Broad ranges of outcome for a serpin-proteinase encounter have been observed. In each individual case, serpins acts as either an inhibitor or a substrate or both. Additionally, complete or partial switch from inhibitor to substrate has been observed (Skriver *et al.*, 1991; Hood *et al.*, 1994). A branched pathway, suicide inhibition mechanism has thus been proposed (Olson, 1985; Rubin *et al.*, 1990; Patston *et al.*, 1991; 1994). According to this mechanism, the initial Michaelis complex (EI) and the subsequent intermediate EI' are common to both substrate and inhibitory pathways; occurring at the branch point, the intermediate EI' can be subverted from the cleavage pathway and became kinetically trapped as a stable covalent complex ($E^{\bullet}I^{\bullet}$) (Jornvall *et al.*, 1979; Jesty, 1979; Longas and Finlay, 1980; Lawrence *et al.*, 1995). The outcome of a serpin-proteinase interaction, thereby, is determined by the relative values of the substrate and inhibitory branch rate constants. It has been proposed also that the inhibitory branch rate constant may depend on the ease of insertion of the N-terminal end of the RCL into ß-sheet A. Thus if loop insertion is rapid, the loop-insertion-dependent inhibitory pathway predominates the normal substrate reaction, and vice versa for slow insertion (Hopkins *et al.*, 1993; Gettins *et al.*, 1996).

Several lines of evidence support the proposal that insertion of the N-terminal end of the RCL into ß-sheet A is a prerequisite for operation of the inhibitory pathway. As shown for AT (Bjork, *et al.*, 1992a; 1992b) and α_1-PI (Schulze *et al.*, 1990; 1992), formation of a binary complex with tetradecapeptide corresponding to the respective RCL P14-P1 sequences converted an otherwise inhibitory serpin exclusively into a substrate. Spectroscopic and stability studies of the resultant complexes revealed that the peptide presumably occupied the strand 4 position of the expanded ß-sheet A, which is present in cleaved, loop-inserted inhibitory serpins. This clearly demonstrated the need for loop insertion as a requirement for inhibition by serpins. Moreover, an epitope, absent from the native serpin, was shown immunologically to be present on cleaved and proteinase-complexed serpins for both C1 inhibitor (De Agostini *et al.*, 1988) and AT (Bjork, *et al.*, 1993). The AT-RCL peptide complex also contained this neopeptide, suggesting that in each case expansion of ß-sheet A has occurred with associated structural changes. Additional evidence in support of loop insertion as an integral part of the inhibitory mechanism came from the following observation using a PAI-I P9Cys variant fluorescently labelled with nitrobenzofuran (NBD). Conversion of this PAI-I variant to either latent or cleaved forms with concomitant loop insertion into ß-sheet A resulted in the same large enhancement of NBD fluorescence as occurred upon the formation of stable complex with trypsin (Shore *et al.*, 1995). Finally, the partial or complete absence

of inhibitory properties for certain RCL variants can be most readily explained by the deleterious effect that particular side chains might have on the rate of loop insertion, and thus on the rate constant of the inhibitory branch (Gettins *et al.*, 1996).

The mechanism of stable proteinase-serpin complex formation is not completely understood. Kinetics studies have suggested that the formation of the stable proteinase-serpin complex involves at least two steps: the association of E and I in a Michaelis complex (EI), followed by its conversion to a stable covalent complex $E^{*}I^{*}$ (Olson and Shore, 1982; Stone *et al.*, 1987; Bruch and Bieth, 1989; Longstaff and Gaffney, 1991; Faller *et al.*, 1993; Morgenstern *et al.*, 1994; Stone and Hermans, 1995). The presence of an intermediate EI' between EI and $E^{*}I^{*}$ is also indicated, again by kinetic evidence (O'Malley *et al.*, 1997). The same study also demonstrates that the partitioning step between inhibitor and substrate pathways precedes P1-P1' cleavage. For the inhibitory pathway, although it is agreed generally that a covalent intermediate is formed, the nature of this intermediate is still under debate. Results from a number of studies suggest that the stable intermediate complex is an acyl form (Fish and Bjork, 1979; Jesty, 1979; Jornvall *et al.*, 1979; Longas and Finlay, 1980; Bjork *et al.*, 1982; Lawrence *et al.*, 1995). However, NMR studies suggest that it may take the form of a tetrahedral intermediate (Matheson *et al.*, 1991).

1.4. Activation of AT by Heparin

Blood coagulation proceeds through a series of reactions in which the plasma zymogens of the serine proteinases, also called clotting factors, are sequentially activated by limited proteolysis culminating in the generation of thrombin; thrombin, in turn, cleaves fibrinogen to produce the filamentous fibrin of the established clot (Fig. 1.2). AT has been identified as the primary inhibitor of the activated clotting factors thrombin (Abilgaard, 1969; Rosenberg and Damus, 1973; Vogel *et al.*, 1979; Jesty, 1986) and factor Xa (FXa) (Kurachi *et al.*, 1976b; Biggs *et al.*, 1970; Fuchs and Pizzo, 1983; Gitel *et al.*, 1984). To a lesser extent, AT also inhibits FVIIa associated with tissue factor (Rao *et al.*, 1993), FIXa (Rosenberg *et al.*, 1975; Kurachi *et al.*, 1976b; Fuchs *et al.*, 1984b), FXIa (Damus *et al.*, 1973; Scott and Colman, 1989), FXIIa (Stead *et al.*, 1976; Pixley *et al.*, 1974), kallikrein (Lahiri *et al.*, 1974), plasmin (Highsmith and Rosenberg, 1974), urokinase (Clemmensen, 1978), and trypsin (Danielsson and Bjork, 1982). The inhibition of serine proteinases by AT alone under physiologic conditions is relatively slow, but greatly accelerated in the presence of the polysulphated glycosaminoglycans, heparin and heparan sulphate. Actually, AT attains its full anti-proteinase activity only upon binding to these specific glycosaminoglycans (Jordan *et al.*, 1979; Olson and Shore, 1981). In addition, four other serpins are relatively inefficient inhibitors until they are activated by a specific glycosaminoglycan including heparin. The activation occurs as a result of the

Fig. 1.2. Coagulation cascade and fibrin formation (Taken from Davie *et al.*, 1991). The initiation of the coagulation cascade occurs following vascular injury and the exposure of tissue factor to the circulating blood. This triggers the extrinsic pathway (right side), shown in heavy arrows. The intrinsic pathway (left side) can be triggered when thrombin is generated, leading to the activation of factor XI. The two pathways converge by the formation of factor Xa. The activated clotting factors (except thrombin) are designated by lowercase a, i.e., IXa, Xa, XIa, etc. PL refers to phospholipid. The phospholipid bound to tissue factor apoprotein is not shown.

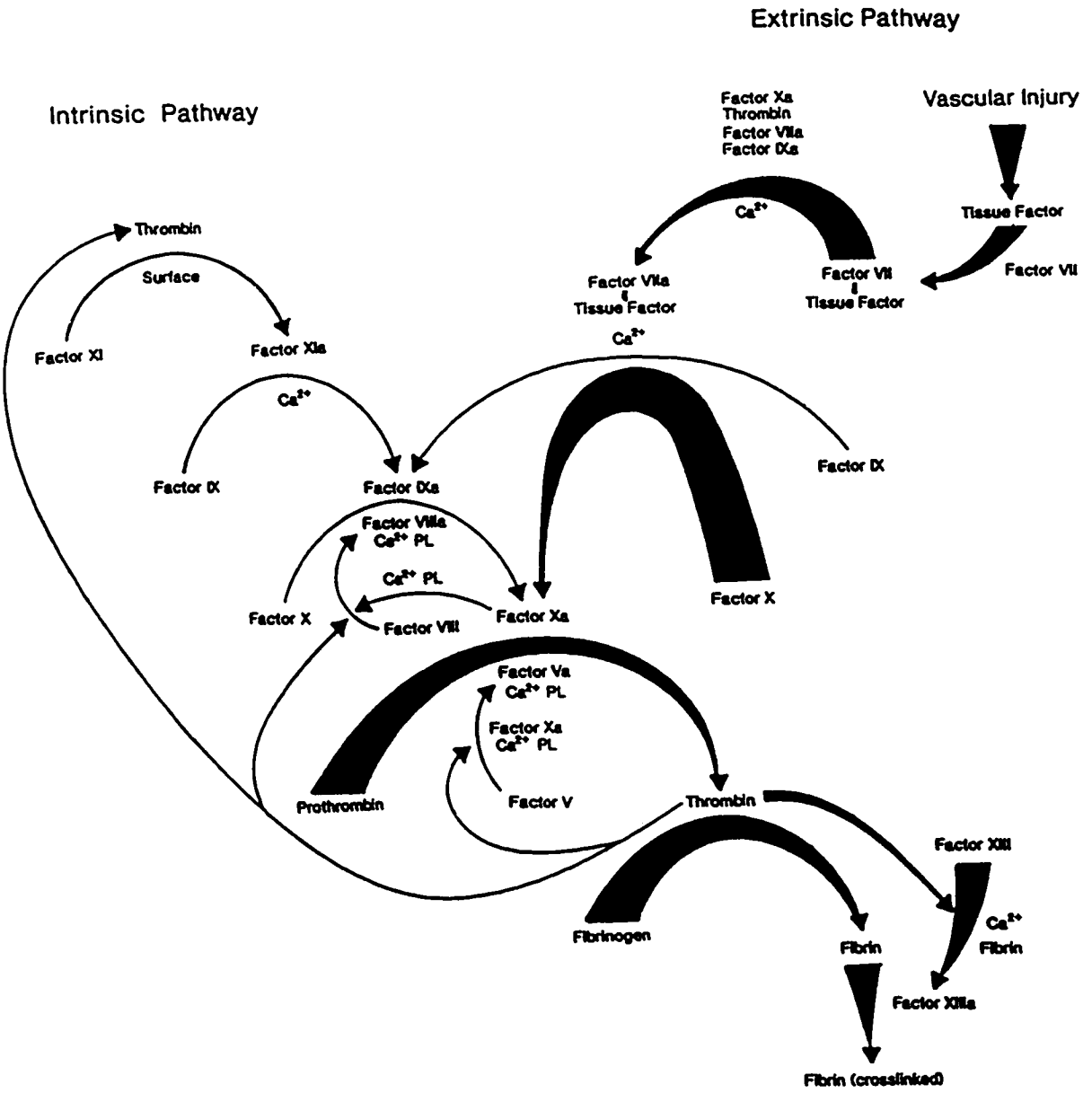
Extrinsic Pathway
Intrinsic Pathway
Vascular Injury
Factor Xa
Thrombin
Factor VIIa
Factor IXa
Tissue Factor
Factor VII
Factor VIIa
Tissue Factor
Factor VII
Tissue Factor
Thrombin
Surface
Factor XI
Factor XIa
Factor IX
Factor IXa
Factor X
Factor VIIIa
Factor VIII
Factor Xa
Factor V
Factor Va
Prothrombin
Thrombin
Fibrinogen
Fibrin
Factor XIII
Factor XIIIa
Fibrin
Fibrin (crosslinked)

binding of the glycosaminoglycan to the inhibitor and is manifested by the up to several thousand-fold enhancement in the rate at which these inhibitors inactivate their proteinases. These heparin activatable serpins, namely HC-II, protease nexin I (PN-I), PAI-I, and PCI, act mainly to regulate proteinases participating in blood coagulation and fibrinolysis.

1.4.1. Heparin and its AT-binding Pentasaccharide

Heparin is a potent anticoagulant and antithrombotic agent widely used for the prophylaxis and treatment of thromboembolism. Like most glycosaminoglycans, heparin is an alternating copolymer of a uronic acid and an amino sugar (Elson and Morgan, 1933), with its structure commonly represented by its prevalent disaccharide sequences. The major uronic acid of heparin is L-iduronic acid, and the major amino sugar is *N*-sulphated D-glucosamine (Jorpes *et al.*, 1950; Perlin *et al.*, 1968; Perlin and Sanderson, 1970). The molecular structure of the major disaccharide sequences of heparin is α-1,4-linked L-iduronic acid 2-sulphate ¬D-glucosamine *N*, 6-disulphate (Perlin *et al.*, 1971).

Heparin is synthesized by mast cells as a proteoglycan. In this heparin precursor variable numbers of the repeating disaccharide chains of 60-100 kDa are linked by the trisaccharide galacosylgalactosylxylose to a core protein of unknown size via the hydroxyl group of its serine residues (Lindahl and Roden 1964; 1965; Lindahl, 1966; Robinson *et al.*, 1978). Five monosaccharide "building

blocks" have been identified as components of the heparin molecule. These are D-glucosamine (Jorpes and Bergstrom, 1936), D-glucuronic acid (Wolfrom and Rice, 1946), L-iduronic acid (Cifonelli and Dorfman, 1962), D-galactose (Lindahl and Roden, 1964; 1965), and D-xylose (Lindahl and Roden, 1964; 1965). Three kinds of substituents are found on the sugar residues of heparin, namely acetyl (Jorpes, 1935), sulphate (Jorpes *et al.*, 1950), and phosphate groups (Rosenfeld and Danishefsky, 1988). Although heparin chains have a common backbone of alternating *N*-sulphated glucosamine and uronic acid units, there are heterogeneities in their fine structure (Casu, 1985). These variations arise from differences in the nature of the uronic acid, *i.e.*, glucuronic or iduronic, the degree of sulphation and positions of sulphate ester groups, and the occurrence of small amounts of *N*-acetylglucosamine and unsubstituted glucosamine. In addition, a dispersion of molecule size has been found in commercial heparins, with the heparin chains present in these preparations generally having molecular weights in the range of 5 to 30 kDa, *i.e.* with approximately 15-100 monosaccharide residues per chain (Lindahl *et al.*, 1965). This structural heterogeneity of heparin gives rise to differences in its affinity for AT (Bjork and Lindahl, 1982; Niedyszynski, 1989). Approximately one-third of the heparin molecules present in commercial preparations binds to AT with high affinity, and these high affinity molecules account for approximately 90% of the anticoagulant activity of the preparations (Lam *et al.*, 1976; Hook *et al.*, 1976; Andersson *et al.*, 1976). A

search for the specific structural features responsible for the anticoagulant activity led to the discovery that a unique pentasaccharide sequence (Fig. 1.3) constitutes the specific AT-binding region of high affinity heparin molecules (Lindahl *et al.*, 1980; Casu *et al.*, 1881; Thunberg *et al.*, 1982; Choay *et al.*, 1983; Atha *et al*, 1984; 1985). This pentasaccharide, not found in low affinity heparin preparations, contributes more than 90% of the free energy associated with the binding of heparin to AT (Lindahl *et al.*, 1984; Atha *et al.*, 1985; Olson *et al.*, 1992). Most high affinity heparin molecules contain only one such specific sequence distributed randomly in their chains, although molecules with longer chains may contain two, resulting in higher anticoagulant activity (Danielsson and Bjork, 1981; Jordan *et al.*, 1982; Nesheim *et al.*, 1986). This pentasaccharide has been synthesized and shown to bind to AT with high affinity comparable to full-length heparin (Choay *et al.*, 1983; Sinay *et al.*, 1984; Olson *et al.*, 1992). Structural analysis of this heparin pentasaccharide shows that the 3-*O*-sulphate group of glucosamine at position three is critical for the AT-heparin binding (Lindahl *et al.*, 1980). In addition, both *N*-sulphate groups of the glucosamine residues at positions three and five, as well as the 6-*O*-sulphate of the first glucosamine residue, are required for high affinity binding (Riesenfeld *et al.*, 1981; Atha *et al.*, 1984). Actually, AT is unique among the heparin activatable serpins in that a sequence-specific pentasaccharide is required for its activation.

Fig. 1.3. Structure of a heparin octasaccharide sequence that displays most of the substituted monosaccharide components identified to date (Taken from Roden, 1989). The pentasaccharide sequence within brackets represents the AT-binding region.

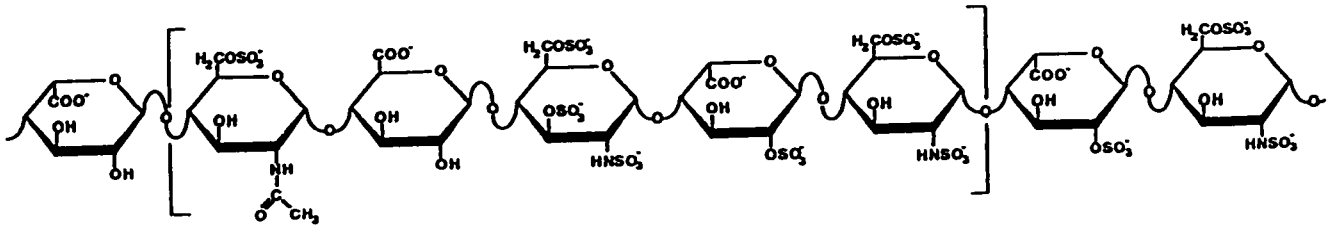
COO⁻
OH
OH
H₂COSO₃⁻
OH
NH
C
O
CH₃
COO⁻
OH
OH
H₂COSO₃
OSO₃⁻
HNSO₃⁻
COO⁻
OH
OSO₃⁻
H₂COSO₃⁻
OH
HNSO₃⁻
COO⁻
OH
OSO₃⁻
H₂COSO₃⁻
OH
HNSO₃⁻

1.4.2. The Putative Pentasaccharide and Heparin Binding Sites of AT

The structural specificity of the AT-binding heparin pentasaccharide implies a well-defined binding site on AT. Our understanding of the pentasaccharide and heparin binding sites of AT has come from structural and functional analysis of both naturally-occurring low heparin affinity AT variants and chemically modified AT associated with reduced heparin binding. Relevant information has also been derived from studies involving site-directed mutagenesis, ^{1}H NMR, molecular modelling, as well as computer sequence alignments of the heparin activatable serpins. Table 1.1 summarizes amino acid residues that have been associated with binding to heparin.

Since the binding of heparin pentasaccharide to AT is critically dependent on the position of the sulphate groups, it would take place predominately by the bonding of the negatively charged sulphates to the positively charged side chains of certain amino acid residues. The pentasaccharide binding site of AT thus should compose of complementary basic residues. A comparison of the homologous sequence alignments of three heparin-binding serpins, namely AT, HC-II, and PN-I, with 30 other members of the family showed the unique conservation of a set of basic residues (Carrell *et al.*, 1987). When these conserved residues were projected on a space-filling model of α_1-PI, they formed a band of positive charge stretching from the base of the A-helix and across the underside of the D-helix, giving a convincing depiction of the pentasaccharide

Table 1.1. Amino acid residues of AT that have been associated with binding to heparin. The indicated residues have been implicated from data about naturally occurring mutants; from studies involving chemical modification, mutagenesis, ^{1}H NMR, molecular modelling; or from combinations of such studies.

Amino acid residue	Natural mutants	Chemical modification	Mutagenesis studies	^{1}H NMR studies	Molecular modelling
ILe7	x				
Arg24	x				
Pro41	x				
Arg47	x				x
Trp49		x	x		
Leu99	x				
Lys107		x			
Lys114		x	x		
Ser116	x				
His120				x	
Lys125		x	x		
Arg129		x			x
Arg132			x		
Lys133			x		
Lys136		x			
Lys139			x		
Arg145		x			

binding site on the D-helix and at the commencement of the A-helix. This site was so formed that the pentasaccharide could be modelled to bond with basic residues within this site (Grootenhuis and Van Boeckel, 1991). Moreover, the amino terminus of AT was tentatively positioned in relationship to the proposed core pentasaccharide binding site, based on the structures of cleaved bovine and intact human AT (Carrell *et al.*, 1994). The amino terminus formed a curve around the core pentasaccharide binding site on the body of the molecule, moving between the D- and E-helices, then turning to form a ß-strand, hydrogen bonded to the peptide loop joining the D- and C-helices.

Satisfying though it is, this model requires supporting evidence to identify it specifically as the pentasaccharide binding site, *i.e.* the high affinity binding site for heparin on AT. The most convincing evidence in support of this putative high affinity binding site for heparin comes from the identification of AT variants with low heparin affinity and associated with inherited thrombotic disease. Of the 11 known variants with low affinity for heparin, five result from replacement of Arg residues: namely Arg24Cys (Borg *et al.*, 1990), Arg47Cys (Koide *et al.*, 1984; Duchange *et al.*, 1986; 1987; Brunel *et al.*, 1987; Mohlo-Sabatier *et al.*, 1989; Perry and Carrell, 1989; Owen *et al.*, 1989; Olds *et al.*, 1990; Ueyama *et al.*, 1990; Roussel *et al.*, 1991), Arg47Ser (Borg *et al.*, 1988), Arg47His (Owen *et al.*, 1987; Perry and Carrell, 1989; Caso *et al.*, 1990; Wolf *et al.*, 1990; Vidaud *et al.*, 1991), and Arg129Gln (Gandrille *et al.*, 1990; Najjam *et al.*, 1994).

The other mutations all predictably cause structural perturbations of the site. For example, Pro41Leu (Chang and Tran, 1986; Daly *et al.*, 1989; Mohlo-Sabatier *et al.*, 1989; Perry and Carrell, 1989; deRoux *et al.*, 1990) affects a critical turn in the amino terminal extension, while the substitution of Asn7 (Brennan *et al.*, 1988) creates a new glycosylation site that would block access of heparin to the binding site in the region of Lys125 and Arg129. The other four mutations, namely Leu99Phe (Olds *et al.*, 1992), Leu99Val (Chowdhury *et al.*, 1995), Ser116Pro (Okajima *et al.*, 1993), and Gln118Pro (Chowdhury *et al.*, 1995), cause readily-modelled perturbations of the tight packing involved in the turn of the amino terminus at the C-helix and its ß-sheet bonding to the CD loop. The observed increased heparin affinity associated with the ß-AT lacking N-glycosylation at Asn135 (Peterson and Blackburn, 1985; Brennan *et al.*, 1987) also supports the location of the high affinity binding site for heparin on AT.

Studies involving specific chemical modifications and recombinant engineering of AT also contributed to the identification of the residues within the high affinity heparin binding site as well. Chemical modification of four Lys residues in AT, i.e. Lys107, Lys114, Lys125, and Lys136 (Liu and Chang, 1987; Peterson *et al.*, 1987; Chang, 1989), demonstrated the involvement of all four in high affinity binding of heparin to AT. Similarly, selective modification of Arg residues indicated that Arg129 and Arg145 were constituents of the high affinity binding site for heparin on AT (Sun and Chang, 1990). AT derivatives chemically

modified at Trp residues also displayed impaired heparin affinity (Bjork and Nordling, 1979; Blackburn and Sibley, 1980; Villanueva *et al.*, 1980; Karp *et al.*, 1984). The loss of high affinity for heparin upon Trp-specific modification was attributed to the selective modification of Trp49 (Blackburn *et al.*, 1984). However, another group of investigators argued that the impaired heparin binding of such chemically modified AT may be a result of change or stabilization of certain conformation of AT other than related to selective modification of the Trp49 residue (Scully *et al.*, 1991; Shah *et al.*, 1990). A recombinant AT variant with a Lys substitution for Trp49 was thus generated (Gettins *et al.*, 1992). This Trp49Lys variant displayed reduced affinity for the pentasaccharide, indicating that Trp49 probably contacts the pentasaccharide through hydrophobic interactions and contributes to the binding of the pentasaccharide to AT. Using recombinant approaches, Lys125 was shown to play an important role in the high affinity binding of heparin to AT (Fan, *et al.*, 1994a; Kridal *et al.*, 1996), as well as two residues outside the putative pentasaccharide binding site, Lys114 and Lys139 (Kridel *et al.*, 1996). However, the locations of Arg132 and Lys133 were shown to be peripheral to the core pentasaccharide binding site (Meagher *et al.*, 1996). In addition to the above, ^{1}H NMR studies combined with recombinant approaches revealed that His120 might play an important role in AT binding to heparin, more likely through maintaining the correct conformation of the heparin binding site (Fan *et al.*, 1994b). In contrast, neither His1 nor His65 appeared to

be involved in heparin binding although they might be in proximity to the core heparin binding site and consequently sensitive to the binding of heparin.

Early studies aimed at defining the high affinity heparin binding site also involved dissection of AT. A proteolytic fragment of AT comprising residues 104-251 was first demonstrated to be able to bind to heparin (Rosenfeld and Danishefsky, 1986). Similarly, AT114-156 was shown to be sufficient to bind heparin (Smith and Knauer, 1987). We characterized three recombinant AT fragments and one AT variant for heparin binding capacity (Wu *et al*, 1992; 1993; 1994). Expression in *E. coli* conferred heparin binding properties on the bacterial protein if residues 90-160 or 22-160 were present, but not when only residues 22-60 were included. The fusion protein containing AT22-160 had higher affinity to heparin than that obtained with AT90-160. The truncated form of AT lacking residues 41-49 also displayed reduced heparin binding. In addition, polyclonal antibodies were raised against a synthetic peptide corresponding to the sequence of residues 124-145 (Smith *et al.*, 1990). These antibodies were found to be able to block the specific binding of heparin to AT and to mimic partially the action of heparin on AT. Further analysis of the region composed of residues 123-139 revealed that it had a strong potential for formation of an amphipathic helix with highly positively charged residues on one face and hydrophobic residues on the other (Smith *et al.*, 1990). Accordingly, the spacial arrangement of the positively charged residues in this region was shown to be essential for binding to heparin

(Lellouch and Lansbury, 1992). Moreover, AT121-134 was suggested to constitute the high affinity heparin binding site (Tyler-Cross *et al.*, 1994). It was found that loss of any single cationic residue in the peptide AT121-134 had a deleterious effect on heparin binding (Tyler-Cross *et al.*, 1996).

The resolution of the structure of a dimeric form of intact AT to 2.6 Å (Skinner *et al.*, 1997) and the determination of the structures of the pentasaccharide-AT complex to 2.9 Å (Jin *et al.*, 1997) have enabled the binding site for the pentasaccharide to be further mapped. In the active molecule of the AT dimer, the side-chains of the key pentasaccharide binding residues Arg47, Lys114, Lys125, and Arg129 are externally oriented towards the binding site and readily available to form ionic interactions with the sulphate groups of the pentasaccharide (Skinner *et al.*, 1997). In the pentasaccharide-AT complex, the pentasaccharide forms well-defined bonds to Arg47 and Arg129 but less well defined to Lys125 although the pentasaccharide overlies this residue (Jin *et al.*, 1997). Thus the role of the D-helix region and surrounding N-terminus, in particular Arg47, Arg129, Lys114, and Lys125, as the binding site for the pentasaccharide has been established.

Although the high affinity binding site for heparin on AT has been mapped to the N-terminal residues centred on the D-helix region, variants with substitutions at the C-terminal portion of AT have been shown to have altered heparin affinity. Substitutions in or near s1C and s4B region, including residues

402-429, result in molecular instability (Lane *et al*, 1993a) and a substantially decreased affinity for both heparin (Lane *et al.*, 1993; Watton *et al.*, 1993) and the pentasaccharide (Mille *et al.*, 1994); P1 mutations increased heparin affinity (Bauer *et al.*, 1983; Lane *et al.*, 1987; Wolf *et al.*, 1987; Erdjument *et al.*, 1988; 1989; Owen *et al.*, 1991). The molecular mechanisms accountable for such changes in heparin affinity are unknown, but a structural link between the C-terminal and those N-terminal residues has been well established (Gettins *et al.*, 1993a; Dawes *et al.*, 1994; Skinner *et al.*, 1997).

1.4.3. Binding of Heparin to AT and Activation of AT by Heparin

Heparin accelerates the reaction of AT with its cognate proteinases up to several thousand-fold (Bjork *et al.*, 1989; Olson and Bjork, 1991a). The binding of heparin to AT is essential for this accelerating effect (Rosenberg and Damus, 1973; Rosenberg, 1977; Jordan *et al.*, 1980). High affinity heparin binds to AT with a dissociation constant (K_d) measured as 10-20 nM at physiological pH and ionic strength (Nordenman *et al.*, 1978; Jordan *et al.*, 1979; Olson *et al.*, 1981; 1992). Ionic interactions are involved as well as non-ionic interactions, as suggested by the observed ionic-strength dependence of this binding (Nordenman *et al.*, 1978; Jordan *et al.*, 1979; Nordenman and Bjork, 1981; Olson *et al.*, 1981; Olson and Bjork, 1991b). The heparin pentasaccharide binds to AT with only a 3- to 4-fold reduced affinity, implying that it accounts for more than 95% of the

binding energy associated with heparin-AT interaction (Atha *et al.*, 1985; Olson *et al*, 1992). Based on the ionic-strength dependence of the binding of the pentasaccharide to AT, 4 to 5 ionic interactions were suggested to be involved (Olson *et al.*, 1992). Moreover, one additional ionic interaction outside the pentasaccharide site was suggested to account for the slightly higher affinity of full-length heparin (Olson *et al.*, 1992).

Binding of heparin to AT causes structural perturbations in AT. These changes are substantial perturbation of the ^{1}H NMR spectrum (Gettins, 1987; Gettins and Wooten, 1987; Horne and Gettins, 1992), a red-shift in the near UV spectrum (Nordenman and Bjork, 1978), large increases in elipticity in the near UV circular dichroism (Nordenman and Bjork, 1978), and a 40% enhancement of the endogenous Trp fluorescence (Einarsson and Andersson, 1977; Villanueva and Danishefsky, 1977; Nordenman *et al.*, 1978; Jordan *et al.*, 1979). The fluorescence enhancement appears to originate from buried Trp residues, rather than from a perturbation of surface residues, suggesting that a major conformational change in the AT molecule is induced by its interaction with heparin (Olson and Shore, 1981). Such heparin-induced conformational changes have also been implicated in studies showing that the binding of heparin to AT leads to an increased reactivity of Lys236 to chemical modifying agents (Chang, 1989), appearance of a new cleavage site on the RCL for a snake-venom proteinase (Kress and Catanese, 1981), and a decreased accessibility of the A-

sheet to forming binary complexes with homologue-loop peptides (Bjork *et al.*, 1992b). Kinetic studies have confirmed that heparin binding induces a conformational change in AT rather than perturbing a pre-existing equilibrium between the two conformational states of AT (Olson *et al.*, 1981). The pentasaccharide has been suggested to induce changes in the AT conformation similar to those elicited by full-length heparin (Olson *et al.*, 1992). Thus, AT conformational changes induced by full-length heparin derive predominantly from the interactions between the pentasaccharide and AT. This conclusion is, however, challenged by a study using a Trp49Lys variant (Gettins *et al.*, 1992). There are four Trp residues in AT, i.e. Trp49, Trp189, Trp215, and Trp307, and they are located at A-helix, F-helix, strand s3A, and H-helix, respectively. The observed enhancement of endogenous Trp fluorescence reflects the sum of the perturbation of one or a number of these Trp residues. This enhancement thus may not detect the difference between the pentasaccharide- and the full-length heparin-induced structural rearrangements since it may exist in such a way that the sum of the perturbation of the involved Trp residues are not changed. In another word, local structures, specially the RCL, can be rearranged differently by the pentasaccharide and full-length heparin; thus not necessarily altering the overall fluorescence enhancement. In a study to probe the functional role of Trp49, a Trp49Lys AT variant was analyzed for both its spectroscopic properties and its heparin cofactor activity. Despite the apparent contribution of Trp49 to

the favourable binding energy of the pentasaccharide, the replacement of Trp49 by a Lys residue did not appear to have adverse effects on the structure or heparin induced activation of AT towards FXa. In contrast, the pentasaccharide induced only a 24% enhancement of AT fluorescence, while high affinity heparin induced an enhancement of 40%. It appears that somehow the pentasaccharide and full-length heparin cause different perturbations of Trp49 since the sum of the perturbations of the other three Trp residues are different in this variant. Small differences in circular dichroism changes also have been observed when comparing the effect of the pentasaccharide with that of longer heparin species; and the differences could reflect an additional conformational change in AT induced by the larger heparin moiety (Stone *et al.*, 1982). Alternatively, such spectroscopic differences were interpreted as evidence for an additional electrostatic interaction by the larger molecule (Lindahl *et al.*, 1984; Olson *et al.*, 1992). This later explanation, however, does not necessarily rule out the possibility of an additional conformational change in AT when interacting with longer chain heparin.

Early studies examining the refolding properties of AT following denaturation suggested that binding of heparin to AT is a two-step process in which a primary binding is followed by a secondary conformational rearrangement (Villanueva and Allen, 1983). Kinetic studies revealed that an initial rapidly equilibrating step with a K_d of $4.3 \pm 1.3 \times 10^{-5}$ M precedes the conformational change

step and that the highly favourable conformational change then results in a greater than 300-fold increase in the affinity of heparin to AT and therefore tight binding (Olson *et al.*, 1981; 1992). This two-step binding mechanism was further suggested by spectrofluorimetry experiments which showed that the initial weak binding pushes AT into a high affinity conformation which in turn results in a tight binding with the pentasaccharide (Petitou *et al.*, 1997). The major function of the conformational change has thus been postulated to increase the affinity of the pentasaccharide for AT. In addition, the initial change in AT conformation has been suggested to result in an increased reactivity of AT towards its cognate proteinases and therefore to be responsible for activating AT to become a better inhibitor (Rosenberg and Damus, 1973). The observed increase in proteolytic vulnerability of the loop (Kress and Catanese, 1981) and the inaccessibility of the A-sheet to peptide insertion (Bjork *et al.*, 1992a; 1992b) both support the concept of a mobile RCL conformationally linked to the heparin binding site. Direct evidence for the transmission of a conformational change from the heparin binding site to the reactive centre of AT has been provided (Gettins *et al.*, 1993a; Dawes *et al.*, 1994). A comparison of the structure of AT with that of other serpins showed two differences surrounding the putative heparin binding site. These were a shift of the D-helix relative to the A-helix and a change in the conformation of the peptide loop connecting the carboxyl terminus of D-helix to strand s2A (Carrell *et al.*, 1994). On the basis of modelling studies, Van Boeckel

and colleagues (1994) have proposed that heparin induces ordered helical structure in this hD-s2A connecting loop, with consequent movement of strand s2A and expulsion of the RCL from the sheet. The RCL would therefore change from its partially inserted form to the fully exposed conformation seen in the other intact inhibitory serpin structures, thereby making it a better target for FXa binding. Evidence for RCL preinsertion with expulsion upon heparin binding has been provided recently (Huntington *et al.*, 1996). Such expulsion frees the RCL from a constrained form to take up an optimal inhibitory conformation, as seen in α_1-PI (Carrell *et al.*, 1997).

1.4.4. Mechanism of Heparin Acceleration of Proteinase Inactivation by AT

The observation of the conformational change in AT upon heparin binding has led to the hypothesis, first proposed by Rosenberg and Damus (1973), that this conformational change is responsible for activating AT to become a better inhibitor of its cognate proteinases by making it more reactive toward the proteinases. This conformational activation is thought to cause the reactive bond of AT to be more accessible or complementary to the active site of the proteinases. According to this hypothesis the heparin pentasaccharide should produce the same rate enhancing effect on proteinase-AT reactions as a full-length heparin, given the assumption that they induce highly similar, if not identical, conformational changes in AT. This is challenged, however, by the

observation of the chain length dependence of heparin's accelerating effect (Laurent *et al.*, 1978; Andersson *et al.*, 1979; Danielsson and Bjork, 1981). The rate of reaction between AT and FXa, FVIIa, FXIIa, or kallikrein is accelerated by various heparin moieties, regardless of their size, whereas the rate enhancement activity for the inhibition of thrombin, FIXa, or FXIa is chain length dependent (Thunberg *et al.*, 1979; Jordan *et al.*, 1980; Holmer *et al.*, 1980; 1981; Oosta *et al.*, 1981; Choay *et al.*, 1983; Lane *et al.*, 1984; Ellis *et al.*, 1986; Olson, 1988; Olson and Choay, 1989; Lormeau *et al.*, 1996). While the pentasaccharide is as effective as larger heparin species for FXa inhibition, it has little effect on thrombin inactivation by AT (Holmer *et al.*, 1981; Choay *et al.*, 1983; Olson *et al.*, 1992). Thus heparin chains just large enough to bind AT and to induce the conformational change are sufficient to account for most of the rate enhancing effect of heparin on FXa inactivation. For heparin to promote thrombin inhibition by AT, additional saccharide residues appear to be required to induce additional conformational changes in AT, or to accommodate both the AT and the thrombin or both. Actually, significant accelerating activity of AT is not observed until the chain length is 18 saccharide long (Lane *et al.*, 1984; Danielsson *et al.*, 1986; Bray *et al.*, 1989), the smallest polysaccharide chain able to bind AT and thrombin simultaneously (Olson *et al.*, 1988). A second mechanism was thus postulated to explain the unusual chain length dependence of the heparin's rate enhancement of thrombin inactivation by AT (Holmer *et al.*,

1979). According to this mechanism, the larger heparin chain required to accelerate thrombin inhibition by AT is necessary to accommodate both the inhibitor and the proteinase on the same polysaccharide chain (Olson and Bjork, 1991). The molecular bridging by heparin of the ternary complex between heparin, thrombin, and AT make a contribution to the rate enhancing effect of heparin on thrombin inactivation by AT. The consequence of this bridging has been thought to limit their interaction to a single plane along the heparin chain such that thrombin approaches the AT in the correct orientation for formation of the complex between the two.

The essential role of heparin-thrombin interaction for the heparin accelerated thrombin inactivation by AT is supported by several lines of evidence. The accelerating effect of heparin can be abolished by the selective modification of Lys or Arg residues within the thrombin molecule, without affecting the bimolecular thrombin-AT interaction (Pomeranz and Owen, 1978; Machovich *et al.*, 1978). Heparin accelerated thrombin-AT reaction is saturable with respect to both AT and thrombin, a kinetic pattern linked to a two-substrate enzyme-catalysed reaction (Griffith, 1982; Hoylaerts *et al.*, 1984; Evington *et al.*, 1986). The observed reaction rates over a wide heparin concentration range can be described mathematically using equations which fit the ternary complex model (Hoylaerts *et al.*, 1984). Moreover, the accelerating effect of heparin on thrombin-AT reaction diminishes at high heparin concentrations, an observation

suggesting that thrombin and AT bound to separate heparin chains at high heparin concentrations (Jordan *et al.*, 1979; 1980; Oosta *et al.*, 1981; Griffith, 1982; Nesheim, 1983; Peterson and Jorgensen, 1983; Hoylaerts *et al.*, 1984; Olson, 1988). Active-site-blocked thrombin reduces the accelerating effect of heparin, apparently by competing with the active thrombin for the binding to heparin in a ternary thrombin-heparin-AT complex (Griffith, 1982; Pletcher and Nelsestuen, 1983; Hoylaerts *et al.*, 1984; Olson, 1988). Kinetic studies have been reported which support the concept that thrombin binds to AT-bound heparin and then diffuses along the polysaccharide chain to meet the AT (Richer and Eigen, 1974; Winter *et al.*, 1981; Hoylaerts *et al.*, 1984). Thrombin appears to bind to heparin mainly through ionic interactions with an affinity lower than that of AT (Nordenman and Bjork, 1978; 1980). No specific saccharide sequence in heparin has yet been identified to account for this binding. In addition, binding of thrombin to the binary AT-heparin complex has been shown to be much tighter than to either AT or heparin alone (Olson and Shore, 1982; Olson and Bjork, 1991b). These observations are consistent with the concept that thrombin binds both AT and heparin in the ternary complex. Two synthetic peptides corresponding to AT404-412 and AT420-429 have been demonstrated to interact directly with thrombin and to increase the amidolytic activity of thrombin (Nishioka and Suzuki, 1992). These latter results suggests that the C-terminal region of AT interacts with thrombin to facilitate the interaction between the

catalytic Ser and the P1 Arg. Modelling of serpin-proteinase complexes also suggests that the C-terminus AT interacts with the proteinase with a changed conformation (Whisstock *et al.*, 1996). In addition, the rate-enhancing effect of heparin has been shown to be mediated through promoting the initial encounter between thrombin and AT, rather than affecting the rate of conversion of the intermediate complex to the stable thrombin-AT complex (Olson and Shore, 1982; Olson and Bjork, 1991b).

In summary, the accelerating effect of heparin on FXa inhibition by AT has been proposed to come mainly from the conformational activation of AT upon binding of the pentasaccharide. The major contribution to the rate enhancing effect of heparin on thrombin inactivation by AT, on the other hand, appears to result from the bridging by heparin of the ternary complex with thrombin and AT. The molecular basis for this difference has not been elucidated. In addition, heparin acceleration of the proteinase-AT reactions is catalytic rather than stoichiometric (Bjork and Nordenman, 1976). The catalytic feature results from an approximately 1000-fold decrease in the affinity of heparin for AT upon stable proteinase-AT complex formation (Jordan *et al.*, 1979; Carlstrom *et al.*, 1977). A similar decrease in heparin affinity occurs when the RCL of AT is cleaved (Bjork and Fish, 1982), or AT is exposed to mild denaturation (Fish *et al.*, 1985), or a complex between AT and its RCL peptide is formed (Bjork *et al.*, 1992). What is common to all these low affinity forms of AT is that their RCLs are inserted

into ß-sheet A, implying that loop insertion disrupts the high affinity interaction between the pentasaccharide and AT. This disrupture has actually been demonstrated in the latent form of AT (Skinner, *et al.*, 1997). As a result of the loop insertion, the side-chains of the key pentasaccharide binding residues Arg47, Lys125, and Arg129 are hydrogen bonded to other regions of the molecule and the side-chain of Lys114 points away from the pentasaccharide binding site (Fig. 1.6.b).

1.4.5. Roles of AT as a Regulator of *in vivo* Coagulation

Although AT attains its full anti-proteinase activity upon binding to heparin, therapeutically used heparin is not the natural activator of AT. Its nearest equivalent in the circulation is heparan sulphate, the side-chains of some endothelial glycoproteins that line the capillaries and sinusoids of the circulation. The structural distinctions between heparin and heparan sulphate are subtle. They are both composed of the same types of monosaccharide units joined by the same types of glycosidic linkages. Heparan sulphate contains the pentasaccharide sequence (Choay *et al.*, 1983; Lindahl *et al.*, 1984; Marcum *et al.*, 1984). Heparan sulphate is thus able to bind to AT; and to locate AT to the microvasculature that is most vulnerable to thrombosis. There is experimental evidence to suggest that heparan sulphate, synthesized by endothelial cells and expressed on the luminal surface of the endothelial cells, accelerates the rate of thrombin inhibition by AT

in vivo (Marcum *et al.*, 1983; 1984; 1986a; 1986b; Marcum and Rosenberg, 1984; 1985; Bauer and Rosenberg, 1991). A small fraction of plasma AT appears to be normally bound to a specific population of heparan sulphate proteoglycans on endothelial cells (Bauer and Rosenberg, 1991), apparently permitting a fraction of AT to be selectively activated at blood surface interfaces where proteinases of the coagulation cascade are commonly generated. It appears that AT is so critically placed that it may effectively neutralize those procoagulant proteinases at the sites of their generation. The physiological importance of localization of AT by heparan sulphate has been suggested by the clinical findings that individuals with inherited AT deficiency who have in their circulation only dysfunctional forms of AT deficient in heparin binding appear to have an increased risk for thrombolic disease (Hirsh *et al.*, 1989). Furthermore, the catalytic nature of the activation of AT by this specific set of heparan sulphate proteoglycans ensures the release of newly formed proteinase-AT complexes into the circulation for catabolic removal and continual regeneration of the nonthrombogenic properties of the endothelium.

1.5. Molecular Genetics of AT

1.5.1. AT Gene structure

The coding region of AT cDNA consists of an open reading frame (ORF) of 1392 nucleotides of which the first 96 encode the 32 amino acid signal

peptide and the next 1296 comprise codons for the 432 amino acid residues of the mature protein (Bock *et al.*, 1982; Prochownik *et al.*, 1983a; Stackhouse *et al.*, 1983). The gene for AT maps to the long arm of chromosome 1 at 1q23-25 (Lovrien *et al.*, 1978; Winter *et al.*, 1982; Kao *et al.*, 1984; Bock *et al.*, 1985). It occurs in a single copy on the haploid genome and is organized into seven exons and six introns (Prowchownik *et al.*, 1983a; Jagd *et al.*, 1985; Bock *et al.*, 1988). The gene spans 13477 base pairs (bp) from the transcriptional initiation site to the last nucleotide of the poly A tail and the nucleotide sequence of the gene has been completed (Olds *et al.*, 1993). Several sequence variations, i.e. polymorphisms, at the AT gene locus have been described (Prochownik *et al.*, 1983b; Bock and Levitan, 1983; Daly *et al.*, 1990; Daly and Perry, 1990; Lane *et al.*, 1991; 1993b). Two of them are PstI restriction fragment length polymorphisms (RFLP), and both PstI RFLPs are very useful in the diagnosis and the mapping of kindreds with AT deficiency (Prochownik *et al.*, 1983b; Bock *et al.*, 1985; Le Paslier et al., 1985).

1.5.2. Inherited AT Deficiency

Inherited AT deficiency is a heterogeneous group of disorders that manifests clinically with an increased risk of venous thromboembolic events in the affected individual. The prevalence of inherited AT deficiency in individuals with thromboembolic events has been estimated to be approximately 5% (Thaler and

Lechner, 1981; Pabinger *et al.*, 1992). In the general population, inherited AT deficiency has been estimated to affect from 1 in 2000 to 1 in 5000 individuals (Abilgaard, 1981; Thaler and Lechner, 1981; Winter *et al.*, 1982). It has been reported recently, however, that the incidence of AT deficiency may be higher than previously estimated. The prevalence of AT deficiency in normal individuals has been estimated, in a Scottish study of healthy blood donors, to be 1 in 250 (Tait *et al.*, 1994). In a similar Canadian study, it has been estimated to be approximately 1 in 500 (Wells *et al.*, 1994).

AT deficiency is inherited in an autosomal-dominant fashion and may be placed into two classes (Manson *et al.*, 1989; Lane *et al.*, 1991; Blajchman *et al*, 1992; Lane *et al.*, 1993; Perry, 1994). Type I the classical deficiency is characterized by a parallel reduction in AT antigenic and functional levels to approximately 50% of that observed in normal individuals, due to the absence of an AT translation product from one of the two autosomal AT alleles. This group of disorders is caused by a wide variety of heterogeneous molecular defects. These defects arise either through a complete or partial deletion of the gene or as a consequence of small insertion or point substitution mutations within the gene that prevent transcription, translation, secretion, or circulation of AT (Bock and Prochownik, 1987). In type II deficiency normal or near normal immunologic levels of AT are associated with decreased functional activity as a result of the presence of a nonfunctional variant in the circulation (Nagy and Lasonczy, 1979).

This type of deficiency is marked by the presence of a nonfunctional mutant AT molecule in the circulation. Such mutations can affect either the reactive centre region or the heparin binding site, or have pleiotropic effects.

1.5.3. Expression of Recombinant AT

The availability of AT cDNA clones has allowed the expression of recombinant AT from a variety of sources, including reticulocyte lysate cell-free systems (Austin *et al.*, 1990; Sheffield *et al.*, 1992; Wu *et al.*, 1992), bacteria (Bock *et al.*, 1982), yeast (Broker *et al.*, 1987), slime mold (Dingermann *et al.*, 1991), insect cells (Gillespie *et al.*, 1991; Kridel *et al.*, 1996), and cultured mammalian cells (Stephens *et al.*, 1987; Wasley *et al.*, 1987; Zettlmeisal *et al.*, 1989). In contrast to the bacteria and the cell-free systems which produce a nonglycosylated form of AT, all the other cells give rise to glycosylated products. Expression in cell culture systems of mammalian origin represents a more "natural" way of producing AT, although all expression systems are by definition artificial. The glycosylation in mammalian cell expressed protein shows a close similarity with that of the plasma AT, including incomplete glycosylation at Asn135 (Bjork *et al.*, 1992c; Fan *et al.*, 1993). Transient expression of AT in transformed African green monkey kidney (COS) cells has been shown to be a convenient tool when small amounts of recombinant AT present in the background proteins can be used to carry out the assay to answer the question asked in a particular study (Stephens

et al., 1987; 1988). Expression of AT in permanently transfected Chinese hamster ovary (CHO) cell lines yields high levels of AT (Stephens *et al.*, 1987; 1988). This allows a thorough physicochemical and kinetic assessment of the recombinant AT. It has been shown that the CHO-derived AT and plasma-derived AT did not differ significantly either in structure when analyzed by circular dichroism, ultraviolet absorbance, or fluorescence spectroscopy, nor in function in terms of heparin binding or the kinetics of thrombin inhibition. Permanent expression of AT in baby hamster kidney cells has also become a good way to characterize AT variants (Gettins *et al.*, 1992; Fan *et al.*, 1994a; Meagher *et al.*, 1996).

1.6. Objectives of the Current Study

AT is the most important physiological inhibitor of thrombin. AT thereby plays an essential role in the regulation of haemostasis. Such a role is clearly indicated by the predisposition to thromboembolism of individuals with AT deficiency. AT is also the major plasma cofactor of heparin. Heparin exerts its therapeutic effect primarily through its ability to increase substantially the rate of inactivation by AT of the procoagulant serine proteinases. Binding of heparin to AT is thus believed to be a prerequisite for this effect. Understanding the interaction between heparin and AT and its consequences, therefore, is a fundamental and important step towards elucidating the molecular mechanism of the rate enhancing effect of heparin. The latter in turn could lead to the

development of recombinant plasma-free products that could represent improvement in such therapeutic agents. Hopefully, this and related information will allow the identification of those individuals who are entering a clinically relevant prethrombotic state and to intervene with appropriate therapy before the onset of overt disease.

In this study, two hypotheses were proposed to explore the molecular details of pentasaccharide-AT and heparin-AT interactions. Hypothesis 1: Arg47 participates in the ionic interaction with heparin pentasaccharide, and therefore its positive charge is required for the binding of the pentasaccharide to AT and for the subsequent activation of AT by the pentasaccharide. Hypothesis 2: the pentasaccharide and full-length heparin, upon binding to AT, cause structural perturbations in AT that are transmitted to the RCL; and these two different heparin species induce different RCL conformations in AT, resulting in different inhibitory activities. To investigate these hypotheses, two specific objectives were set out. Objective 1: to test the consequences of alterations to Arg47 on the binding of the pentasaccharide to AT and the activation of AT by the pentasaccharide. Objective 2: to demonstrate the transmission of structural perturbations to the RCL of AT upon pentasaccharide and heparin binding and to differentiate the pentasaccharide- and heparin-induced conformations of the RCL of AT using an AT variant with a Pro397Trp substitution.

2. MATERIALS AND METHODS

2.1. Materials

Involved materials including those mentioned in the methods sections were all listed here. The location of the source of the companies was only presented when it was referred to at the first time.

2.1.1. General Chemicals and Reagents

Dimethyl sulphoxide (DMSO), di-sodium hydrogen orthophosphate (Na_2HPO_4), ethylenediaminetetraacetic acid (EDTA), phenylmethylsulfonyl fluoride (PMSF), polyethylene glycol (PEG) 8000, propan-2-ol, sodium acetate (NaOAc), sodium dihydrogen orthophosphate ($NaH_2PO_4.H_2O$), and urea were purchased from BDH Chemicals (Toronto, ON). Acrylamide, bromophenol blue, Coomassie brilliant blue R-250, glycine, N,N'-methylene-bis-acrylamide (BIS), N,N,N',N'-tetramethylethylenediamine hydrochloride (TEMED), tris(hydroxymethyl)aminomethane (Tris) were supplied by Bio-Rad Laboratories (Mississauga, ON). Electrophoresis grade agarose, ammonium persulphate (APS), dithiothreitol (DTT), SDS, ß-D-isopropyl-thiogalactopyranoside (IPTG), and 5-bromo-4-choloro-3-indolyl-ß-D-galactoside (X-gal) were Gibco Bethesda Research Laboratories (Gibco BRL) products from Life Technologies (Burlington, ON). Ethidium bromide (EtBr), 5-bromo-4-chloro-3-indolyl phosphate (BCIP), nitro

blue tetrazolium (NBT), and the phosphatase substrate, p-Nitrophenyl phosphate (PNPP), disodium, hexahydrate (Sigma 104^R phosphatase substrate), were obtained from Sigma Chemical Company (St. Louis, MO). All other chemicals and regents were of the highest purity commercially available.

2.1.2. Media and Regents for Cell Cultures

Dulbecco's modified eagle medium-low glucose without L-Gln, L-Met, or L-Cys (D-MEM-Gln$^-$Met$^-$Cys$^-$), qualified and heat-inactivated fetal bovine serum (FBS), geneticin^R selective antibiotic (G-418 sulphate), L-Gln-200 mM (100X), the lipofectin^R reagent, penicillin-streptomycin, and trypsin-EDTA (1X) (0.05% trypsin, 0.53 mM EDTA.4Na) were Gibco BRL products. Minimum essential medium α-medium (α-MEM), D-MEM, and sterile phosphate-buffered saline (PBS) were supplied from McMaster University (Hamilton, ON).

2.1.3. Radiochemicals

[^{35}S] deoxyadenosine 5'-(α-thio) triphosphate (dATP) was purchased from DuPont Canada (Mississauga, ON) through Mandel Scientific (Guelph, ON). For metabolic radiolabelling of the cultured COS-1 cells, the *in vitro* L-(^{35}S) cell labelling mix containing 70% L-[^{35}S] Met and 30% L-[^{35}S] Cys was obtained from Amersham Canada (Oakville, ON).

2.1.4. Enzymes

Restriction endonucleases and all other enzymes including lysozyme, RNase, T4 DNA kinase, and T4 DNA ligase were either from Pharmacia (Baie d'Urfe´, QC) or Gibco BRL products. The enzymes were stored and used in accordance with the manufacturers' instructions.

2.1.5. Oligodeoxyribonucleotides

The oligodeoxyribonucleotides designed as primers for both site-directed mutagenesis and DNA sequencing (listed in Table 2.1) were synthesized at the Institute for Molecular Biology and Biotechnology, McMaster University.

2.1.6. AT cDNA and Plasmid Vectors

A cDNA encoding the mature AT, cloned into the polycloing site of plasmid pGEM3Zf(+) between the restriction endonuclease sites EcoRI and Hind III, was a generous gift from Dr. R.C. Austin (McMaster University). This cDNA comprised of an ORF of His1 to Lys432 of the mature AT led by an initial Met codon. Most DNA manipulation was carried out with this cDNA within the plasmid pGEM3Zf(+) backbone, designed as pGEM3Zf(+)-$AT_{1\text{-}432}^{wt}$. In particular, this recombinant plasmid was used as a template for both *in vitro* site-directed mutagenesis and DNA sequencing. In order to create various AT expressing constructs, another AT cDNA whose ORF included the native 96

nucleotide secretory signal sequence was also employed in this study. This AT cDNA was cloned between the EcoRI and HindIII sites of the plasmid vector pGEM3Zf(+). This recombinant plasmid was designated as pGEM3Zf(+)-$AT_{-32-432}^{wt}$, and kindly provided by Dr. R.C. Austin also.

The plasmid pGEM3Zf(+) lacks the *rop* gene which normally lies close to the origin of DNA replication and participates in the control of copy number. As a result, it replicates to high copy numbers in its hosts. This vector expresses the N-terminal fragment of the *LacZ* gene product (ß-galactosidase) and displays α-complementation in appropriate hosts. Recombinants can thus be identified by histochemical screening. It also carries the ampicillin resistance gene. The expression of this gene allows bacteria that have been successfully transformed to be selected with ampicillin.

Mammalian expression plasmid vector pCMV5 was kindly provided by Dr. K. High (University of Pennsylvania, Philadelphia, PA). This plasmid carries the human cytomegalovirus (CMV) immediate early gene promoter which enables high expression of a foreign gene in many eukaryotic cultures. It has been used for expression of interested genes in both transiently transfected COS cells and permanently transfected CHO cell lines. The pCMV5 vector also carries the ampicillin resistance gene. Plasmid pSV2Neo contains a dominant geneticin resistance gene which can be expressed in eukaryotic cells. Introduction of this gene into cells can confer resistance to geneticin, enabling the cells to grow in

media containing geneticin.

2.1.7. Cell Lines

Subcloning efficiency competent *Escherichia Coli* (*E. coli*) DH5α cells were a Gibco BRL product. These cells were used for routine transformations for the purpose of manipulation of plasmid DNA. After transformation, transformed cells were selected on Lauria-Bertani Broth (LB)-agar plates [1.5% (w/v) bacto-agar in LB medium comprised of 1% (w/v) bacto-tryptone, 0.5% (w/v) bacto-yeast extract, 1% (w/v) NaCl, pH 7.5] containing a selective antibiotic. Since both pGEM3Zf(+) and pCMV5 carry the ampicillin resistance gene, 100 μg/ml ampicillin was supplemented into the LB-agar plates for selection of transformed resistant bacteria. Transformed cells were then routinely grown at 37 °C with shaking in LB medium in the presence of 100 μg/ml ampicillin. Competent *E. coli* BMH 71-18 *mutS* cells were a Clontech Laboratories (Palo Alto, CA) product purchased through Bio/Can Scientific (Mississauga, ON). This strain of *E. coli* was defective in mismatch repair and thus suitable for facilitating the enrichment of the mutated, mismatched plasmid.

The Pro-5 (Ovary, proline auxotrophy, Chinese hamster) was a clonal derivative of the original Chinese hamster ovary cell line CHO. One of the advantages of this line was that it could be maintained in either a suspension or monolayer system. This feature facilitated the amplification of the culture to a

large scale to produce large quantities of AT sufficient for its purification and further extensive characterization. COS-1 (Kidney, SV40 transformed, African green monkey) was a fibroblast-like cell line established from CV-1 simian cells which were transformed by an origin-defective mutant of simian virus 40 (SV40). These COS cells express high levels of the SV40 large tumour (T) antigen, required for initiating viral DNA replication. The T antigen-mediated replication can amplify the plasmid copy number to a great extent, allowing high expression of the transfected DNA. Both the Pro-5 CHO and COS-1 were cell repository lines from American Type and Culture Collection (Rockville, MD).

2.1.8. Protein Standards

The low range prestained SDS-PAGE standards were from BioRad Laboratories. These protein standards (kDa) were used for molecular mass determination on SDS-PAGE. They included 104, rabbit muscle phosphorylase B; 80, bovine serum albumin; 46.9, chicken egg white ovalbumin; 33.5 bovine erythrocyte carbonic anhydrase; 28.3, soybean trypsin inhibitor; and 19.8, chicken egg white lysozyme.

2.1.9. Other Materials

All solutions were made with deionized and distilled water (dd H_2O). All labwares for manipulations of DNA and cell cultures were sterilized by

autoclaving. All solutions for manipulation of DNA and cell cultures were sterilized either by autoclaving or by filtering through a 0.2 μm sterilization filter unit from Nalgene (Rochester, NY; distributed by VWR Canlab, Mississauga, ON). Amplify™, the flurographic reagent for the treatment of polyacrylamide gels, was from Amersham Canada. The FXa inhibitor 1,5-dansyl-glu-gly-arg chloromethyl kekone, dihydrochloride (1,5-DNS-GGACK, HCl), the thrombin inhibitor D-phe-L-propyl-arg chloromethyl kekone (PPACK), and Omnisorb™ cells were from Calbiochem (La Jolla, CA). The Transformer™ site-directed mutagenesis kit was from Clontech Laboratories. The 1kb DNA ladder suitable for sizing linear ds DNA fragments from 500 bp to 12 kb was a Gibco BRL product. Adenosine 5'-triphosphate (ATP), CNBr-activated Sepharose 4B, Hitrap^R heparin, Q-Sepharose^R fast flow, Sephaglas™ BandPrep kit, and the ^{T7}Sequencing™ kit were from Pharmacia. QIAGEN^R plasmid maxi kit was from QIAGEN (Chatsworth, CA). Bovine serum albumin (BSA), ampicillin sodium salt used for selection of resistant bacteria, and heparin sodium salt were obtained from Sigma Chemical Company. Affinity-purified sheep anti-human AT IgG was prepared by Mr. M. Kulczyky in our laboratory. This IgG was used as the primary antibody in Western blotting and employed in immunoprecipitation as well as in an enzyme-linked immunosorbent assay (ELISA). This IgG was biotinylated in accordance with the manufacturers' instructions; the biotinylated IgG was also used in the ELISA. The affinity-purified antigen specific antibody rabbit anti-

sheep IgG (H+L)-alkaline phosphatase (AP) conjugate served as the secondary antibody in Western blotting was from Zymed laboratories (Burlingame, CA). S&S NC™ nitrocellulose was purchased from Schleicher & Schuell (Keene, NH). Spectro/Por® molecularporous membrane tubings with a molecular weight cut-off (MWCO) of 1000 and a MWCO of 12000-14000, respectively, were from Spectrum medical industries Inc. (Houston, Texas). Human AT, thrombin, and FXa exclusively were used in this study. AT was obtained from Cutter Biologicals (Elkhart, IN). α-thrombin was a generous gift from Dr. J. Fenton (New York State Division of Biologicals, Albany, NY). FXa was kindly provided by Dr. F. Ofosu (McMaster University).

2.1.10. Apparatus

Precision pipettes (Pipetman P20, P200, P1000) were purchased from Gilson through Mandel Scientific. Accumet™ pH meter model 620 was from Fisher Scientific (Pittsburgh, PA). Sorvall™ RC-5 superspeed refrigerated centrifuge and Sorvall™ RT6000B refrigerated centrifuge were from DuPont Canada. Eppendorf® micro centrifuge model 5415C was from Brinkmann (Mississauga, ON). The centrifugal concentrators, Centriprep-10 and Centricon-10, were from Amicon (Beverly, MA). Hoefer HE 33 mini and Hoefer HE 99X max submarine electrophoresis units were from Pharmacia. Fotodyne™ transilluminator Foto/prep I and Fotodyne™ polaroid camera were purchased

through Bio/Can Scientific. Model S2 sequencing gel electrophoresis apparatus was a Gibco BRL product, electrophoresis constant power supply ECPS 3000/150 was from Pharmacia, and model 583 gel dryer was from Bio-Rad. Mini-PROTEIN II electrophoresis cell suitable for SDS-polyacrylamide gel electrophoresis (SDS-PAGE) with discontinuous buffer systems and mini trans-blot electrophoretic transfer cell for transfer of proteins from SDS-polyacrylamide gel to solid support were from Bio-Rad. Electrophoresis power supply EC-105, used for agarose and SDS-polyacrylamide gel electrophoresis as well as protein transfer, was purchased through Mandel Scientific. Prep/Scale^{TM}-TFF 1 ft^2 cartridge (PLTK 30 K regenerated cellulose) and MasterFlex^R industrial/process Easy-Load^R pump were from Millipore (Mississauga, ON). Peristaltic pump P-1, RediFrac fraction collector, and Gradient mixer GM-1 were from Pharmacia. Fluorescence measurements were made on a luminescence spectrometer LS 50 from Perkin Elmer (Mississauga, Ontario) and was made available for use by Dr. V.S. Ananthanarayanan (McMaster University).

2.1.11. Software

The scientific Fig.Processor, Fig.P^R (version 6.0), was a product of the Fig.P software corporation (Durham, NC) distributed by Biosoft (Ferguson, MO). Minitab^{TM} (version 8.0) was from Minitab Inc. (State college, PA). SigmaPlot^R scientific graphing software was from Jandel Scientific Software (San Rafal, CA).

2.2. Construction of Mammalian Expression Plasmids

2.2.1. Transformation of *E. Coli* Cells with Plasmids

E. coli cells were routinely transformed according to the manufacturer's protocol. Briefly, 50 μl of competent cells was incubated with 10-20 ng plasmid DNA on ice for 30 min, followed by heat shock at 37°C for 20 s. After standing on ice for 2 min, 1 ml of LB medium was added and the cells were allowed to recover at 37°C for 1 h with shaking. The cells were collected by centrifugation and resuspended in 110 μl of LB medium. 10 μl of cell suspension supplied with 90 μl of LB medium and the remaining 100 μl of the cell suspension were then spread onto LB plates containing 100 μg/ml ampicillin, respectively. These plates were incubated at 37°C overnight. After characterization, the desired individual transformants were cultured and stored at -70°C in the presence of DMSO, following quick freezing in liquid N_2.

2.2.2. Isolation of Plasmid DNA from Transformed *E. Coli* Cells

Plasmid DNA was routinely used for sequencing, restriction analysis, and transformation. For such tasks, plasmid DNA was isolated from transformed *E. coli* cells in a small scale using a modified alkaline lysis miniprep method (Zhou *et al.* 1990). Briefly, cells from a 1.5 ml of overnight culture were harvested by centrifugation and resuspended in 100 μl of LB medium. 300 μl of a freshly prepared alkaline solution TENS [10 mM Tris-HCl, 1 mM EDTA, 0.1

N NaOH, and 0.5% (w/v) SDS] was added to the resuspended cells, followed by the addition of 150 μl of 3.0 M NaOAc [pH 5.2]. Precipitated chromosomal DNA and cell debris were discarded following centrifugation, and the supernatant was mixed with 0.9 ml of ethanol which had been prechilled to -20°C. Plasmid DNA and RNA were then pelleted by centrifugation. The pellet was washed twice with 1 ml of 70% ethanol, dried under vacuum for 2-5 min, and resuspended in 20 μl of TE buffer [10 mM Tris-Cl, 1 mM EDTA, pH 8.0] containing 25-50 μg/ml RNase.

Plasmid DNA used for subcloning and transfecting mammalian cells was prepared using the QIAGEN^{R} plasmid kit. *E. coli* DH5α cells, transformed by various recombinant pGEM3Zf(+) or pCMV5 plasmids, were cultured overnight in 125 ml of LB medium. A modified alkaline lysis procedure was applied initially, followed by binding of plasmid DNA to QIAGEN anion-exchange resin under appropriate low salt and pH conditions. RNA, proteins, and low molecular weight impurities were removed by a medium salt wash. The bound plasmid DNA was eluted with a high salt buffer. Finally, the isolated plasmid DNA was concentrated and desalted by isopropanol (propan-2-ol) precipitation, and resuspended in 50-100 μl of TE buffer.

2.2.3. Quantitation and Agarose Gel Electrophoresis of DNA

Two types of methods were used to measure the amount of DNA in a

preparation (Sambrook *et al.*, 1989a). Quantitation of a concentrated, pure DNA sample was determined by spectrophotometric measurement of the amount of ultraviolet (UV) irradiation absorbed by the base. An aliquot of 1-10 μl of the sample was diluted to 1 ml in dd H_2O, and the optical density (OD) readings were taken at 260 nm and 280 nm. The concentration of DNA was calculated on the assumption that an OD_{260} of 1 corresponded to approximately 50 μg/ml for double-stranded (ds) DNA. An estimate of the purity of the DNA was provided by the ratio between the readings at 260 nm and 280 nm (OD_{260}/OD_{280}). For a dilute DNA sample or a sample containing significant amounts of impurities, quantitation was determined from the intensity of the UV-induced fluorescence emitted by EtBr intercalated into the DNA. Since the amount of fluorescence was proportional to the total mass of DNA, the amount of DNA in the sample was estimated by a comparison of the fluorescence yield of the DNA with that of a series of standards following electrophoresis on agarose gel containing EtBr.

The standard method used to separate, identify, and purify DNA fragments was electrophoresis through agarose gels. Gel preparation and gel electrophoresis was performed essentially as described by Maniatis *et al.* (1982). A 1% (w/v) agarose solution in 1X TAE (40 mM Tris-acetate, 1 mM EDTA) was prepared by heating to 100°C. When it was cooled to approximately 50°C, the fluorescent dye EtBr was added to a final concentration of 0.5 μg/ml to enable the visualization of the elctrophoresized DNA fragments. DNA samples were

prepared by mixing with 5 volumes of 6X DNA loading buffer [0.25% (w/v) bromophenol blue, 0.25% xylene cyanol, and 40% (w/v) sucrose in 6X TAE buffer], and electrophoresized in 1X TAE at 40 V for 2-4 h. The separated DNA bands were visualized and photographed.

2.2.4. Extraction of Individual DNA Bands From Agarose Gels

Extraction of individual DNA bands from agarose gels following electrophoresis was carried out using Sephaglas™ BandPrep kit as instructed by the manufacturer. Basically, the agarose slice containing the DNA band to be extracted was solubilized in sodium iodide. Sephaglas™ BandPrep was added to allow the binding of the DNA fragment. The matrix-bound DNA was then washed with a buffered ethanol wash buffer and allowed to air-dry. Finally, the DNA was recovered from the dry matrix in an elution buffer of low ionic strength. The resulting DNA was ready for subsequent enzymatic manipulation.

2.2.5. *In Vitro* Site-directed Mutagenesis

In vitro site-directed mutagenesis was carried out as outlined in the transformer™ site-directed mutagenesis kit (see Fig. 2.1) based on the method of Deng and Nickoloff (1992). Plasmid pGEM3Zf(+)-$AT_{1\text{-}432}^{wt}$ was used as the template. Following denaturation of the ds DNA plasmid, two oligodeoxynucleotide primers, a mutagenic and a selection primer, were annealed

Fig. 2.1. Schematic representation of the strategy used for generating specific base changes of AT cDNA at Arg47 and Pro397, respectively.

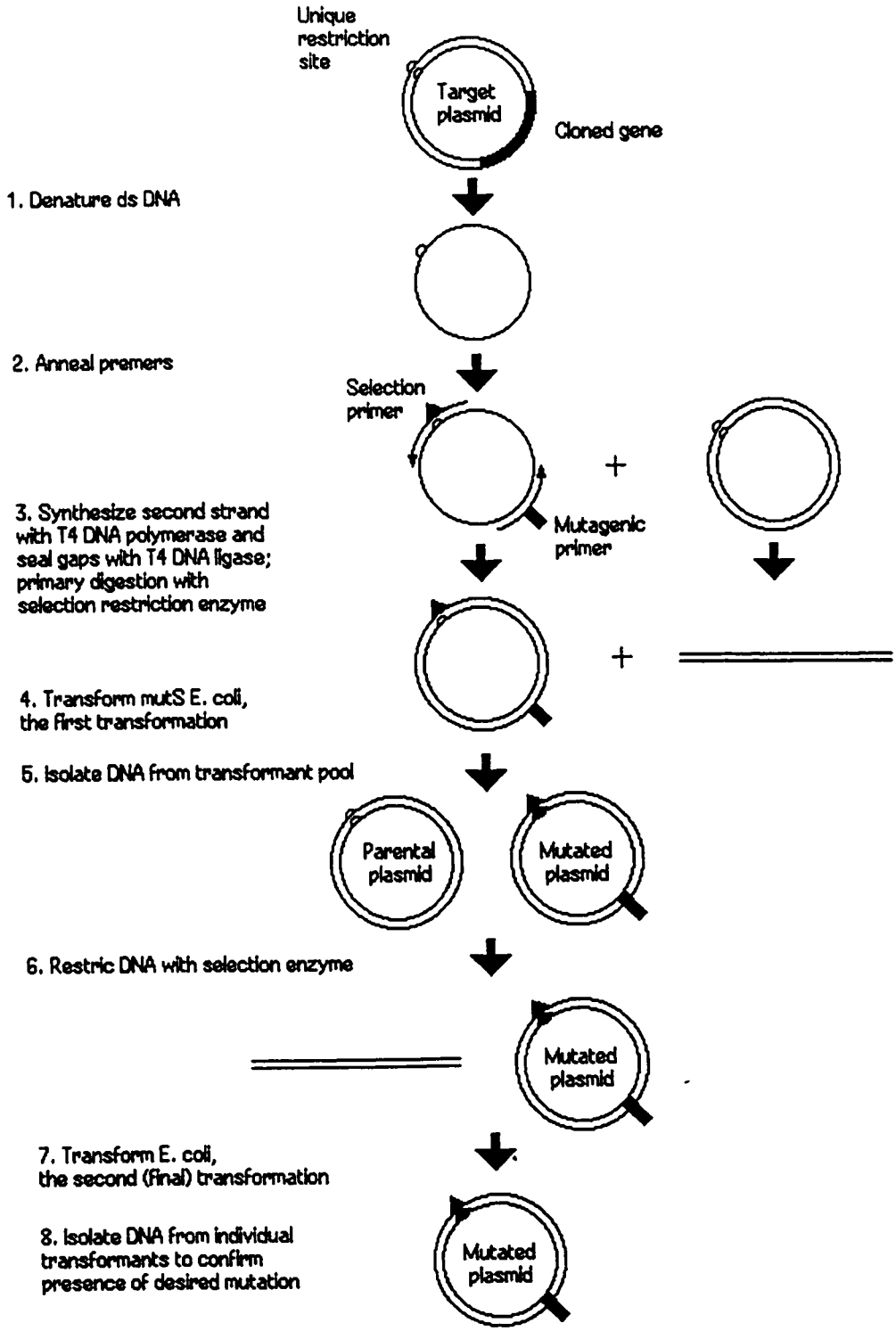
Unique restriction site
Target plasmid
Cloned gene
1. Denature ds DNA
2. Anneal premers
Selection primer
Mutagenic primer
3. Synthesize second strand with T4 DNA polymerase and seal gaps with T4 DNA ligase; primary digestion with selection restriction enzyme
4. Transform mutS E. coli, the first transformation
5. Isolate DNA from transformant pool
Parental plasmid
Mutated plasmid
6. Restric DNA with selection enzyme
Mutated plasmid
7. Transform E. coli, the second (final) transformation
8. Isolate DNA from individual transformants to confirm presence of desired mutation
Mutated plasmid

simultaneously to one strand of the denatured template. While the mutagenic primer introduces the desired mutation, the selection primer carries the substitution of a unique restriction site with another. To create AT moieties with substitution mutations at Arg47, two mutagenic primers, AB2302 and AB3216 (see table 2.1 for sequence), were designed. In AB2302, a random insertion at the first two positions of codon 47 confers 15 possible codons, namely Ala, Asn, Asp, Cys, Gly, His, Ile, Leu, Phe, Pro, Ser, Thr, Tyr, Val, and the wt Arg. The degenerative primer AB3216 potentially codes Asn, Asp, Glu, and Lys. To generate Pro397Trp moiety, the oligodeoxynucleotide AB2301 (see table 2.1 for sequence), in which the Pro397 codon CCC was substituted with the Trp codon TGG, was employed as the mutagenic primer. In all mutagenesis reactions, oligodeoxynucleotide AB3374 was used as the selection primer conveying the replacement of the restriction EcoRI site by EcoRV site. After standard DNA elongation and ligation, a selective restriction digestion by EcoRI was performed to linearize the unmutated DNA. Such treated DNA was transformed into *E. coli* BMH 71-18 *mutS* cells. Since the linearized plasmid was 100-fold less efficient in transformation and the BMH 71-18 *mutS* cell was defective in DNA mismatch repair, a primary selection in favour of the mutated DNA was thus achieved. The pooled transformants were then amplified. Plasmid DNA was extracted from the mixed population and restricted by EcoRI. To enrich for, amplify, and clone the mutated plasmid, transformation of *E. coli* DH5α cells was then followed. Finally,

Table 2.1. The oligodeoxyridonucleotides designed and employed as primers for site-directed mutagenesis and DNA sequencing. The underlined bases indicate a mismatch with the wt sequence. Letter "N" in AB2302 represents a random insertion of A, C, G, or T. A/G and A/C in AB3216 symbolize a random insertion of A or G and A or C, respectively.

Name	Sequence	Description
AB1594	5'-GATGCATTCCATAAGGC-3'	sequencing primer annealing to codons 366-371
AB2301	5'-TCGCTAAACTGGAACAGGGTG-3'	mutagenic primer for Pro397Trp
AB2302	5'-ACCAACCGGNNTGTCTGGGAA-3'	mutagenic primer for Arg47X
AB2802	5'-GAATTCATTTACCGCTCCCCGGAG-3'	sequencing primer annealing to codons 22-27
AB3216	5'-ACCAACCGGA/GAA/CTGGGAA-3'	mutagenic primer for Arg47X
AB3374	5'TATAGGGCGATATCGAGCTCGC-3'	selection primer for EcoRV site

plasmid DNA was extracted from individual transformants and the presence of the intended mutations was confirmed by DNA sequencing analysis with primer AB2802 for the Arg47 variants and AB1594 for the Pro397Trp moiety (see table 2.1 for primer sequence).

2.2.6. Dideoxy Chain-termination Sequencing of DNA

To confirm the introduction of the desired mutations in AT cDNA, interested regions were sequenced using the ^{T7}Sequencing^{TM} kit, based using on the dideoxy sequencing method of Sanger *et al.* (1977). The basis of this dideoxy sequencing was base-specific termination of enzyme-catalyzed primer-extension reactions. Six steps were involved in sequencing DNA with T7 DNA polymerase and a radioactive label. (1). Preparation of template DNA. ds plasmid DNA was extracted from transformed *E. coli* cells as described previously. The template was then denatured to single-stranded DNA for the sequencing reaction to take place. (2). Annealing of a primer to the template. Such annealing took place adjacent to the target sequence. In this study, interested regions of AT cDNA were sequenced from specific internal AT primers available in the laboratory (see table 2.1 for sequence). (3). Labelling reaction. T7 DNA polymerase-catalyzed extension of the primer was initiated in the presence of limiting concentrations of all four deoxynucleotides of which dATP was radiolabelled with ^{35}S. (4). Termination reaction. The labelled and extended primer from the labelling

reaction was terminated in four separate reactions, each contained a specific dideoxynucleotide in addition to all four deoxynucleotides. (5). Electrophoresis. The chain-terminated reaction products were elctrophoresized in four adjacent lanes of a thin polyacrylamide gel under denaturing conditions. The sequencing gel was composed of 8% (w/v) acrylamide [the 40% stock solution contained 38% (w/v) acrylamide and 2% (w/v) BIS], 8 M urea in 1X TBE [89 mM Tris-Cl, 89 mM Boric acid, 2 mM EDTA, pH 8.0], and gel formation was initiated by 0.05% APS (w/v) and 0.05% TEMED. Electrophoresis was carried out at a constant power of 50 W for approximately 2 h per loading. (6). Autoradiography. After electrophoresis, the sequencing gel was transferred to Whatman 3MM chromatography paper and dried under vacuum at 80°C for 2 h on a gel dryer. The dried gel was then wrapped with X-ray film and exposed for approximately 20 h. Finally, the film was developed and DNA sequencing was read carefully.

2.2.7. Construction of AT-expressing Plasmids in pCMV5

To create AT expressing constructs, various AT cDNAs were liberated from their plasmid backbone, pGEM3Zf(+), and subcloned into mammalian expression plasmid vector pCMV5 between the EcoRI and HindIII sites at its polycloning site. The construct that allows expression of wt AT was designated as pCMV5-$AT_{-32-432}^{wt}$. To generate this construct, plasmids pGEM3Zf(+)-$AT_{-32-432}^{wt}$ and pCMV5 were restriction digested with EcoRI and HindIII, respectively

(see Fig. 2.2). Such restriction digestion linearized pCMV5 and released the AT cDNA insert from its plasmid backbone pGEM3Zf(+). The restricted AT cDNA and pCMV5 were purified using Sephaglas™ BandPrep Kit as described above, and joined together by T4 DNA ligase to assemble the pCMV5-$AT_{-32-432}^{wt}$ construct. Ligation was carried out at 4°C overnight in One Phor All^{R} buffer supplemented with 1 mM ATP. A portion of the ligation reaction mixture was then used to transform *E. Coli* DH5α cells. The desired plasmid with the desired insert was first confirmed by restriction enzyme mapping and then by DNA sequencing analysis.

To construct the AT Pro397Trp variant expressing plasmid, three plasmids, namely pGEM3Zf(+)-$AT_{-32-432}^{wt}$, pGEM3Zf(+)-$AT_{1-432}^{Pro397Trp}$, and pCMV5 were enzymatically manipulated (see Fig. 2.3). Plasmids pGEM3Zf(+)-$AT_{-32-432}^{wt}$ and pGEM3Zf(+)-$AT_{1-432}^{Pro397Trp}$ were digested first with NsiI and HindIII, respectively. Since NsiI cleaved AT cDNA once at codon 367 and HindIII cleaved plasmid pGEM3Zf(+) once at the polycloning site downstream AT cDNA, restriction digestion of pGEM3Zf(+)-$AT_{-32-432}^{wt}$ with NsiI and HindIII yielded pGEM3Zf(+)-$AT_{-32-367}^{wt}$. Meanwhile, the same restriction digestion of pGEM3Zf(+)-$AT_{1-432}^{Pro397Trp}$ released a portion of the AT cDNA insert corresponding to $AT_{367-432}^{Pro397Trp}$ from its plasmid backbone pGEM3Zf(+). These two fragments were ligated and the resultant plasmid pGEM3Zf(+)-AT-32-432Pro397Trp was restriction digested with EcoRI and HindIII. The liberated

Fig. 2.2. Schematic representation of the strategies used to construct the pCMV5 plasmid expressing wt AT, pCMV5-$AT_{-32-432}^{wt}$. To create the pCMV5-$AT_{-32-432}^{wt}$ construct that allows expression of wt AT, plasmids pCMV5 and pGEM3Zf(+)-$AT_{-32-432}^{wt}$ were restriction digested with EcoRI and HindIII, respectively. Ligation of the restricted AT cDNA and pCMV5 assembled the desired plasmid.

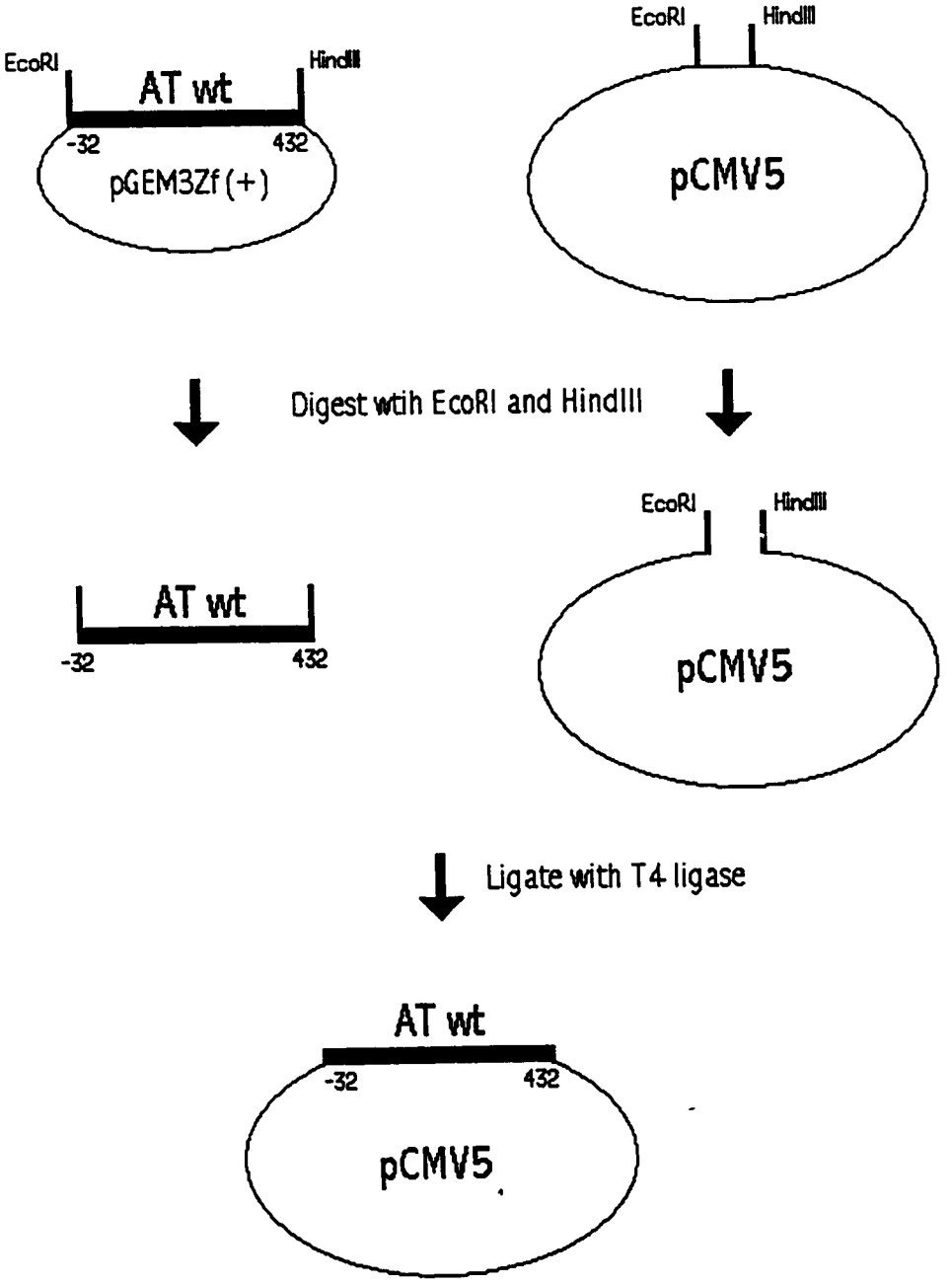
EcoRI
HindIII
AT wt
-32
432
pGEM3Zf(+)
EcoRI
HindIII
pCMV5
Digest wtih EcoRI and HindIII
AT wt
-32
432
EcoRI
HindIII
pCMV5
Ligate with T4 ligase
AT wt
-32
432
pCMV5

Fig. 2.3. Schematic representation of the strategies used to construct the pCMV5 plasmid expressing the AT Pro397Trp variant, pCMV5-$AT_{-32-432}^{Pro397Trp}$. To create this construct, three plasmids, namely pGEM3Zf(+)-$AT_{-32-432}^{wt}$, pGEM3Zf(+)-$AT_{1-432}^{Pro397Trp}$, and pCMV5, were enzymatically manipulated. While restriction digestion of pGEM3Zf(+)-$AT_{-32-432}^{wt}$ with NsiI and HindIII generated pGEM3Zf(+)-$AT_{-32-367}^{wt}$, the same restriction digestion of pGEM3Zf(+)-$AT_{1-432}^{Pro397Trp}$ produced $AT_{367-432}^{Pro397Trp}$. Ligation of these two fragments assembled plasmid pGEM3Zf(+)-$AT_{-32-432}^{Pro397Trp}$. Subsequent restriction digestion of this plasmid with EcoRI and HindIII liberated $AT_{-32-432}^{Pro397Trp}$ cDNA, which was then inserted into the pCMV5 between the EcoRI and HindIII sites.

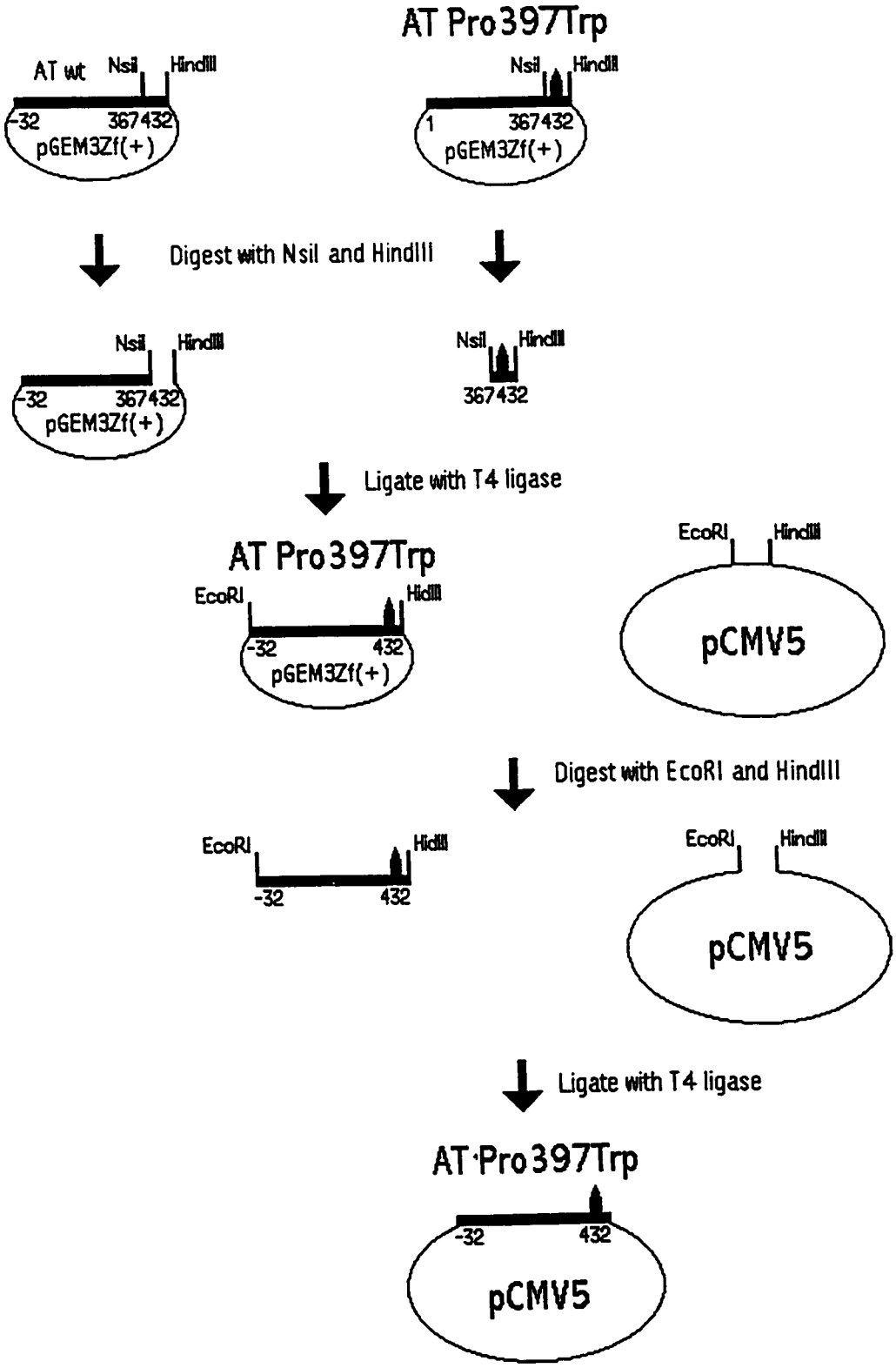
AT wt
NsiI
HindIII
-32
367432
pGEM3Zf(+)
AT Pro397Trp
NsiI
HindIII
1
367432
pGEM3Zf(+)
Digest with NsiI and HindIII
NsiI
HindIII
-32
367432
pGEM3Zf(+)
NsiI
HindIII
367432
Ligate with T4 ligase
AT Pro397Trp
EcoRI
HidIII
-32
432
pGEM3Zf(+)
EcoRI
HindIII
pCMV5
Digest with EcoRI and HindIII
EcoRI
HidIII
-32
432
EcoRI
HindIII
pCMV5
Ligate with T4 ligase
AT·Pro397Trp
-32
432
pCMV5

$AT_{-32-432}^{Pro397Trp}$ cDNA was then inserted into the pCMV5 between the EcoRI and the HindIII sites to generate the expression construct pCMV5-$AT_{-32-432}^{Pro397Trp}$.

The expression plasmids differing from the pCMV5-$AT_{-32-432}^{wt}$ at codon 47 were denoted as pCMV5-$AT_{-32-432}^{Arg47X}$, where X represents the three-letter code for the mutant amino acid residue. To construct this set of recombinant plasmids, pGEM3Zf(+)-AT_{1-432}^{Arg47X} and pCMV5-$AT_{-32-432}^{wt}$ were digested with SacII and HindIII, respectively (see Fig. 2.4). Since SacII cleaved AT cDNA once at codon 12 and HindIII cleaved the plasmid pGEM3Zf(+) once at the polycloning site downstream AT cDNA, digestion of pCMV5-$AT_{-32-432}^{wt}$ with NsiI and HindIII produced pCMV5-AT_{-32-12}^{wt}. This fragment contained the plasmid pCMV5 and a minor portion of the AT cDNA, AT_{-32-12}^{wt}. Similarly, restriction digestion of pGEM3Zf(+)-AT_{1-432}^{Arg47X} released a major portion of the insert corresponding to AT_{12-432}^{Arg47X} from its plasmid backbone pGEM3Zf(+). Subsequent ligation of these two fragments assembled the various desired expressing plasmid constructs, pCMV5-$AT_{-32-432}^{Arg47X}$.

2.3 Expression of AT in Transfected Mammalian Cells

Unless otherwise indicated, manipulations of cell cultures in 100-mm and 150-mm plates were carried out with a 10-ml and a 25-ml volume, respectively.

Fig. 2.4. Schematic representation of the strategies used to construct the pCMV5 plasmids expressing the AT Arg47 variants, pCMV5-$AT_{-32-432}^{Arg47X}$. To create the set of pCMV5-$AT_{-32-432}^{Arg47X}$ constructs, pCMV5-$AT_{-32-432}^{wt}$ and pGEM3Zf(+)-AT_{1-432}^{Arg47X} were digested with SacII and HindIII, respectively. Such restriction digestion of pCMV5-$AT_{-32-432}^{wt}$ generated pCMV5-$AT_{-32-12}^{wt,}$ while the same restriction digestion of pGEM3Zf(+)-AT_{1-432}^{Arg47X} yielded AT_{12-432}^{Arg47X}. Subsequent ligation of these two fragments produced the desired plasmid.

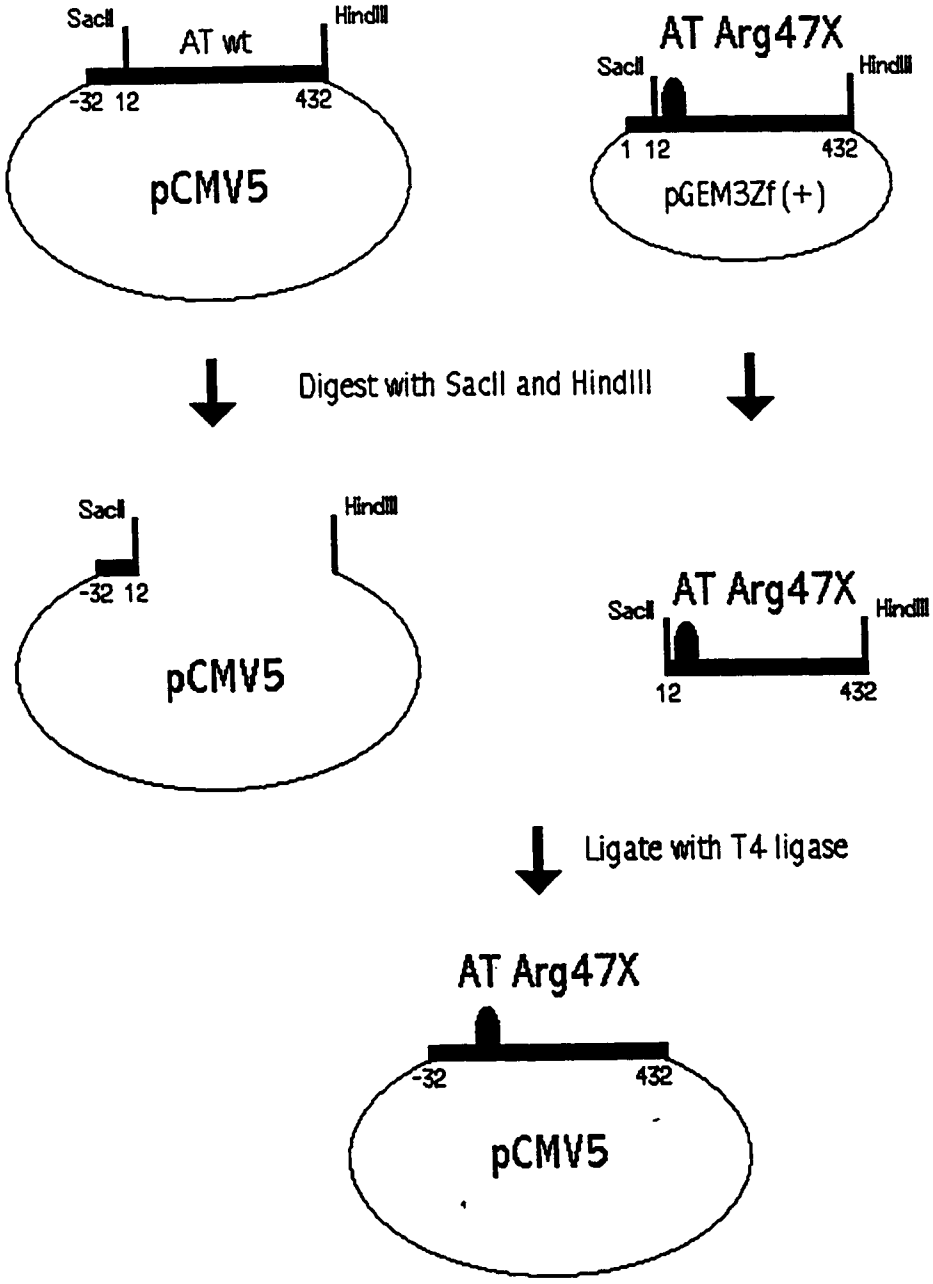
SacII
AT wt
HindIII
-32 12
432
pCMV5
AT Arg47X
SacII
HindIII
1 12
432
pGEM3Zf(+)
Digest with SacII and HindIII
SacII
HindIII
-32 12
pCMV5
AT Arg47X
SacII
HindIII
12
432
Ligate with T4 ligase
AT Arg47X
-32
432
pCMV5

2.3.1. Expression of AT in Transiently Transfected COS-1 cells

Various AT moieties were expressed in transiently transfected COS-1 cells in both radioactive and non-radioactive forms. To express wt AT and its variants, COS-1 cells were transiently transfected with the various pCMV5 mammalian expression constructs, respectively. Transfection of plasmid DNA into COS-1 cells were carried out employing the lipofectin^R reagent. Briefly, COS-1 cells were grown in monolayer in 100-mm plates in D-MEM supplemented with 10% FBS and 1% penicillin-streptomycin. Transfection was initiated when the cultured cells reached 70-80% confluency. These cells were washed twice with sterile PBS. 10 μg plasmid DNA and 50 μg the lipofectin^R reagent were diluted in 5 ml of D-MEM without serum, respectively. The two were combined and then added slowly to the washed cells. After a 4-6 h incubation, the lipofectin-DNA containing medium was removed. In order to obtain radioactive AT proteins, these cells were washed and allowed to recover for 36-40 h in D-MEM supplemented with serum and antibiotics. To increase the efficiency of incorporation of the radiolabelled amino acids, the intracellular pools of these amino acids were depleted before the metabolic radiolabelling took place. Following two washes with PBS and one wash with D-MEM depleted of Met and Cys [D-MEM-Gln$^-$Met$^-$Cys$^-$ supplemented with 2 mM Gln], cells were incubated in Met and Cys deficient medium for 30 min. The starved cells were then washed and fed with 200 μCi of ^{35}S-labelled Met and Cys (from the *in vitro* L-(^{35}S) cell

labelling mix) in 3 ml of D-MEM-Met$^-$Cys$^-$ for 3 h. Finally, the conditioned medium of the radiolabelled cells was harvested, clarified by centrifugation, aliquoted, and frozen at -70 °C until analyzed. For producing non-radioactive AT proteins, cells were allowed to recover for 20-24 h in the serum containing medium. The serum containing medium was replaced by serum free medium following three washes with PBS. Cells were incubated for 24 h prior to harvesting the medium. The clarified conditioned medium was concentrated using a concentrator with a MWCO of 10000. The endogenous heparin-like species were removed by the Probe-Tek heparin adsorbent and the adsorbent subsequently removed by centrifugation. AT concentration in the conditioned medium was determined by a capture ELISA.

2.3.2. Establishment of Permanent AT-producing CHO Cell Lines

To establish CHO cell lines that could produce AT permanently, a mammalian expression plasmid and a Neo-resistant plasmid were cotransfected into the CHO cells employing the lipofectin^R reagent. Stably transfected cells were selected by geneticin and then screened for AT expression levels by an ELISA. Subsequently, the high AT producers were subcloned by the limited dilution method. Finally, the three highest AT producers for each of the AT moieties were chosen for further expansion.

Practically, monolayer of CHO cells were maintained in 100-mm plates

in α-MEM supplemented with 10% FBS and 1% penicillin-streptomycin. The cultured cells were cotransfected at 30-40% confluency with 10 μg plasmid pCMV5 and 1 μg plasmid pSV2Neo in the presence of 50 μg the lipofectin^R reagent. Following a 24 h recovery after the transfection, such treated cells were split 1:10 and geneticin was added to the medium at a concentration of 1 mg/ml. Stably transfected cells were selected by resistance to geneticin. After a 10-12 day selection with geneticin, each individual geneticin resistant colony was picked up with the aid of a glass cylinder. Briefly, the cylinder was glued to the plate around the individual colony which was to be picked up. The cells within the cylinder were detached by trypsinization, and transferred to a 24-well tissue plate and then a 60-mm plate. These transfected cells then were cultured using the selection pressure of 0.25 mg/ml geneticin. To screen their AT production levels, they were incubated in serum free medium for 24 h and the conditioned medium was assayed for AT by an ELISA. Subsequently, the two high producers for each AT moiety were subcloned by limited dilution. Practically, each was diluted to 1-10 cells per well in a 96-well tissue plate. 60 fast-growing colonies were expanded and their AT expression levels again checked by an ELISA. The three high producers were then clonally expanded and stored in liquid N_2 in α-MEM in the presence of 20% FBS and 10% DMSO.

2.3.3. Expression of AT in Permanently Transfected CHO Cells

Amplification of permanently transfected CHO cell cultures to a large scale in suspension facilitated the production of wt AT and its Pro397Trp variant in large quantities which, in turn, enabled the purification and extensive characterization of these AT moieties. Basically, high AT producer cells were grown in 100-mm plate in α-MEM containing 10% FBS, 1% penicillin-streptomycin, and 0.25 mg/ml geneticin to 90-95% confluency. Cells from two such plates were transferred into five 150-mm plates. When cells reached 90-95% confluency, they were washed with PBS, trypsinized, and collected by centrifugation. After another wash with PBS, all cells were transferred to a spinner flask containing 500 ml of serum free medium and AT was allowed to be expressed and secreted into the serum free medium for 60 h. The conditioned medium was then collected by centrifugation and the supernatant stored at -70°C until required for purification.

2.4. Characterization of Recombinant AT

2.4.1. Analysis of COS-produced Radioactive AT by Immunoprecipitation

Immunoprecipitation coupled with SDS-PAGE was used to detect and analyze target antigens, the COS-produced radioactive AT, in mixtures of proteins because of its extreme selectivity. In this case, immunoprecipitation involved binding the recombinant AT to the sheep anti-human AT IgG; precipitating the antigen-antibody complex by the Omnisorb™ immunoadsorbent cells, a

preparation of heat-inactivated, formalin-fixed, and protein G-bearing *Staphylococcus aureus* cells; washing the precipitate; dissociating the protein from the immune complex in SDS/DTT; and analyzing the dissociated protein by SDS-PAGE.

Coupling of COS-produced AT to the sheep anti-human AT IgG was accomplished by incubating 100 μl of conditioned medium from COS-1 cell culture with 3 μg this IgG in 1 ml of 1X RIPA buffer [10 mM Tris-Cl (pH 8.0), 140 mM NaCl, 0.025% NaN_3, 1% Triton X-100, 0.1% (w/v) SDS, 1% (w/v) sodium deoxycholate, 1% (w/v) bovine hemoglobin, 1 mM PMSF, 1 mM iodoacetamide] at 22°C for 2 h. Adsorption of the antigen-antibody complex to the Omnisorb™ cells was accomplished by incubation with 100 μl of a 10% suspension of this cells pre-equilibrated with Tris-buffered saline (TBS) [20 mM Tris-Cl, 150 mM NaCl, pH 7.4]. To remove proteins that were nonspecifically adsorbed to the cells, the cells were washed sequentially with 1 ml of 1X RIPA buffer three times, TBS twice, and ddH_2O once. The cells were then suspended in 50 μl of 2X SDS-PAGE sample buffer containing DTT [10 mM Tris-Cl (pH 6.8), 1 mM EDTA, 5% (w/v) SDS, 10% glycerol, 0.025% (w/v) bromophenol blue, 200 mM DTT] and proteins specifically associated with the cells were denatured by heating to 100°C for 3 min. Subsequently, the cells, which had served as the immunoadsorbent, were removed by centrifugation. All immunoprecipitation was carried out in duplicate, the duplicate samples were

pooled, and an aliquot of the sample was analyzed by SDS-PAGE under reducing conditions.

2.4.2. Quantification of AT by an ELISA

Quantification of AT by a trapping or "capture" ELISA was established and kindly carried out by Mr. M. Kulczyky. Briefly, each polystyrene microtiter plate well was coated with the sheep anti-human AT IgG by incubating 500 ng this IgG in coating buffer [100 mM Na_2CO_3, pH 9.6] at 4°C for 18-24 h. The unbound IgG was removed by suction and three washes with TBS-T. Each well was incubated with 200 μl of Blotto [1% skim milk powder in TBS-T; TBS-T: 10 mM Tris-Cl, 150 mM NaCl, 0.05% Tween-20, pH 7.4] for 1 h at 25°C to block nonspecific binding sites, and again washed three times with TBS-T. The standard AT (ranging from 7.8 ng/ml to 250 ng/ml) and samples to be tested (diluted into the standard range) were then applied in triplicate. After a 1.5 h incubation at 37°C, each well was washed three times with TBS-T. This was followed by addition of 100 ng the biotinylated sheep anti-human AT IgG, diluted 1/1000 in TBS-T+BSA [1% BSA in TBS-T], and a further incubation at 37°C for 1 h. After three washes, streptoavidin-AP, diluted 1/5000 in TBS-T+BSA, was then applied. Following a 1 h incubation at 25°C and three subsequent washes, 100 μg PNPP in DEA substrate buffer [1 M DEA, 0.5 mM $MgCl_2$, pH 9.8] was added. After a 1 h incubation at 25°C, the colour reaction was stopped by adding 30 μl of 100

mM NaOH to each well. Finally, the OD reading of each well was taken at 405 nm by an ELISA reader and the data obtained were analyzed by Minitab™, version 8.0. Unless otherwise stated, reagents were added in a 100-μl per well volume and washes were carried out with 200 μl per well of TBS-T.

2.4.3. Analysis of Proteins by SDS-Polyacrylamide Gel Electrophoresis

In this study, all analytical electrophoresis of proteins were carried out in polyacrylamide gels under conditions that ensured dissociation of the proteins into their individual polypeptide subunits with minimization of aggregation. One dimensional SDS-PAGE using a discontinuous buffer system was performed as described by Laemmli (1970) in vertical gels that composed of a upper stacking gel and a lower resolving gel. In this discontinuous buffer system, the sample and the stacking gel contained Tris-Cl (pH 6.8), the upper and lower buffer reservoirs Tris-glycine (pH 8.3), and the resolving gel Tris-Cl (pH 8.8), while 0.1% (w/v) SDS was present in all components of the system. Resolving gel monomer solution was prepared by combining the following reagents to a final concentration of 12% (w/v) acrylamide [stock solution: 29.2% (w/v) acrylamide and 0.8% (w/v) BIS], 375 mM Tris-Cl (pH 8.8), 0.1% (w/v) SDS, 0.05% (w/v) APS and 0.05% TEMED. The stacking gel monomer solution was composed of 3% acrylamide, 125 mM Tris-Cl (pH 6.8), 0.1% (w/v) SDS, 0.05% (w/v) APS and 0.1% TEMED. Prior to being loaded, samples were mixed with 3 volumes of 4X

SDS-PAGE sample buffer containing DTT [20 mM Tris-Cl (pH 6.8), 2 mM EDTA, 10% (w/v) SDS, 20% (w/v) glycerol, 0.05% (w/v) bromophenol blue, 400 mM DTT] and heated at 100°C for 3 min. The samples were then electrophoresed at 200 V in 1X electrophoresis buffer [0.30% (w/v) Tris, 1.44% (w/v) glycine, 0.1% (w/v) SDS, pH 8.3] until the tracking dye migrated to the bottom of the gel; which took approximately 40-45 min. Following electrophoresis each gel was fixed and stained by soaking in staining solution [0.05% (w/v) Coomassie brilliant blue R-250, 35% methanol, 10% glacial acetic acid] for 1-2 h. Excess dye was allowed to diffuse from the gel during a prolonged period of destaining in destaining solution [35% methanol and 10% glacial acetic acid]. To make a permanent record, the gel was dried on Whatman chromatography 3MM paper on a gel dryer at 80°C for 1 h. When fluorography was indicated for ^{35}S-radiolabelled samples, following electrophoresis the gel was soaked in destaining solution for 30 min to fix proteins and wash out free radiolabel and transferred into Amplify™ for 15 min. The gel was then dried on the gel dryer with the temperature reduced to 70°C so as not to destroy the fluor, packed on X-ray film, and an autoradiogram was made.

2.4.4. Western Blotting (Electrophoretic Transfer and Immunological Detection)

To identify various AT proteins, Western blotting (Towbin *et al.*, 1979; Burnette, 1981) was employed. Western blotting allows electrophoretically

separated proteins to be transferred from a gel to a solid support and probed with reagents that are specific for the target proteins. The probes usually are antibodies that react specifically with antigenic epitopes displayed by the target protein attached to the solid support. Following SDS-PAGE as usual, the polyacrylamide gel was equilibrated in 500 ml of transfer buffer (25 mM Tris, 192 mM glycine) for 30 min at 25°C, and the transfer assembly was prepared as described by Sambrook *et al.* (1989b). Transfer was carried out at 80 V for 2 h in transfer buffer with the apparatus being kept cool within an ice bath. After electrophoretic transfer, the blot was incubated in Blotto for 1 h at 25°C to saturate nonspecific binding sites on the nitrocellulose membrane. Following the initial blocking incubation and three subsequent washes with TBS-T, the blot was incubated with primary antibody, the sheep anti-human AT IgG (22.5 μl of this IgG diluted in 15 ml of Blotto), at 25°C for 1 h. This was followed by three washes, a further 1 h incubation at 25°C with the secondary antibody AP-rabbit anti-sheep IgG, and three subsequent washes. The various AT proteins which were immobilized on the nitrocellulose and probed by the antibodies were then visualized by incubating the blot with chromogenic substrate mixture [165 μg/ml BCIP and 300 μg/mg NBT] in 10 ml of AP buffer [100 mM Tris-Cl (pH 9.5), 100 mM NaCl, 5 mM $MgCl_2$] for 5-15 min at 25°C.

2.4.5. Purification of CHO-derived Recombinant AT

Essentially, AT was isolated from the conditioned medium of stably transfected CHO cell cultures by affinity chromatography on heparin Sepharose, the Hitrap^{R} heparin. 2 L of the conditioned medium was concentrated 10-fold using a Prep/Scale^{TM}-TFF filter cartridge (with a MWCO of 30 kDa) in accordance with the manufacturer's instructions. The concentrated medium was then clarified by centrifugation. In the preliminary experiments, the concentrated medium was applied to a 3-ml Hitrap^{R} heparin column. The column was washed thoroughly with TBS buffer till the OD_{280} reading reached 0. The bound proteins were eluted with a NaCl gradient prepared by having 50 ml of each TBS buffer and 2.0 M modified TBS buffer in a gradient mixer and AT recovery rate was calculated according to the ELISA-based quantitation. In the preparatory experiments, the concentrated medium was applied to a 3-ml anion exchanger Q-sepharose (Q-Sepharose^{R} fast flow) column prior to affinity chromatography on heparin Sepharose. The column was washed with 60 ml of 0.3 M modified TBS buffer [10 mM Tris-Cl, 300 mM NaCl, pH 7.4]. The wash was collected, and its salt concentration was adjusted as in the TBS buffer. The flow through and the wash were pooled, and then applied to a 3-ml Hitrap^{R} heparin column. The column was washed first with TBS buffer till the OD_{280} reading reached 0 and then with 45 ml of 0.5 M modified TBS buffer. After such thorough wash, the bound proteins were eluted with 2.0 M modified TBS buffer. The OD readings of the collected fractions were taken at 280 nm. The 2.0 M AT-containing

fractions were pooled and concentrated with a centriprep-10 concentrator. Such AT preparation was dialyzed against two 4 L of PBS-plus buffer [20 mM Na_2HPO_4, 150 mM NaCl, 0.1 mM EDTA, 0.1% PEG 8000, pH 7.4] overnight at 4°C using a membrane tubing with a MWCO of 12-14 kDa. The dialyzed AT preparation was then placed on a 100-μl Q-sepharose column which had been pre-equilibrated with the PBS-plus buffer. The column was washed with 200 μl of 0.3 M modified PBS buffer. After adjusting its salt concentration to that as in the PBS-plus buffer, the wash was pooled with the flow through. This final preparation of purified AT was stored at 4°C, and characterization of AT was carried out within 5 days after its preparation.

2.4.6. Preparation of High affinity Heparin

High affinity heparin was kindly prepared by Mr. M. Kulczyky through affinity chromatography on an AT-Sepharose column. Such a column was prepared by coupling 140 mg AT to 4 g CNBr-activated Sepharose 4B in 14 ml of TBS for 2 h at 25°C and packing the gel at 4°C for overnight. Following equilibration of the column with TBS buffer, 200 mg standard heparin sodium salt was applied onto the column. The column was washed thoroughly with 200 ml of TBS buffer, and the bound heparin eluted with 2.0 M modified TBS buffer. The heparin concentration in each fraction was determined by a protamine sulphate assay (Hatton, *et al.*, 1978). The heparin-containing fractions were pooled and

dialyzed against 4 L of TBS overnight at 4°C using a membrane tubing with a MWCO of 1 kDa. After dialysis, the heparin concentration again was determined by the protamine sulphate assay.

2.4.7. Determination of the Heparin Binding Property of the COS-produced AT

The heparin binding ability of AT moieties was assessed by affinity chromatography on heparin Sepharose, the Hitrap^R heparin, essentially according to Mille-Anderson *et al.* (1974). For COS-produced AT proteins, 3 ml of the conditioned medium, pretreated with the Probe-Tek heparin adsorbent, was incubated with 300 μl of the Hitrap^R heparin at 25°C for 1 h. The heparin Sepharose was washed thoroughly with 10 bed volumes of TBS. The bound proteins were eluted sequentially with the modified TBS buffers containing increasing concentrations of NaCl ranging from 0.2 to 2.0 M. The resultant fractions were subsequently analyzed by an ELISA.

2.4.8. Determination of the K_ds of the Pentasaccharide- and Heparin-AT Complexes

The binding of the pentasaccharide and high affinity heparin to AT was quantified spectroscopically by monitoring the accompanying changes in fluorescence of the aromatic amino acids as described previously (Olson *et al.*, 1993). A 600 μl of AT in PBS-plus buffer at 25°C was titrated with 2-μl aliquots

of a concentrated high affinity heparin or pentasaccharide solution, respectively, up to a twenty-fold molar ratio of saccharide/protein with minimal dilution (less than 5% dilution). The emission spectrum at 340 nm was measured on a luminescence spectrophotometer with excitation at 280 nm. Protein fluorescence was measured before titration and after each addition of the specific saccharide. Three readings were taken and averaged for each titration point. Titrations were performed three times in such a way that the titrant additions were staggered. Suitable corrections for buffer blanks and dilution were applied. The corrected data were then fitted into the equilibrium binding equation:

$$\triangle F=(F_{obs}-F_0)/F_0=$$

$$\triangle F_{max}\times\{[AT]_0+n[H]_0+K_d-\{([AT]_0+n[H]_0+K_d)^2-4[AT]_0n[H]\}^{1/2}\}/2[AT]_0$$

by nonlinear least-squares analysis using the SigmaPlot^R program to determine the K_d. [AT] represents total AT concentration; [H], total heparin concentration (applicable for the pentasaccharide); F_0, AT fluorescence before the titration; F_{obs}, the observed fluorescence after each addition of the specific saccharide; F_{max} the maximal fluorescence change; and n, the apparent stoichiometry for the interaction, which was assumed to be 1.

2.4.9. Complexes of AT with FXa

Both the purified AT proteins derived from CHO cells and the COS-expressed protein in the conditioned medium of transiently transfected COS-1

cells were assayed for their ability to form a covalent complex with FXa. In most cases, 200 nM AT which had been pre-warmed at 37°C was incubated with 10 nM FXa at 37°C in a total volume of 100 μl in both the absence and the presence of 100 nM pentasaccharide. Under certain circumstances, 500 nM AT was reacted with 50 nM FXa in the absence and the presence of 100 nM pentasacchride. When it was included in the reaction, the pentasaccharide was pre-incubated with AT at 37°C for 3 min. A 10-μl aliquot was taken at various time points and its reaction was stopped by the addition of 30 μl of 1,5-DNS-GGACK, HCl at a final concentration of 2 μM. Under certain circumstances, FXa-AT complexing reaction was carried out in duplicate and the duplicate samples were pooled. Immediately after the reaction, the FXa-AT complexes were detected and quantified by an ELISA. This was carried out by Dr. J. Yang from Dr. F. Ofosu's laboratory as described previously (Gouin-Thibault *et al.*, 1995). Briefly, each microtiter plate well was coated with the affinity-purified chicken anti-human FXa-AT IgY by incubating 200 ng this IgG in 100 μl of the coating buffer at 4°C for 18 h. After the unbound IgY was removed, each well was washed with 200 μl of PBS-T buffer [10 mM Na_2HPO_4, 150 mM NaCl, 0.05% Tween-20, pH 7.4], blocked with TBS-T+BSA buffer [0.1 mg/ml BSA in TBS-T] for 1 h at 37°C, and washed again four times with the PBS-T buffer. Subsequently, 100 μl of the test samples and the FXa-AT standards, prepared by incubating AT and FXa in a molar ratio of 2:1 in the presence of 0.05 unit/ml heparin, were applied in

triplicate. After a 1 h incubation at 37°C, each well was washed four times. This was followed by the addition of 100 μl of biotinylated rabbit anti-human AT IgG (diluted 1/4000 in TBS-T+BSA) and a further 1 h incubation at 37°C. After four washes, 100 μl of streptavidin-AP (diluted 1/5000 in TBS-T+BSA) was applied. Following a 1 h incubation at 37°C and four subsequent washes, 100 μl of p-nitrophenyl phosphate was added. The colour yield at 405 nm was then quantified after a 30 min incubation at 37°C.

2.4.10. Complexes of AT with α-Thrombin

The COS-expressed radioactive AT was assayed in the conditioned medium of transiently transfected COS-1 cells for its ability to form a covalent complex with thrombin in both the absence and the presence of heparin. Briefly, 1 nM AT was incubated with 20-fold excess thrombin at 37 °C in a total volume of 800 μl. When it was included in the reaction, heparin at a final concentration of 5 nM, was pre-incubated with AT at 37°C for 3 min. A 100-μl aliquot was taken at various time points and its reaction was stopped by the addition of 20 μl of PPACK at a final concentration of 1 μM. Each reaction was carried out in duplicate and the duplicate samples were pooled. Immediately after the reaction, the thrombin-AT complexes were analyzed by SDS-PAGE under reducing conditions following immunoprecipitation.

3. RESULTS

3.1. The Consequences of Alterations to Arg47 in AT

3.1.1. Generation of Arg47 Variant cDNAs by Site-directed Mutagenesis

To create AT moieties with substitution mutations at Arg47, the transformer™ site-directed mutagenesis of AT cDNA was carried out as described in section 2.2.5 (see Fig. 2.1). The introduction of the intended mutations at Arg47 in AT cDNA was confirmed by DNA sequencing analysis as outlined in section 2.2.6. Of the fourteen possible substitution mutations at codon 47 given by the sequence of the primer AB2302, eight new codons were obtained. They were Ala, His, Leu, Pro, Ser, Thr, Tyr, and Val (shown in Fig. 3.1). In order to generate AT variants in which Arg47 was replaced by residues with charged side-chains, oligodeoxynucleotide AB3216 was applied as the mutagenic primer. As a result, Arg47Lys and Arg47Glu were obtained (shown in Fig. 3.1). Thus ten AT variants with substitutions at Arg47 were generated. Among them, Ala, Val, Leu, and Pro had nonpolar side-chains; Ser, Thr, and Tyr, uncharged polar side-chains; Lys and His, basic side-chain; Glu, acidic side-chains. Since at least one amino acid from each group was generated, the sum of these variants would be sufficient to test the consequences of alterations to Arg47, in particular, hypothesizing that its positive charge is required for the binding of the pentasaccharide to AT and for the subsequent activation of AT by the pentasaccharide.

Fig. 3.1. Partial nucleotide sequences of AT cDNA showing the region around codon 47. Dideoxy chain-termination sequencing analysis of DNA was carried out to confirm the introduction of the intended substitutions at Arg47. The AT cDNA insert of plasmid DNA from individual transformants was sequenced with the oligodeoxynucleotide primer AB2802. At amino acid position 47, CGT encodes the wt Arg; AAA, Lys; ACT, Thr; AGT, Ser; CAT, His; CCT, Pro; CTT, Leu; TAT, Tyr; GAA, Glu; GCT, Ala; and GTT, Gly.

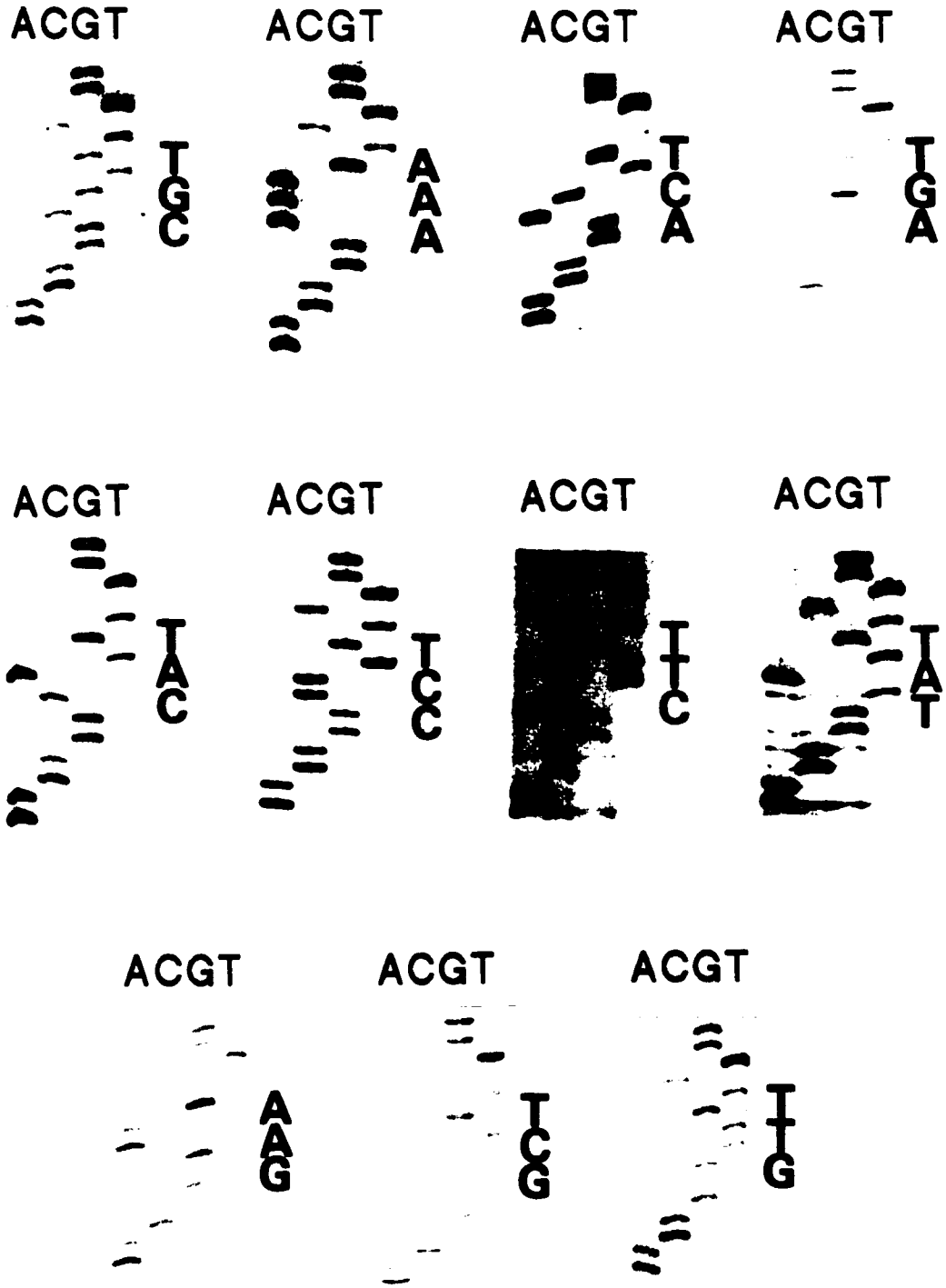
ACGT
TGC
ACGT
AAA
ACGT
TCA
ACGT
TGA
ACGT
TAC
ACGT
TCC
ACGT
TC
ACGT
TAT
ACGT
AAG
ACGT
TCG
ACGT
TTG

3.1.2. Expression of wt AT and the Arg47 Variants in Transiently Transfected COS-1 Cells

The pCMV5 plasmid constructs that allow expression of wt AT and the Arg47 variants were assembled as outlined in section 2.2.7. To eliminate the possibility of having reintroduced a wt sequence in the steps of excision of the AT cDNA and ligation into the expression vector, DNA sequencing was carried out prior to transfection of COS-1 cells. Dideoxy sequencing analysis confirmed that the intended mutations were present in the corresponding plasmids used for transfection of COS-1 cells.

Wt AT and the Arg47 variants were expressed in transiently transfected COS-1 cells in both radioactive and non-radioactive forms as detailed in 2.3.1. To minimize variations between batches of the lipofectin^{R} reagent and differences between plasmid DNA preparation as well as cell culture manipulations at different times, all the eleven expression constructs were purified at the same time under the same experimental conditions, so was transfection and other manipulations of the cell cultures. Characterization of the recombinant AT moieties was also carried out at the same time under the same experimental conditions.

In order to detect and analyze the various recombinant AT proteins by immunoprecipitation coupled with SDS-PAGE, the COS-expressed AT moieties were metabolically radiolabelled with L-[^{35}S] Met and L-[^{35}S] Cys. The expression

levels of the radioactive AT proteins were determined by a capture ELISA. Under the experimental conditions detailed in section 2.3.1, a 3 h incubation with 200 μCi of ^{35}S-labelled Met and Cys in 3 ml of serum-free medium per 100-mm plate produced various radioactive AT proteins in the range of 220-330 ng/ml. The AT expression levels of the different constructs did not differ significantly from each other (data not shown). In other words, nucleotide substitutions at the codon 47 of AT cDNA did not affect the efficiency of expression and secretion of the AT moieties by transiently transfected COS-1 cells.

The ^{35}S-labelled wt AT and the Arg47 variants were analyzed by SDS-PAGE following immunoprecipitation (shown in Fig. 3.2). These AT moietieswere immunoprecipitated from the conditioned media of transfected COS-1 cells with the sheep-anti-human AT IgG and visualized by SDS-PAGE on a 12% polyacrylamide gel under reducing conditions, followed by autoradiography. Analysis of the conditioned medium of COS-1 cells transfected with the pCMV5-$AT_{-32-432}^{wt}$ construct revealed a protein which migrated with an apparent molecular mass (Mr) of 58 kDa (shown in lane 1 in Fig. 3.2), very similar to that of the plasma-derived AT (compare lane 1 to lane 14 in Fig. 3.2). Furthermore, this compound was absent in the immunoprecipitants of the conditioned media of both non-transfected COS-1 cells (shown in lane 12 in Fig. 3.2) and COS-1 cells transfected with the vector pCMV5 alone (shown in lane 13 in Fig. 3.2). Thus, transfection of the expression plasmid construct pCMV5-$AT_{-32-432}^{wt}$ into COS-1

Fig. 3.2. SDS-PAGE analysis of wt AT and the Arg47 variants following immunoprecipitation. ^{35}S-labelled AT moieties in the conditioned media of the COS-1 cells, transiently transfected with the various AT expressing constructs, were immunoprecipitated and visualized by SDS-PAGE on a 12% polyacrylamide gel under reducing conditions, followed by fluorography. Lane 1 shows the wt AT; lane 2, the Arg47Ser variant; lane 3, the Arg47Lys variant; lane 4, the Arg47His variant; lane 5, the Arg47Pro variant; lane 6, the Arg47Val variant; lane 7, the AT Arg47Leu variant; lane 8, the Arg47Tyr variant; lane 9, the Arg47Thr variant; lane 10, the Arg47Glu variant; lane 11, the Arg47Ala variant; lane 12, control material from non-transfected COS-1 cells; lane 13, control material from COS-1 cells transiently transfected with the vector pCMV5 alone without any AT cDNA insert; and lane 14, plasma-derived AT. Plasma AT was visualized by SDS-PAGE on the same 12% polyacrylamide gel as the immunoprecipitants of those COS-expressed ^{35}S-labelled AT moieties.

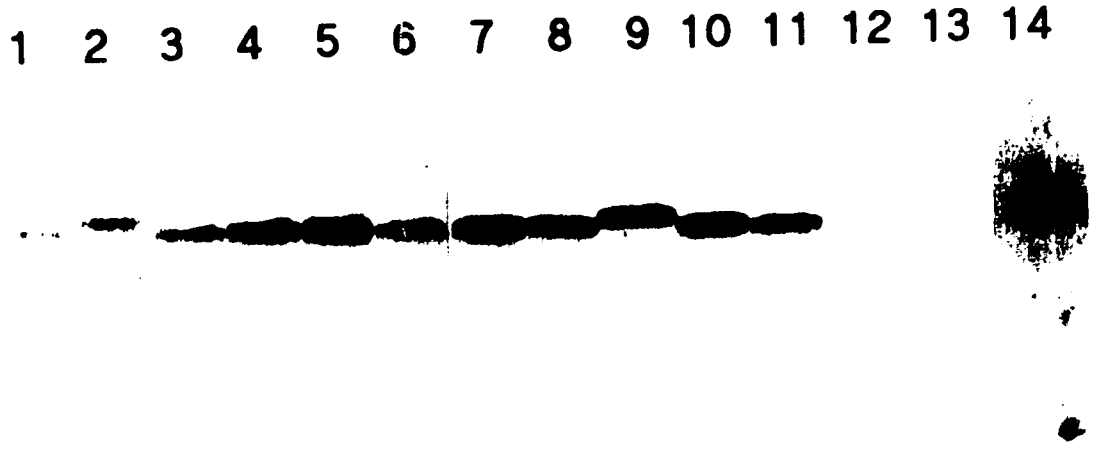
1 2 3 4 5 6 7 8 9 10 11 12 13 14

cells resulted in the appearance in the conditioned medium of a novel, undegraded 58 kDa protein that was recognized by the sheep-anti-human AT IgG. This recombinant protein, therefore, was the COS-expressed wt AT. In other words, transfected COS-1 cells synthesized wt AT and secreted it into the conditioned medium. In addition, AT produced in these cells was glycosylated and the extent of the glycosylation in this recombinant protein appeared to be similar to that of the plasma-derived AT. Novel synthesis of undegraded proteins that could be recognized by the sheep-anti-human AT IgG was also observed in COS-1 cells transfected with the other ten expression plasmid constructs. Among these ten Arg47 variants, eight co-migrated with the wt AT. These were variants AT Arg47Lys (shown in lane 3 in Fig. 3.2), AT Arg47His (shown in lane 4 in Fig. 3.2), AT Arg47Pro (shown in lane 5 in Fig. 3.2), AT Arg47Val (shown in lane 6 in Fig. 3.2), AT Arg47Leu (shown in lane 7 in Fig. 3.2), AT Arg47Tyr (shown in lane 8 in Fig. 3.2), AT Arg47Glu (shown in lane 10 in Fig. 3.2), and AT Arg47Ala (shown in lane 11 in Fig. 3.2). The other two variants, AT Arg47Ser (shown in lane 2 in Fig. 3.2) and AT Arg47Thr (shown in lane 9 in Fig. 3.2), however, migrated slower than the wt AT. The reduced mobility of these two variants suggested that they had an increased apparent Mr. Introduction of a Ser or Thr at the amino acid position 47 resulted in the generation of the fifth glycosylation consensus sequences Asn-X-Ser/Thr in AT. The increased apparent Mr of these two variants thus could be the consequence of N-linked glycosylation at Asn45.

In summary, COS-1 cells, when transfected with the various expression constructs, synthesize and secrete correspondingly wt AT and the 10 Arg47 variants into the conditioned medium. Except for AT Arg47Ser and AT Arg47Thr, the other nine recombinant AT moieties have an apparent Mr similar to that of the plasma-derived AT. AT Arg47Ser and AT Arg47The have a slightly increased apparent Mr most likely due to extra glycosylation at Asn45.

Higher levels of expression would facilitate characterization of the Arg47 AT variants. A convenient way to improve the yield of recombinant AT in the conditioned medium of transiently transfected COS-1 cells was to increase the conditioning time. Since the establishment of ELISAs for both AT and FXa-AT eliminated the demand on radioactive AT proteins for subsequent detection and quantitation of AT, AT moieties were expressed in non-radioactive form. A 20-24 h incubation in 10 ml of serum free medium per 100-mm plate allowed the production of recombinant AT in the conditioned medium to reach higher levels. According to ELISA-based quantitation, the yield for the various AT moieties achieved the range of 1.7-6.7 μg/ml. Additionally, the AT production levels of the different constructs did not differ significantly from each other (data not shown). These non-radioactive AT proteins were analyzed by Western blotting probed with the sheep-anti-human AT IgG following SDS-PAGE under reducing conditions (shown in Fig. 3.3). Similarly, no AT was produced by non-transfected COS-1 cells nor COS-1 cells transfected with the no-insert vector pCMV5.

Recombinant wt AT and the eight Arg47 variants co-migrated as the plasma-derived AT. In addition, two components which migrated closely to each other were present in each of the 9 lanes. These two components should be the α-AT and the ß-AT, respectively. Again, AT Arg47Ser and AT Arg47Thr migrated with a reduced mobility, suggesting an increased Mr probably due to N-glycosylation at Asn45. Since these two variants differed from wt AT not only in the amino acid composition at position 47 but in also the glycosylation status, they were excluded from further characterization. Among the other nine moieties, five were chosen to be characterized subsequently for their heparin binding and the pentasaccharide cofactor properties. They were wt AT, the AT Arg47Lys variant (with a basic side-chain), the AT Arg47Tyr variant (with a uncharged polar side-chain), the AT Arg47Pro variant (the α-helix breaking residue with a nonpolar side-chain), and the AT Arg47Glu variant (with an acidic side-chain).

3.1.3. Quantification of the FXa-AT Complexes by an ELISA

Quantification of the FXa-AT complexes was carried out by an ELISA as detailed in section 2.4.9. To confirm the specificity of this ELISA, plasma AT, various recombinant AT proteins in the conditioned medium of transfected COS-1 cells, FXa, the pentasaccharide, the conditioned medium from non-transfected COS-1 cells, and PBS were incubated at 37 °C for 5 min, respectively. These samples were then applied to ELISA and none of them yielded significant

Fig. 3.3. Western blotting analysis of wt AT and the Arg47 variants. Following SDS-PAGE of the conditioned media of the COS-1 cells transiently transfected with the various AT expressing constructs on a 12% polyacrylamide gel under reducing conditions, AT moieties were analyzed by Western blotting, probed with the sheep anti-human AT IgG. Lane 1 shows the wt AT; lane 2, the Arg47Ser variant; lane 3, the Arg47Lys variant; lane 4, the Arg47His variant; lane 5, the Arg47Pro variant; lane 6, the Arg47Val variant; lane 7, the Arg47Leu variant; lane 8, the Arg47Tyr variant; lane 9, the Arg47Thr variant; lane 10, the Arg47Glu variant; lane 11, the Arg47Ala variant; lane 12, control material from non-transfected COS-1 cells; lane 13, control material from COS-1 cells transiently transfected with the vector pCMV5 alone without any AT cDNA insert; and lane 14, plasma-derived AT.

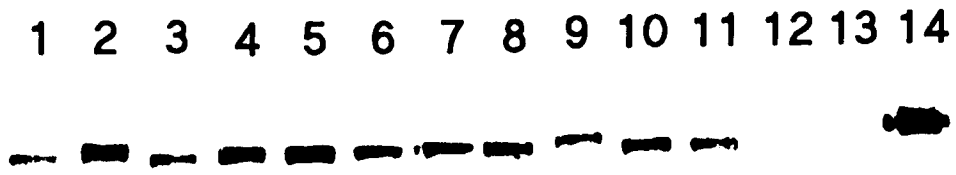
1 2 3 4 5 6 7 8 9 10 11 12 13 14

amounts of FXa-AT complexes above blank wells (data not shown). To control variations between plates, standard FXa-AT was employed to each and every individual plate in a series of dilutions. All samples were calculated for their FXa-AT complex concentrations according to the linear regression equation of the standard from the same plate. In preliminary experiments, the effect of storage conditions on the FXa-AT complex samples was also investigated. The amount of the FXa-AT complexes was found to be reduced significantly upon overnight storage of the prepared samples either at 4 °C, at -20 °C, or at -80 °C (data not shown). Due to this instability, quantification of the FXa-AT complexes was carried out immediate after each sample preparation.

3.1.4. The Production of Endogenous Heparin-like Species by COS-1 Cells

Due to limited expression of AT proteins by transiently transfected COS-1 cells, purification of these recombinant proteins and their characterization in purified system was not attempted. Since the heparin binding and the pentasaccharide cofactor properties of AT moieties were to be determined in the presence of the concentrated conditioned medium of COS-1 cells, it was imperative to test first whether COS-1 cells produced endogenous heparin-like species. The most convenient and sensitive way to detect the presence of a glycosaminoglycan with a heparin-like structure that can bind to and activate AT would be to assay the interaction of AT with FXa in the presence of this

compound. Thus, the effects of the conditioned medium on time-dependent complexation to FXa was examined. To do so, conditioned medium of the non-transfected COS-1 cells was concentrated 20-fold, plasma-derived AT was added to it, and the final concentrations of the conditioned medium was adjusted to 20X, 5X, and 1X, respectively. Plasma AT was also added to PBS; this latter preparation served as a control. For each experimental condition, 200 nM plasma AT was incubated with 10 nM FXa. Plasma AT in PBS was also allowed to complex with FXa in the presence of 50 nM pentasaccharide. As shown in Fig. 3.4 by the typographic symbol ♦, plasma AT in PBS buffer complexed with FXa very slowly. Within the first min, less than 0.13 nM FXa-AT complexes was formed. Even at 5 min, only 0.70 nM FXa, equivalent to 7% of total FXa, formed complexes with AT. Plasma AT in the 1X conditioned medium of non-transfected COS-1 cells interacted with FXa not significantly differing from that in PBS buffer (shown by the symbol ■). When plasma AT was added to the 5X conditioned medium, however, the rate of FXa inhibition by AT was significantly enhanced and the absolute amount of the FXa-AT complexes formed was significantly increased (shown by the symbol ▲). 1.3 nM complexes was detected as early as at 15 s and 2.6 nM complexes formed by 5 min. The 5X conditioned medium enhanced the rate at which plasma AT complexed with FXa to a similar extent as 50 nM pentasaccharide (shown by the symbol ◇). In the presence of the 20X conditioned medium, the reaction rate was further enhanced (shown by the

Fig. 3.4. Effects of the conditioned medium of the non-transfected COS-1 cells on the complexing reaction of plasma AT with FXa. 200 nM plasma AT in 1X (shown by the symbol ■), 5X (shown by the symbol ▲), and 20X (shown by the symbol ▼) conditioned medium, as well as in PBS (shown by the symbol ◆), was incubated with 10 nM FXa, respectively. For plasma AT in PBS, the formation of complexes with FXa was also examined in the presence of 50 nM pentasaccharide (shown by the symbol ◇). Each reaction was carried out in duplicate and the duplicate samples for each time point were pooled.

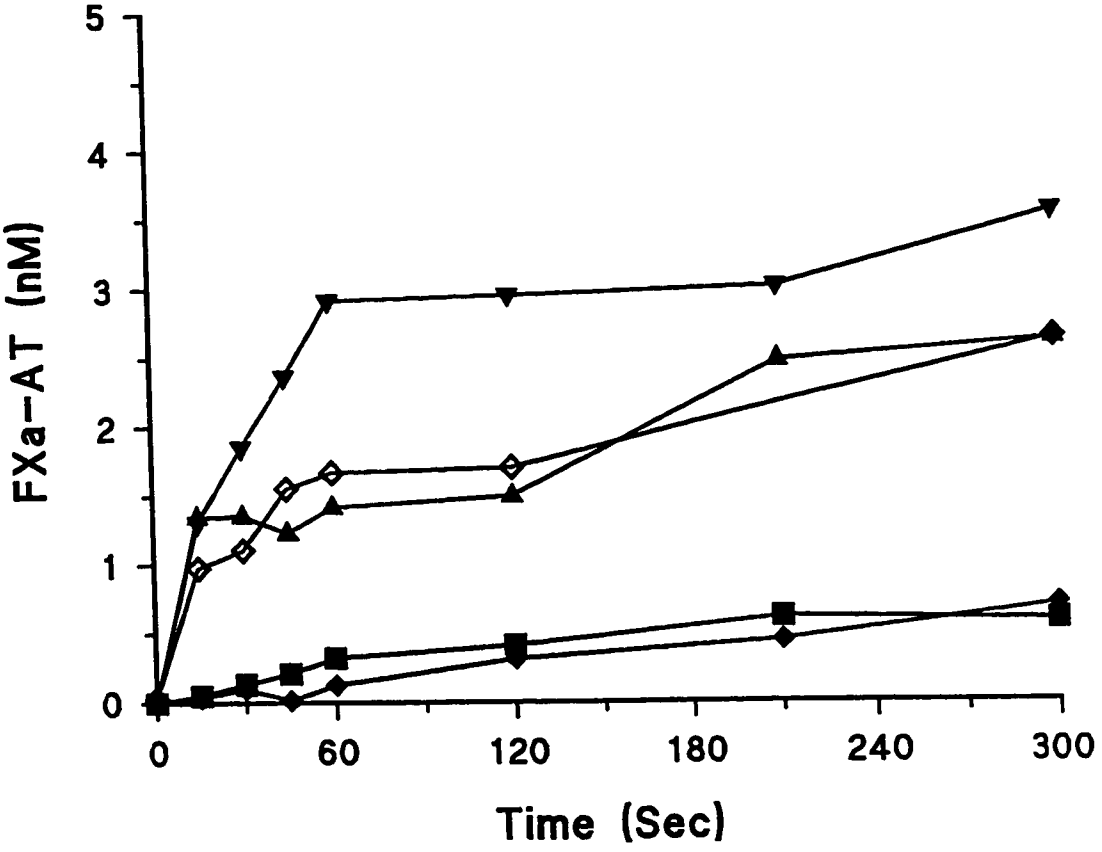
FXa-AT (nM)
5
4
3
2
1
0
0
60
120
180
240
300
Time (Sec)

symbol ▾). A logical explanation for the observed accelerating effect of the conditioned medium would be the production and secretion of endogenous heparin-like species by COS-1 cells. In an attempt to confirm this hypothesis and remove the endogenous heparin-like species, plasma AT added to the 20X conditioned medium was incubated with the Probe-Tek heparin adsorbent prior to its incubation with FXa. Such treatment lowered the rate of the complexes of plasma AT, in the presence of the 20X conditioned medium, with FXa back to the baseline (shown in Fig. 3.5 by the typographic symbol ■), as demonstrated by the preparation of plasma AT in PBS (shown in Fig. 3.5 by the symbol ♦). In other words, the accelerating effect of the conditioned medium was abolished by a heparin neutralizing agent. Thus, COS-1 cells produced and secreted endogenous heparin-like species and the Probe-Tek heparin adsorbent removed them from the conditioned medium. The production of the endogenous heparin-like species by transfected COS-1 cells expressing recombinant wt AT and the removal of these heparin-like species by the Probe-Tek heparin adsorbent is shown in Fig. 3.6. Possible contamination with this heparin adsorbent in the attempt to remove the endogenous heparin-like species, however, could neutralize the activities of the exogenous pentasaccharide, and thereby interfere with the experimental observation of the pentasaccharide cofactor activity. Special caution was taken when separating the adsorbent basin from AT solution. In addition, when it was added to the pre-treated AT preparation (shown in Fig. 3.5 by the symbol □), the

Fig. 3.5. Removal of the endogenous heparin-like species from the conditioned medium of the non-transfected COS-1 cells with the Probe-Tek heparin adsorbent, demonstrated by the effect of its removal on complex formation between plasma AT and FXa. 200 nM plasma AT was incubated with 10 nM FXa in the absence (shown by the solid symbols) and the presence of 50 nM pentasaccharide (shown by the open symbols). Each reaction was carried out in duplicate and the duplicate samples for each time point pooled. AT in PBS is shown by the symbols ♦ and ◇; AT in the 20X conditioned medium with no pretreatment, by the symbols ▾ and ▽; and AT in the 20X conditioned medium pretreated with the Probe-Tek heparin adsorbent, by the symbols ■ and □.

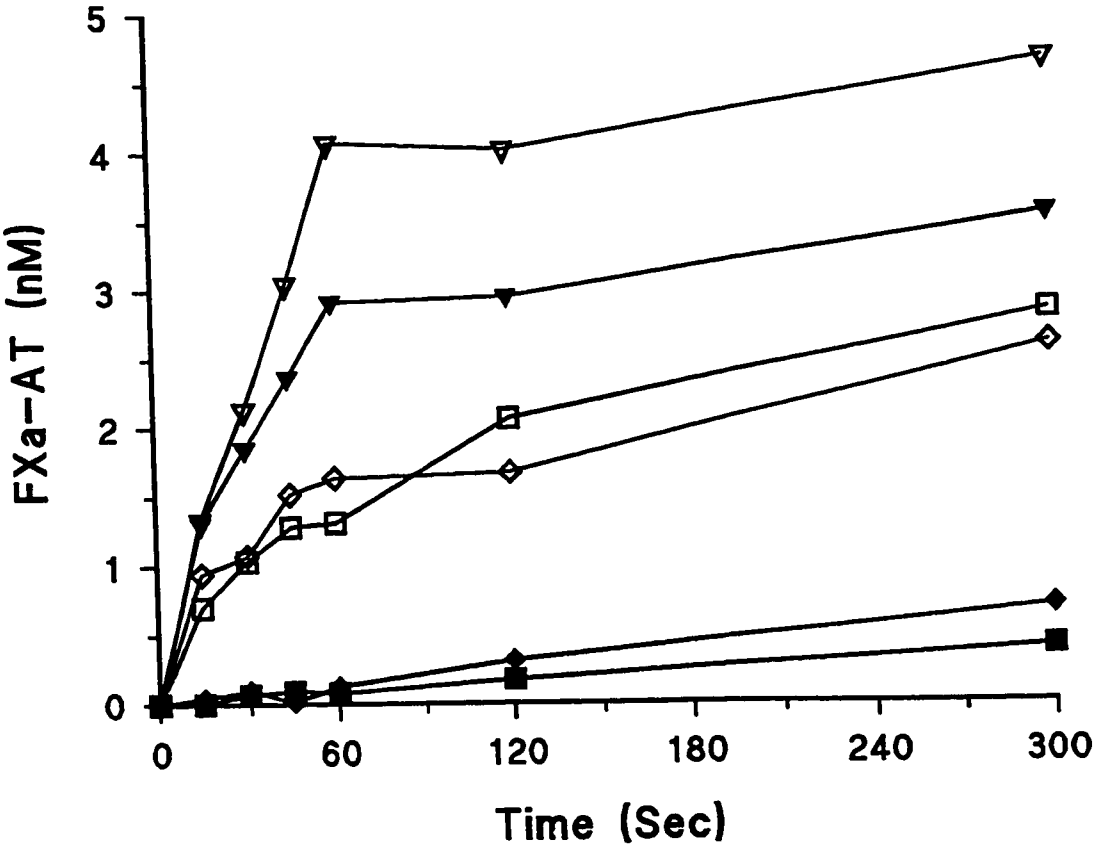
FXa-AT (nM)
5
4
3
2
1
0
0
60
120
180
240
300
Time (Sec)

symbol □), the pentasaccharide enhanced the rate of complexation of plasma AT to FXa to a similar extent as added to AT in PBS (shown in Fig. 3.5. by the symbol ◇). Therefore, all conditioned medium of COS-1 cells was treated routinely with this adsorbent before functional characterization of the COS-expressed AT proteins.

3.1.5. Determination of the Heparin Binding Ability of the Arg47 AT Variants

The heparin binding properties of the four Arg47 variants, namely AT Arg47Lys, AT Arg47Pro, AT Arg47Tyr, and AT Arg47Glu, were examined, along with wt AT, by affinity chromatography on Hitrap^{R} heparin as outlined in section 2.4.7. Shown in Fig. 3.7 is the elution profile for each of these AT moieties. Under the experimental conditions specified above, only approximately 8% of total applied wt AT was present in the 10 bed volume flow through and the 10 bed volume 0.15 M wash (see Fig. 3.7.a). The majority of AT bound to heparin and was eluted off the heparin-Sepharose peaking at 0.8 M NaCl. A careful examination of the eluting profile for wt AT revealed that a very small portion of wt AT could be off the heparin-Sepharose peaking somewhere around 1.4 M NaCl. This second peak could be an artifact of the experimental system. Alternatively, it could represent the ß-form AT having a higher affinity with heparin. For the AT Arg47Lys variant, the majority bound to heparin with approximately 10% left in the flow through and the 0.15 M wash (see Fig. 3.7.b). The majority of the bound protein was off the column peaking at 0.6 M NaCl. A

Fig. 3.6. Removal of the endogenous heparin-like species from the conditioned medium of transiently transfected COS-1 cells with the Probe-Tek heparin adsorbent, demonstrated by assay of the interaction between the COS-expressed wt AT and FXa. 200 nM the COS-expressed recombinant wt AT in the 20X conditioned medium with no pretreatment (shown by the symbol ▼) and pretreated with the Probe-Tek heparin adsorbent (shown by the symbol ■) was incubated with 10 nM FXa, respectively. Each reaction was carried out in duplicate and the duplicate samples for each time point pooled.

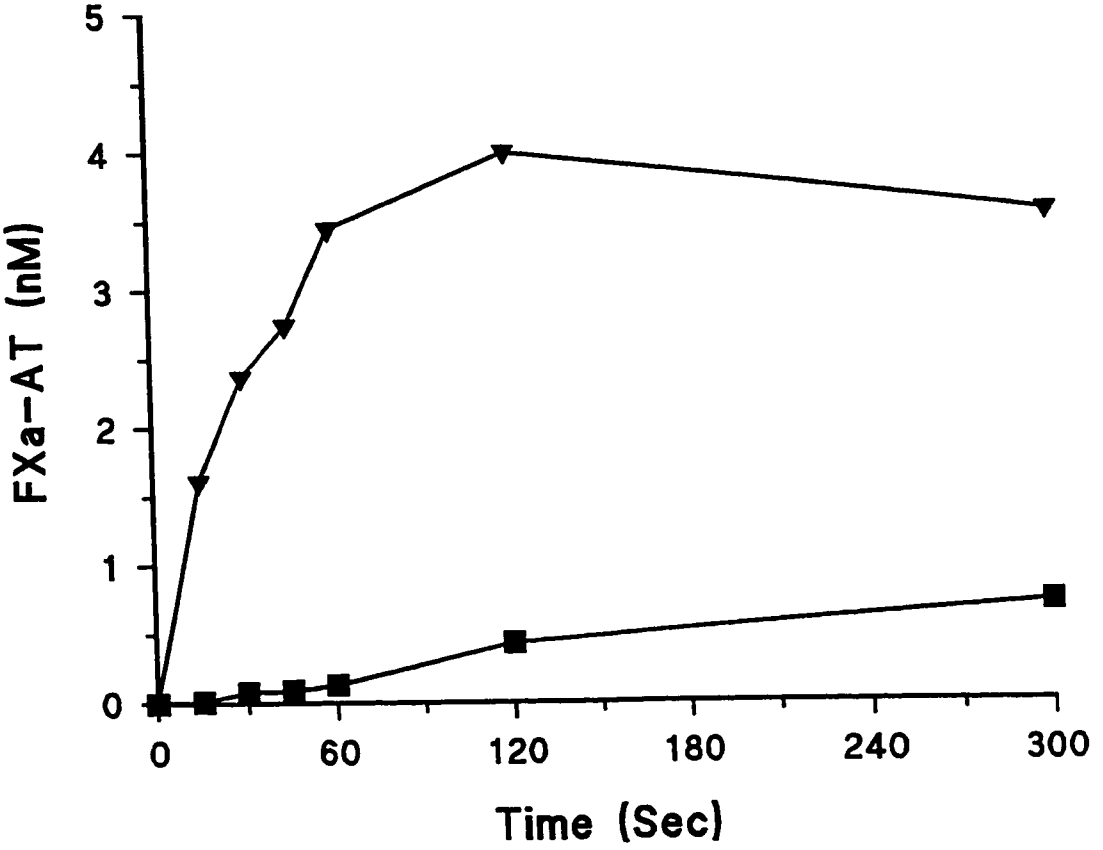
5
4
3
2
1
0
FXa-AT (nM)
0
60
120
180
240
300
Time (Sec)

Fig. 3.7. Heparin chromatography of wt AT and the Arg47 variants. Panel a shows wt AT; panel b, the AT Arg47Lys variant; panel c, the AT Arg47Glu variant; panel d, the AT Arg47Tyr variant; and panel e, the AT Arg47Pro variant.

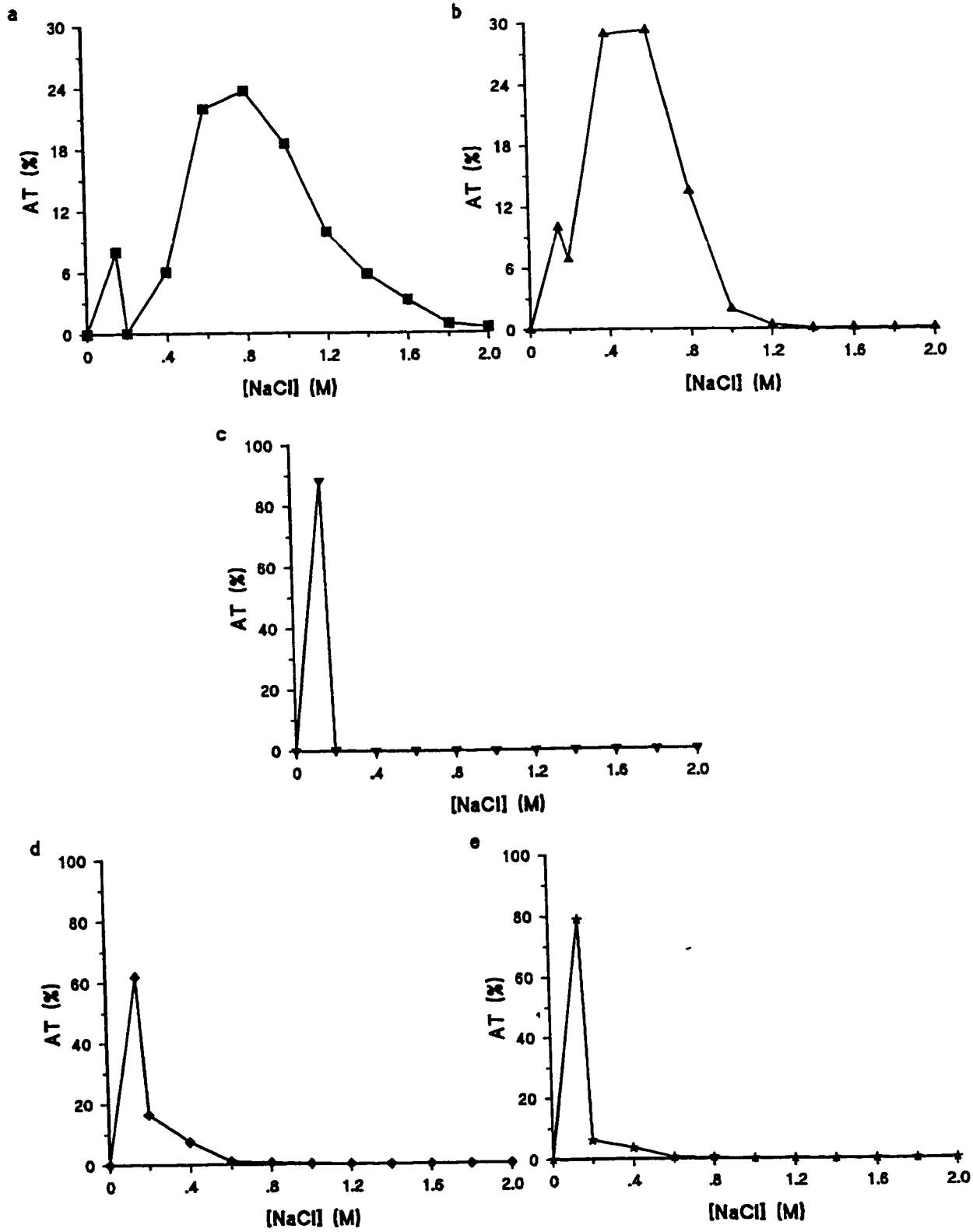
a
b
c
d
e
AT (%)
[NaCl] (M)
0
6
12
18
24
30
20
40
60
80
100
.4
.8
1.2
1.6
2.0

possible second peak, if not an artifact of the system applied, would be peaking maximally at 1.0 M NaCl. Thus, the Arg47Lys variant appears to be able to bind to heparin, but with a slightly reduced affinity. Due to the limitation of the system employed, we could not make more quantitative calculation of the binding. The elution profiles of the Arg47Tyr and the Arg47Pro variants were very similar (compare Fig. 3.7.c and Fig. 3.7.d). For both, the majority did not bind to heparin and therefore was present in the flow through and the 0.15 M wash. Only a very small portion of the variant proteins was retained in the 0.4 M wash, demonstrating significantly reduced heparin binding affinity for these two variants. For the Arg47Glu variant, approximately 90% of the total protein, which represented almost 100% of the protein recovered, did not bind to heparin at all (see Fig. 3.7.e). Moreover, the majority of the recovered protein was in the flow through and the very early fractions of the 0.15 M wash. It thus appeared that as a result of the substitution of the basic Arg residue at position 47 with an acidic residue Glu, the heparin binding ability of the AT molecule was totally lost. In summary, the effect of alteration to residue 47 on heparin binding has been investigated by affinity chromatography on heparin-Sepharose. In terms of heparin binding, whereas a residue with a negatively charged residue at this position is not compatible, a residue with a positively charged side-chain is favoured. Between the two positively charged residues examined, Arg at position 47 fits the AT-binding site of heparin better than Lys.

3.1.6. Determination of the Pentasaccharide Cofactor Property of the Arg47 AT Variants

To determine the pentasaccharide cofactor property of the four Arg47 variants as well as wt AT, 200 nM of each recombinant protein was incubated with 10 nM FXa in the presence of 100 nM pentasaccharide. Shown in Fig. 3.8.a is time-dependent complexation of wt AT to FXa. In the absence of the pentasaccharide, wt AT complexed with FXa very slowly (shown by the symbol ◇). Within the first min, less than 0.17 nM FXa-AT complexes could be detected. Even at 3 min, only 0.36 nM FXa-AT complexes were formed. When the pentasaccharide was included in the reaction, the rate of complexation of wt AT to FXa was significantly enhanced (shown by the symbol ♦). As early as at 10 sec, 1.59 nM AT was already complexed with FXa. In other words, within 10 sec there was a 13-fold net increase in the amount of the complexes formed. At 1 min, 2.72 nM complexes (represent a 16-fold increase) was detected and the amount of the complexes went up to 4.69 nM (equivalent to a 13-fold increase) at 3 min. The accelerating effect of the pentasaccharide on complexation of wt AT to FXa was also observed when wt AT was incubated with FXa at a higher concentration. Shown in Fig. 3.8.b is the results of incubation of 500 nM wt AT with 50 nM FXa in the absence and the presence of 250 nM pentasaccharide. Again, wt AT complexed with FXa (shown by the symbol ◇), and the pentasaccharide accelerated FXa inactivation by AT (shown by the symbol ♦). At 10 sec, the

Fig. 3.8. Time-dependent complexation of wt AT to FXa in the absence (shown by the symbol ◇) and the presence of the pentasaccharide (shown by the symbol ♦). Panel a shows the results of incubation of 200 nM wt AT in the 20X conditioned medium, pretreated with the Probe-Tek heparin adsorbent, with 10 nM FXa in the absence and the presence of 100 nM pentasaccharide. Each reaction was performed in duplicate and shown is the mean of the duplicates and the standard deviation. In panel b, 500 nM wt AT was incubated with 50 nM FXa in the absence and the presence of 250 nM pentasaccharide. In this case, each reaction was carried out in duplicate and the duplicate samples for each time point pooled.

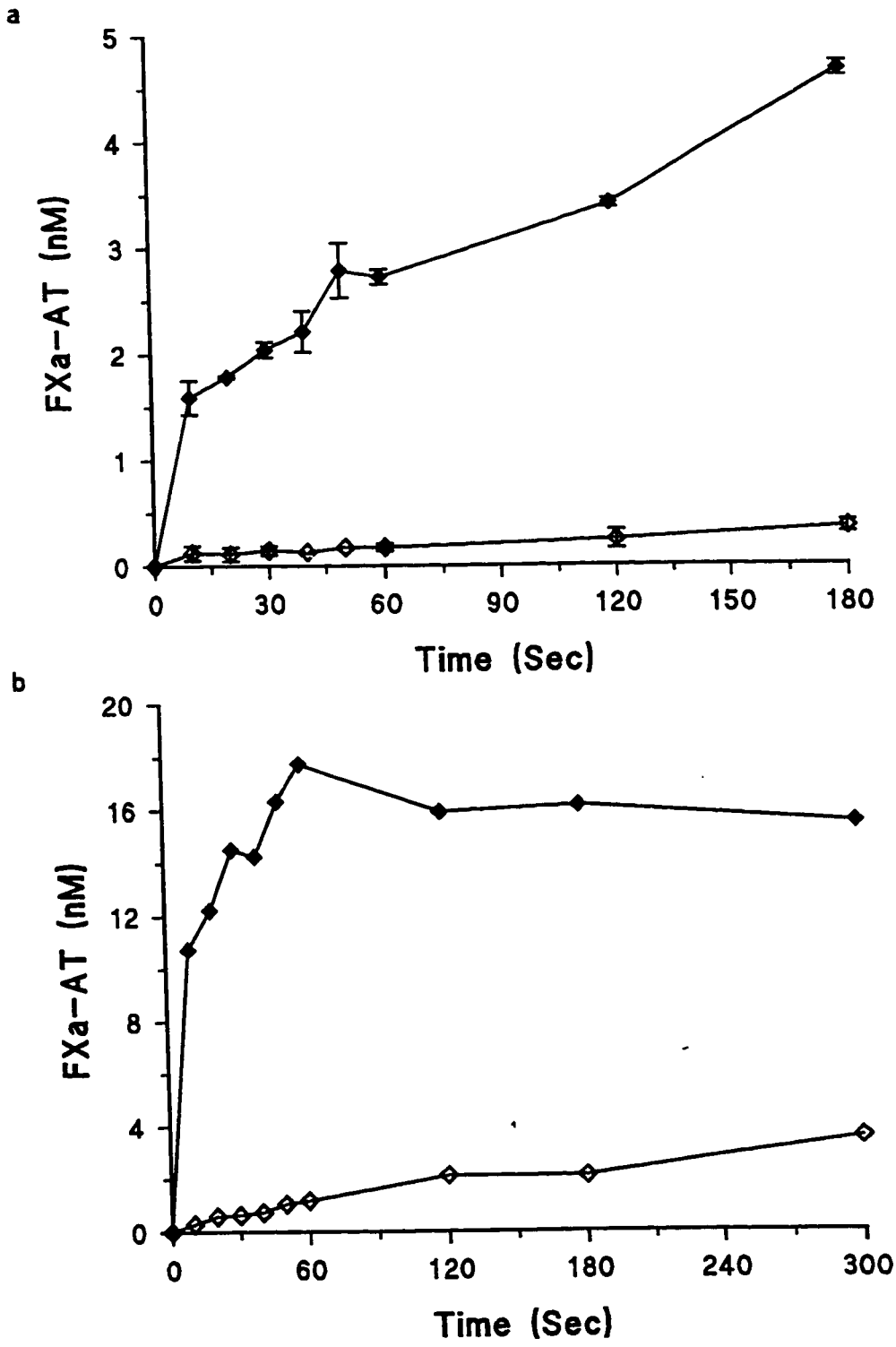
a
FXa-AT (nM)
0
1
2
3
4
5
0
30
60
90
120
150
180
Time (Sec)
b
FXa-AT (nM)
0
4
8
12
16
20
0
60
120
180
240
300
Time (Sec)

pentasaccharide increased the amount of the formed FXa-AT complexes from 0.31 nM (in the absence of the pentasaccharide, shown in Fig. 3.8.b by the symbol ◇) to 10.7 nM (in the presence of the pentasaccharide, shown in Fig. 3.8.b by the symbol ♦), which represented a 35-fold increase in the net amount of the complexes formed. By 1 min, the amount of the complexes went up to 17.7 nM from 0.53 nM, equivalent to a 33-fold increase. Time-dependent complexation of the AT Arg47Lys variant to FXa is shown in Fig. 3.9.a. In the absence of the pentasaccharide, this AT moiety complexed with FXa in a progressive manner very similar as wt AT (compare Fig. 3.9.a to Fig. 3.8.a, shown by the symbol ◇). The pentasaccharide also enhanced the rate at which AT Arg47Lys complexes with FXa. The rate-enhancing effect of the pentasaccharide on the complexation of this AT variant to FXa, however, was reduced significantly when compared to wt AT (compare Fig. 3.9.a to Fig. 3.8.a, shown by the symbol ♦). At 10 sec, the pentasaccharide increased the amount of the FXa-AT complexes from 0.09 nM (in the absence of the pentasaccharide, shown by the symbol ◇) to 0.28 nM (in the presence of the pentasaccharide, shown by the symbol ♦), which was only a 3-fold increase. By 5 min, the amount of the formed complexes reached 1.56 nM, equivalent to a 4-fold increase. When 500 nM of the AT Arg47Lys was incubated with 50 nM FXa in the presence of 250 nM pentasaccharide, the rate-enhancing effect of the pentasaccharide was also observed (shown in Fig. 3.9.b). At 10 sec, the detected amount of the complexes increased 6-fold from 0.27 nM (in the

Fig. 3.9. Time-dependent complexation of the AT Arg47Lys variant to FXa in the absence (shown by the symbol ◇) and the presence of the pentasaccharide (shown by the symbol ♦). Panel a represents 200 nM of the AT Arg47Lys variant in the 20X conditioned medium, pretreated with the Probe-Tek heparin adsorbent, incubated with 10 nM FXa in the absence and the presence of 100 nM pentasaccharide. Each reaction was performed in duplicate and shown is the mean of the duplicate with its standard deviation. In panel b, 500 nM the AT Arg47Lys variant was incubated with 10 nM FXa in the absence and the presence of 250 nM pentasaccharide. In this case, each reaction was carried out in duplicate and the duplicate samples for each time point pooled.

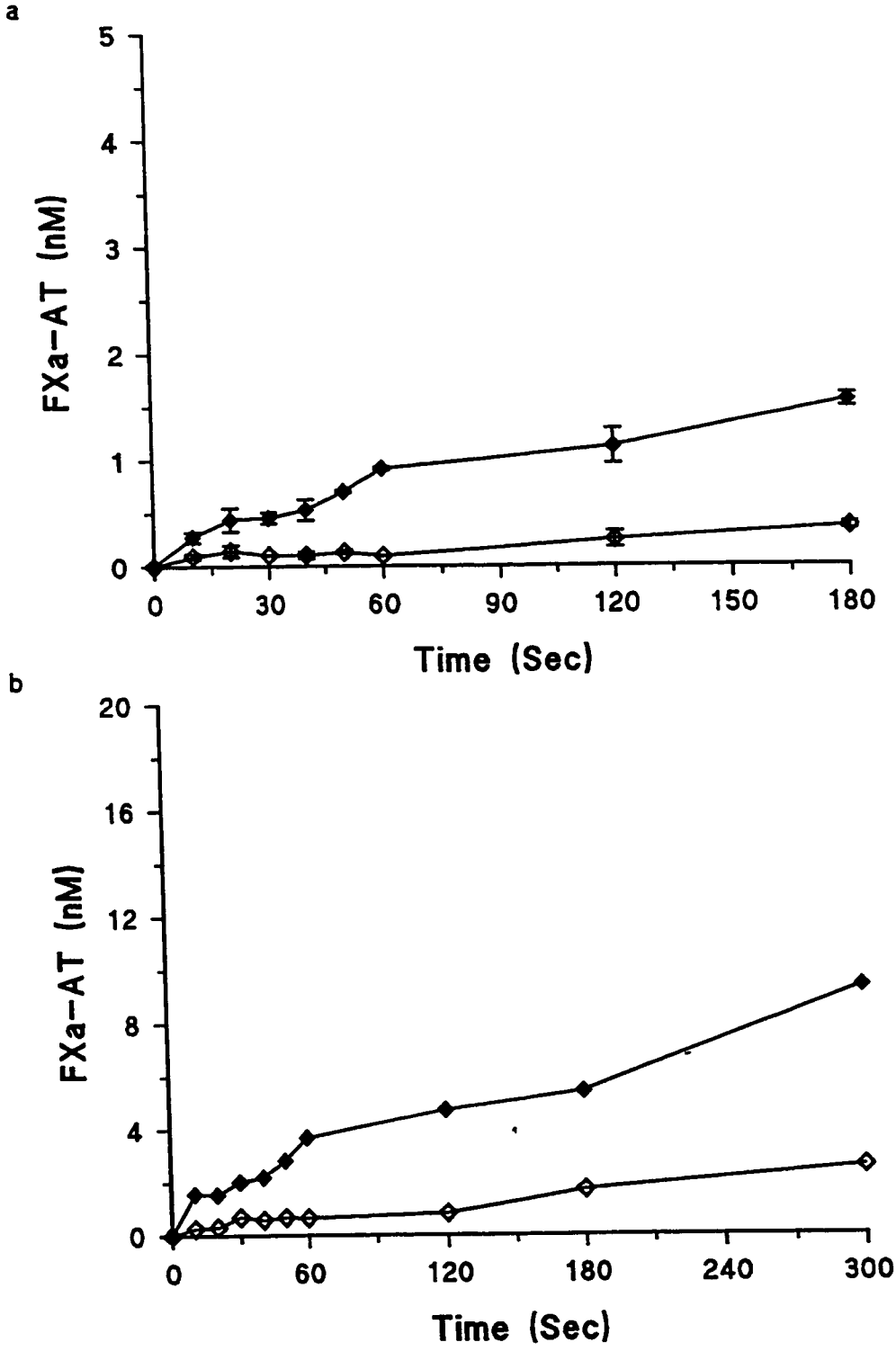
a
FXa-AT (nM)
0
1
2
3
4
5
0
30
60
90
120
150
180
Time (Sec)
b
FXa-AT (nM)
0
4
8
12
16
20
0
60
120
180
240
300
Time (Sec)

absence of the pentasaccharide) to 1.58 nM (in the presence of the pentasaccharide); and at 1 min, from 0.65 nM to 3.70 nM, again an 6-fold increase. Thus, the pentasaccharide accelerates the rate of the complexation of AT Arg47Lys to FXa, but to a lesser extent when compared to wt AT.

Under the same experimental conditions, however, the pentasaccharide did not alter the rate of FXa inactivation by the other three variants, as shown in Fig. 3.10.a, for AT Arg47Tyr; in Fig. 3.10.b, for AT Arg47Pro; and in Fig. 3.10.c, for AT Arg47Glu. Similarly, when 500 nM of each of these AT variants was incubated with 50 nM FXa in the absence and the presence of 250 nM pentasaccharide, there was no difference between the rate of complexation (data not shown). Thus, the pentasaccharide cofactor activity towards FXa inhibition was lost in these three variants.

In summary, the pentasaccharide enhances the rate at which wt AT complexes with FXa. To a lesser extent, it accelerates the complexation of the AT Arg47Lys variant to FXa. The rate of the FXa-complexing reaction for each of the other three AT variants, namely AT Arg47Tyr, AT Arg47Pro, and AT Arg47Glu, was not altered by the pentasaccharide. In other words, the substitution of Arg47 with Lys reduced the anti-FXa pentasaccharide cofactor activity of AT, whereas substitutions with Tyr, Pro, and Glu abolished this activity. It thus appears that an amino acid residue with a positively charged side-chain at position 47 is required for the pentasaccharide accelerated FXa inhibition by AT.

Fig. 3.10. Time-dependent complexation of three AT variants to FXa in the absence and the presence of the pentasaccharide. 200 nM AT in the 20X conditioned medium, pretreated with the Probe-Tek heparin adsorbent, was incubated with 10 nM FXa in the absence (shown by the open symbols) and the presence of 100 nM pentasaccharide (shown by the solid symbols). Each reaction was performed in duplicate and shown is the mean of the duplicates with its standard deviation. Panel a represents AT Arg47Tyr; panel b, AT Arg47Pro; and panel c, AT Arg47Glu.

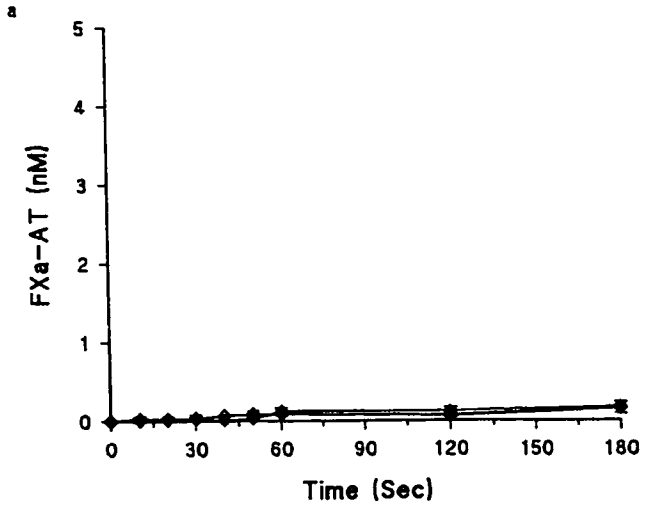
a
FXa-AT (nM)
0
1
2
3
4
5
0
30
60
90
120
150
180
Time (Sec)

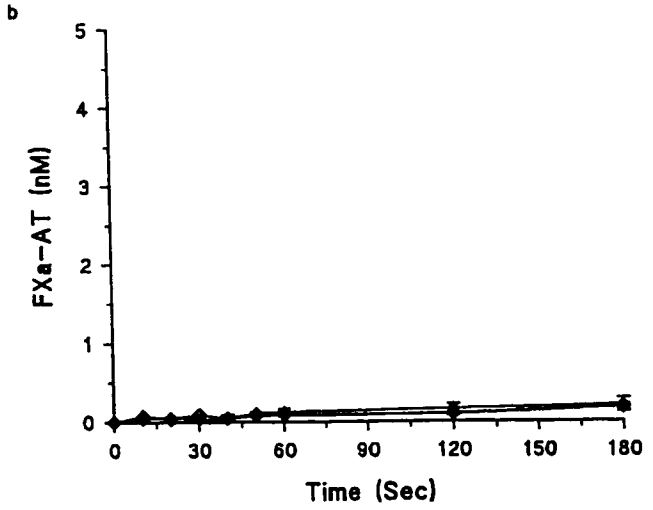
b
FXa-AT (nM)
0
1
2
3
4
5
0
30
60
90
120
150
180
Time (Sec)

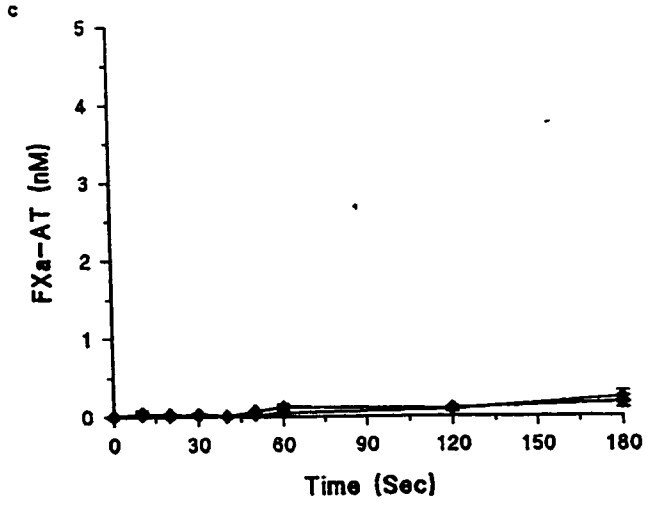
c
FXa-AT (nM)
0
1
2
3
4
5
0
30
60
90
120
150
180
Time (Sec)

It also appears that Tyr, Pro, and Glu substitutions led to loss of progressive AT activity.

3.2. The Pentasaccharide- and Heparin-induced Conformations of the RCL of AT

3.2.1. Creation of AT Pro397Trp cDNA by Site-directed Mutagenesis

An AT moiety with a Pro397Trp mutation was generated by site-directed mutagenesis. To confirm the substitution of the Pro397 codon (CCC) with the Trp codon (TGG), the inserted sequences of recombinant plasmid DNAs from individual transformants were analyzed as outlined in section 2.2.6. Shown in Fig. 3.11 is the sequencing of wt and the intended mutated AT cDNA around the region of codon 397. Construction of the plasmid that allows the expression of the Pro397Trp variant was carried out as outlined in section 2.2.7. Prior to transfection into COS-1 and CHO cells, DNA sequencing analysis was performed. The presence of the intended mutation in the plasmid construct used for transfection was thus confirmed.

3.2.2. Expression in Transiently Transfected COS-1 Cells and Characterization of the Pro397Trp Variant

Before permanently transfected CHO cell line that could express the Pro397Trp variant was established this AT moiety was expressed in transiently

Fig. 3.11. Partial nucleotide sequence of AT cDNA showing the region around codon 397. Dideoxy chain-termination sequencing of DNA was carried out to confirm the intended generation of the AT cDNA with the Pro397Trp substitution. The AT cDNA insert from individual transformants was analyzed with the oligodeoxynucleotide primer AB1594 that anneals to AT cDNA at codons 366-371. At amino acid position 397, CCC encodes wt Pro while GGT encodes Trp.

ACGT
ACGT
CCC
GGT

transfected COS-1 cells and its heparin binding property, progressive thrombin inhibitory activity, and heparin cofactor activity were examined. The COS-expressed Pro397Trp variant was analyzed first by SDS-PAGE following immunoprecipitation (shown in Fig. 3.12). Analysis of the conditioned medium from COS-1 cells transfected with the pCMV5-$AT_{-32-432}^{Pro397Trp}$ construct revealed a protein that was recognized by the sheep-anti-human AT IgG. This protein migrated with an apparent Mr of 58 kDa (shown in lane 3 in Fig. 3.12), which is the same as the wt AT produced in the same system (compare lane 3 and lane 2 in Fig. 3.12). Thus, transfected COS-1 cells synthesized and secreted this AT variant. According to ELISA-based quantitation, this variant was produced at levels within the range of expression seen for wt AT, suggesting that the introduction of the nucleotide substitutions at codon 397 of AT cDNA did not affect the efficiency of expression and secretion by COS-1 cells. In addition, the extent of glycosylation of this moiety appeared to be similar to that of the plasma-derived AT.

This recombinant protein next was analyzed for its heparin binding properties. To obtain a heparin affinity profile, this AT variant, as well as wt AT, were applied to heparin-Sepharose, the Hitrap^{R} heparin, as outlined in section 2.4.7. Under these experimental conditions, the majority of the COS-expressed Pro397Trp variant bound to heparin and were eluted off the heparin-Sepharose peaking at 0.8 M NaCl (shown in Fig. 3.13.b). The observed elution profile of this

Fig. 3.12. SDS-PAGE analysis of COS-expressed wt AT and the AT Pro397Trp variant following immunoprecipitation. ^{35}S-labelled AT moieties in the conditioned media of COS-1 cells transiently transfected with the various AT expressing constructs were immunoprecipitated and visualized by SDS-PAGE on a 12% polyacrylamide gel under reducing conditions, followed by fluorography. Lane 1 contains control material from the COS-1 cells transiently transfected with the vector pCMV5 alone without AT cDNA insert; lane 2, wt AT; and lane 3, the Pro397Trp variant.

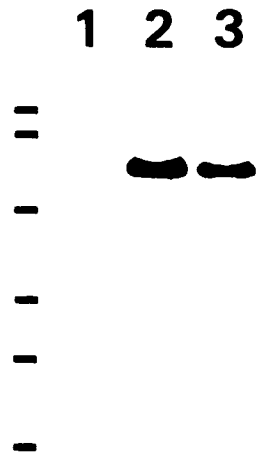
1 2 3

Fig. 3.13. Heparin chromatography of COS-derived wt AT (panel a) and the Pro397Trp variant (panel b).

a

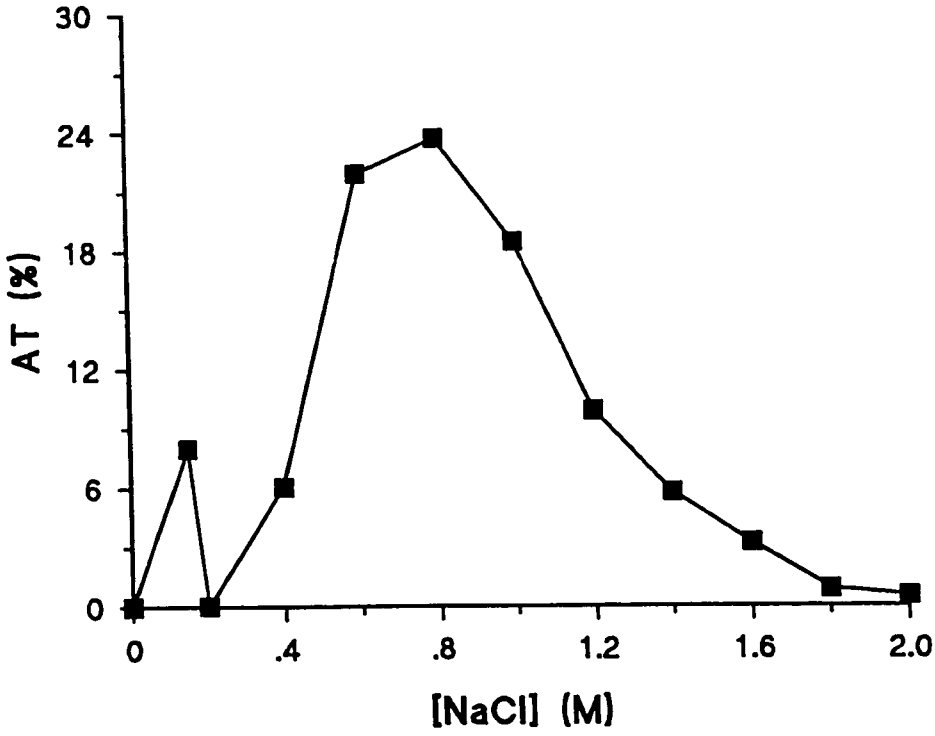
30
24
18
12
6
0
AT (%)
0
.4
.8
1.2
1.6
2.0
[NaCl] (M)

b

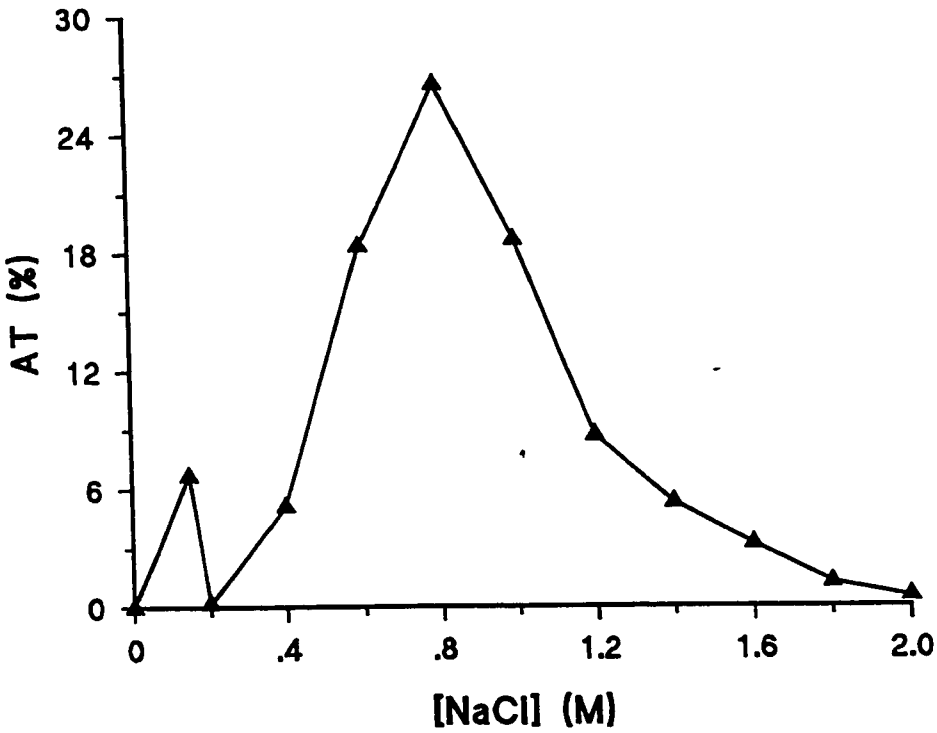
30
24
18
12
6
0
AT (%)
0
.4
.8
1.2
1.6
2.0
[NaCl] (M)

variant was very similar to that of wt AT (compare Fig. 3.13.b to Fig. 3.13.a), implying that it bond to heparin with an affinity similar to that of wt AT.Finally, the progressive thrombin inhibitory activity and the heparin cofactor activity of wt AT (shown in Fig. 3.14) and the Pro397Trp variant (shown in Fig. 3.15) were assayed by analyzing time-dependent complexation to thrombin both in the absence and the presence of heparin, using the conditions described in section 2.4.10. When incubated with α-thrombin, the COS-expressed wt AT formed a SDS-stable thrombin-AT complex of higher Mr of approximately 94 kDa (shown in Fig. 3.14.a). Heparin, as shown in Fig. 3.14.b, enhanced the rate at which wt AT complexed with thrombin. Under the same experimental conditions, the Pro397Trp variant also formed a SDS-stable thrombin-AT complex in a time-dependent manner (shown in Fig. 3.15.a), similar to that seen with wt AT (compare Fig. 3.15.a and Fig. 3.14.a). When heparin was present, the rate of complexation was also enhanced (compare Fig. 3.15.b and Fig. 3.15.a). Thus this variant retained both progressive thrombin inhibitory activity and heparin cofactor activity, despite of the substitution of Pro with Trp residue at the P4' position of its RCL.

In summary, wt AT produced in transiently transfected COS-1 cells is glycosylated and secreted into the culture medium in its biologically active form. The amino acid substitution in the AT Pro397Trp variant does not appear to alter the functional properties of AT. The heparin binding properties of AT and the

Fig. 3.14. Time-dependent complexation of wt AT to α-thrombin in the absence and the presence of heparin. 1 nM AT in the conditioned medium, pretreated with the Probe-Tek heparin adsorbent, was incubated with a 20-fold excess α-thrombin in the absence (panel a) and the presence of 5 nM heparin (panel b). Immediately after each reaction, AT and the thrombin-AT complexes were immunoprecipitated and visualized by SDS-PAGE on a 12% polyacrylamide gel under reducing conditions, followed by fluorography. Lane 1 represents AT without thrombin; and lanes 2-8, represent incubation times of 15 sec, 30 sec, 1 min, 2 min, 5 min, 10 min, and 20 min, respectively.

a

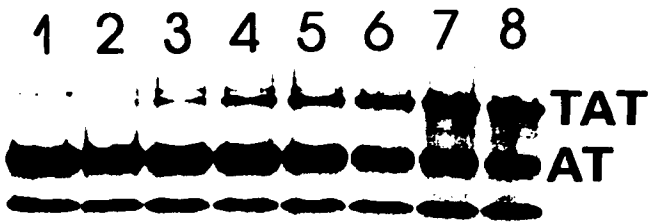

b

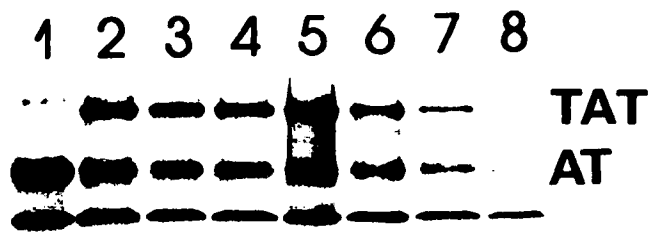

Fig. 3.15. Time-dependent complexation of the AT Pro397Trp variant to α-thrombin in the absence and the presence of heparin. 1 nM AT in the conditioned medium, pretreated with the Probe-Tek heparin adsorbent, was incubated with a 20-fold excess α-thrombin at 37 °C in the absence (panel a) and the presence of 5 nM heparin (panel b). Immediately after each reaction, AT and the thrombin-AT complexes were immunoprecipitated and visualized by SDS-PAGE on a 12% polyacrylamide gel under reducing conditions, followed by fluorography. Lane 1 represents AT without thrombin; and lanes 2-8 represent incubation times of 15 sec, 30 sec, 1 min, 2 min, 5 min, 10 min, and 20 min, respectively.

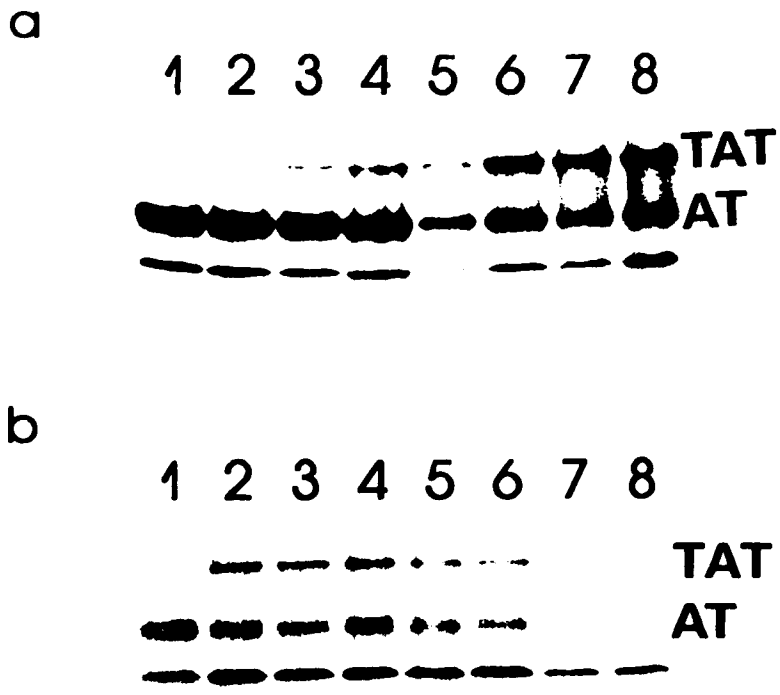
a
1 2 3 4 5 6 7 8
TAT
AT
b
1 2 3 4 5 6 7 8
TAT
AT

formation of covalent thrombin-AT complex are very sensitive to the overall folding of the molecule, it thus appears that the folding of this recombinant protein is not significantly different from that of wt AT.

3.2.3. Establishment of AT-producing CHO Cell Lines

To further explore the fluorescent and functional properties of this AT variant and the feasibility of using it to differentiate the pentasaccharide- and heparin-induced conformations of the RCL, a high-yield expression system that could produce sufficient amount of AT allowing for its purification was required. Thus the expression of wt AT and the Pro397Trp variant in permanently transfected CHO cell lines was attempted. To establish permanent AT-producing CHO cell lines, a mammalian expression plasmid construct, pCMV5-$AT_{-32-432}^{wt}$ and PCMV5-$AT_{-32-432}^{Pro397Trp}$, respectively, and a Neo-resistant plasmid pSV2Neo were cotransfected into CHO cells, employing the lipofectin^{R} reagent. Transfection with the plasmid pSV2Neo would confer geneticin resistance to the cells, thus allowing the selection of the cells transfected with the desired AT expression construct. Since the two plasmids were employed in a ratio of pCMV5:pSV2Neo of 10:1, most of the cells which were transfected with pSV2Neo should theoretically had been cotransfected with pCMV5, and this was shown experimentally to be the case for both the wt and the mutant constructs. Thus, the transfected cells were first selected by resistance to geneticin and subsequently

subsequently screened for AT expression. According to ELISA-based quantitation, among the eighty-two geneticin-resistant colonies that were exposed to the wt AT expression construct, 91.5% were positive for AT expression. For the mutant construct, AT was expressed in 91.1% of the seventy-eight examined geneticin-resistant colonies. Due to the nature and the practical means of the selection used, such AT-expressing cells could be contaminated with non-AT-producing cells that were transfected with the pSV2Neo plasmid only. Two high producers for each AT moiety were subcloned by the limited dilution method. Thus, each high AT producer was diluted to 1-10 cells per well in a 96-well tissue plate. For each AT moiety, 60 fast-growing colonies were expanded and their AT expression levels again checked by an ELISA. Finally the three highest AT producers, per AT moiety, were clonally expanded and stored for further expansion. Such subcloning served not only to purify the AT-expressing colony, thus increasing the AT expression levels, but also to select for cells with fast-growing characteristics. As a result of this subcloning step, a 3- to 4-fold increase in the AT expression level was achieved.

3.2.4. Expression in Permanently Transfected CHO Cells and Purification of CHO-produced AT Moieties

To produce wt AT and its Pro397Trp variant in quantities sufficient for their purification and characterization, permanently transfected CHO cell cultures

were amplified in suspension. AT was allowed to be expressed and secreted into serum free medium for up to 72 h and the expression levels checked by an ELISA. According to such ELISA-based quantitation assays, a 60 h incubation was optimal in terms of AT expression (data not shown), and this incubating period was used for subsequent production of recombinant AT proteins. Under these experimental conditions, AT was expressed at levels of 0.5-1.5 μg/ml.

The CHO-derived AT proteins were affinity-purified on heparin-Sepharose as detailed in section 2.4.5. In preliminary experiments, the concentrated medium was applied directly to a Hitrap^R heparin column. Shown in Fig. 3.16 is the elution profile for wt AT. Two major peaks, peak I and peak II, were observed. While peak I eluted off the heparin-Sepharose at less than 0.5 M NaCl, peak II eluted off at approximately 1.2 M NaCl. Fractions from both peaks were analyzed by SDS-PAGE. Whereas many proteins with different sizes constituted fractions of peak I; in the fractions from peak II, there was only one major component which migrated with an apparent molecular mass of 58 kDa (data not shown). Fractions from peak II were pooled, concentrated, and dialyzed against PBS plus buffer. Western blotting analysis demonstrated that the major component, that had a mobility similar to the plasma-derived AT, was recognized by the sheep-anti-human IgG (data not shown). The recovered AT, based on ELISA quantitation, however, was less than 10% of total AT in the applied conditioned medium. Approximately 60-70% of AT did not bind to the column

Fig. 3.16. Heparin chromatography of the conditioned medium of permanently transfected CHO cells expressing wt AT.

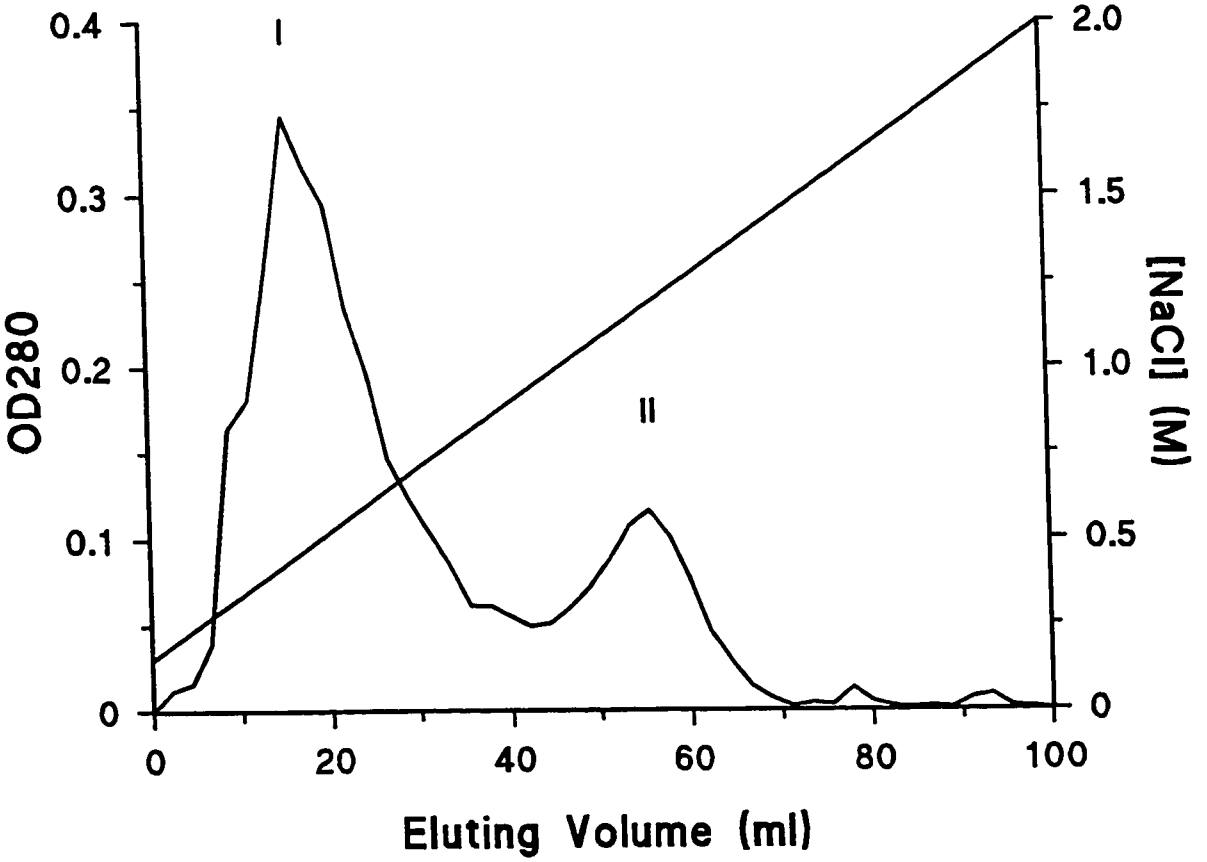
0.4
0.3
0.2
0.1
0
OD280
I
II
2.0
1.5
1.0
0.5
0
[NaCl] (M)
0
20
40
60
80
100
Eluting Volume (ml)

and thus was present in the flow through and the 0.15 M wash. In an attempt to improve the binding of recombinant AT to heparin and thus the recovery rate, an anion exchanger Q-Sepharose (Q-Sepharose^{R} fast flow) was applied to the conditioned medium prior to affinity chromatography on heparin-Sepharose. Approximately 70-85% of the applied wt AT was present in the flow through and the low salt wash up to 0.3 M NaCl. These fractions were pooled and their salt concentration adjusted to 0.15 M. This AT-containing preparation was then subjected to heparin chromatography. Pretreatment with Q-Sepharose improved the binding of wt AT to heparin. As a consequence, the recovery rate of AT over heparin-Sepharose increased 3- to 5-fold. Thus, clearing the concentrated conditioned medium through Q-Sepharose was applied in all the preparatory experiments prior to affinity chromatography on heparin-Sepharose.

When applied to the heparin-Sepharose, a very similar elution profile was observed for the AT Pro397Trp variant (data not shown). Application of Q-Sepharose prior to heparin chromatography also improved the binding of this AT moiety to heparin and consequently increased its recovery (data not shown). Thus, the pretreatment with Q-Sepharose was applied in all the preparatory experiments for the Pro397Trp variant. Actually, this recombinant protein was purified under the same conditions as that used for wt AT.

Contamination of purified AT samples with heparin from heparin-Sepharose column could interfere with subsequent characterization of these

recombinant AT proteins. In order to eliminate any heparin present, another Q-Sepharose chromatography was applied after dialysis of the purified AT samples following the heparin chromatography step. More than 80% of AT was recovered in the flow through and the 0.3 M wash of this Q-Sepharose chromatography and the salt concentration of the final AT preparation was adjusted to 0.15 M NaCl.

The purified recombinant AT proteins, along with BSA and the plasma-derived AT, were analyzed by SDS-PAGE on a 12% acrylamide gel under reducing conditions (shown in Fig. 3.17.a). Both purified recombinant proteins migrated with an apparent Mr similar to that of plasma AT. To confirm their identities, Western blotting was performed probed with sheep-anti-human AT IgG (shown in Fig. 3.17.b). In sharp contrast to the BSA, the purified recombinant AT proteins, as well as the plasma AT, were all recognized by this affinity-purified human AT specific IgG. The purified recombinant proteins thus represented CHO-expressed wt AT and the Pro397Trp variant, respectively. According to SDS-PAGE (see Fig. 3.17.a), they were purified to greater than 98% homogeneity. As judged by Western blotting, no major degradation occurred during the purification process (see Fig. 3.17.b).

In summary, full length AT was produced in permanently transfected CHO cells in a glycosylated form and secreted into the culture medium. The Pro397Trp variant exhibits the same characteristics as wt AT during purification by Q-Sepharose, heparin affinity, and subsequent Q-Sepharose chromatography.

Fig. 3.17. Analysis of the purified CHO-derived AT proteins by SDS-PAGE and Western blotting. Following SDS-PAGE of the purified AT proteins on a 12% polyacrylamide gel under reducing conditions (panel a), they were analyzed by Western blotting, probed with the sheep anti-human AT IgG (panel b). Lane 1 shows the molecular weight markers; lane 2, BSA; lane 3, the plasma-derived AT; lane 4, the purified CHO-derived wt AT; and lane 5, the purified CHO-derived Pro397Trp variant.

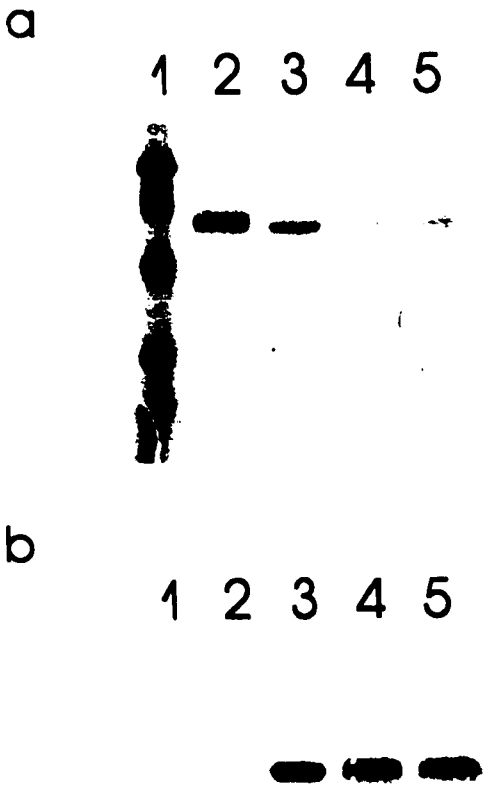
a
1 2 3 4 5
b
1 2 3 4 5

Both recombinant proteins were purified to greater than 98% homogeneity with overall yields of approximately 25%.

3.2.5. Determination of the K_ds for the Pentasaccharide-AT and Heparin-AT Complexes

Interactions of heparin and the pentasaccharide with wt AT and its Pro397Trp variant, as well as the plasma-derived moiety, were studied as described in section 2.4.8 by following changes in endogenous Trp fluorescence that accompanied the binding during titration. In order to determine the K_ds of these complexes, the emission spectrum at 340 nm of each AT moiety after excitation at 280 nm was measured on a luminescence spectrophotometer before titration and after the addition of each specific saccharide. Shown in Fig. 3.18 are changes in Trp fluorescence of plasma AT, the CHO-derived wt AT, as well as the CHO-derived Pro397Trp variant, shown as a function of added heparin at ionic strength (I) of 0.15 M. Titrations of the pentasaccharide with these three AT moieties are shown in Fig. 3.19. K_ds were determined by nonlinear least square fitting of the observed endogenous Trp fluorescence enhancement upon titration with heparin and the pentasaccharide. Table 3.1 summarizes the K_d values for the complexes formed with each of these AT moieties, for both the pentasaccharide and high affinity heparin at I 0.15. The K_d for heparin and plasma AT was estimated, in this experimental system, to be 11.5±1.4 nM, in good agreement with

Fig. 3.18. Changes in Trp fluorescence of the various AT moieties as a function of added heparin at I 0.15. Panel a shows titration of high-affinity heparin with plasma AT; panel b, the CHO-derived wt AT; and panel c, the CHO-derived Pro397Trp variant.

a

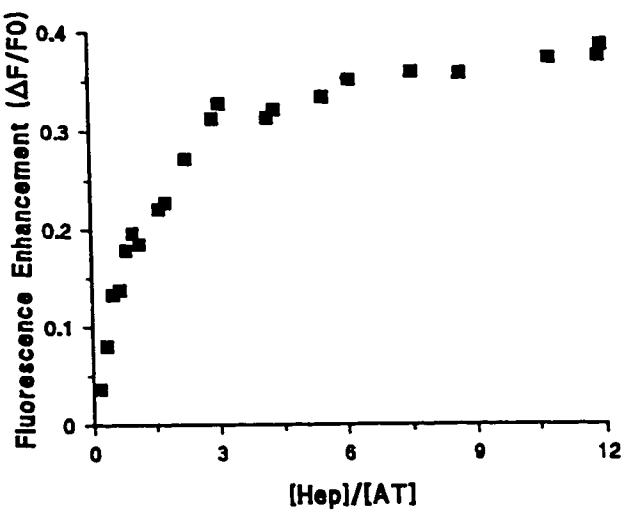
Fluorescence Enhancement (ΔF/F0)
0.4
0.3
0.2
0.1
0
0
3
6
9
12
[Hep]/[AT]

b

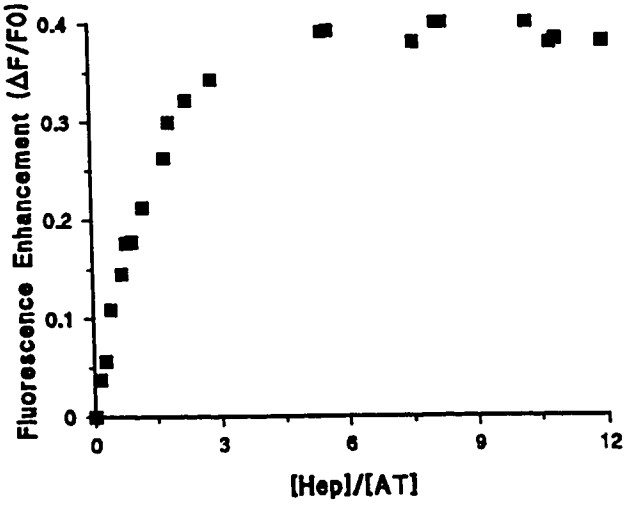
Fluorescence Enhancement (ΔF/F0)
0.4
0.3
0.2
0.1
0
0
3
6
9
12
[Hep]/[AT]

c

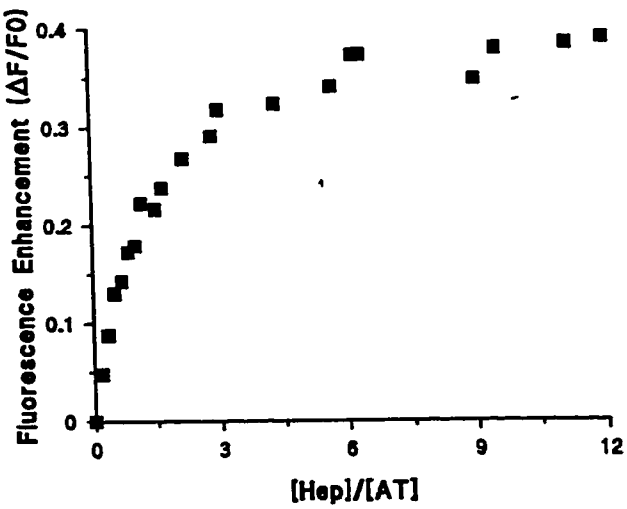
Fluorescence Enhancement (ΔF/F0)
0.4
0.3
0.2
0.1
0
0
3
6
9
12
[Hep]/[AT]

Fig. 3.19. Changes in Trp fluorescence of the various AT moieties as a function of added the pentasaccharide at I 0.15. Panel a shows the titration of the pentasaccharide with plasma AT; panel b, the CHO-derived wt AT; and panel c, the CHO-derived Pro397Trp variant.

a

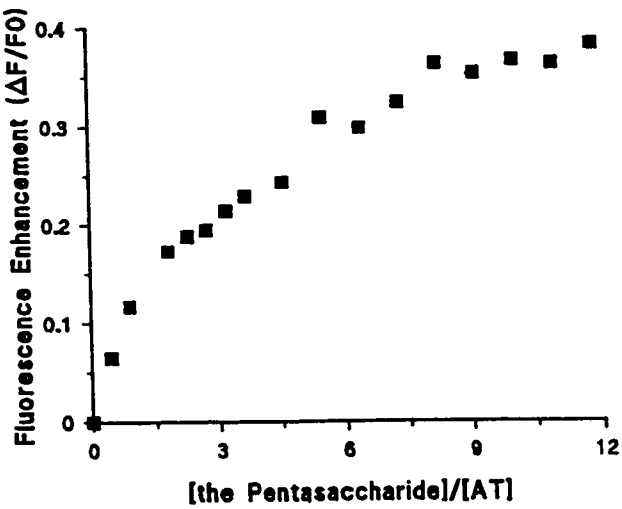
Fluorescence Enhancement (ΔF/F0)
0.4
0.3
0.2
0.1
0
0
3
6
9
12
[the Pentasaccharide]/[AT]

b

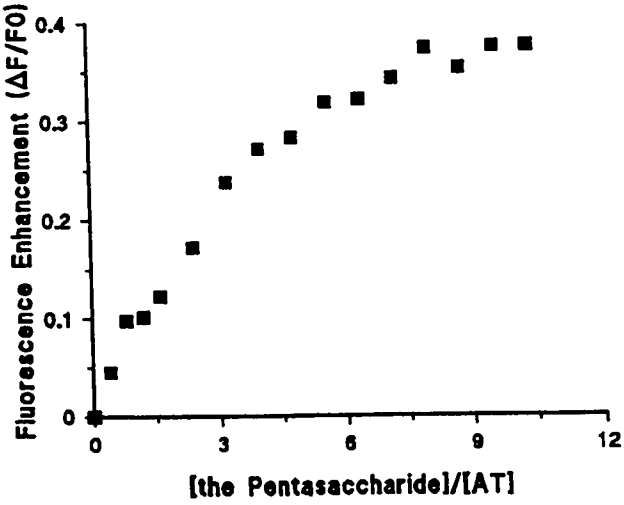
Fluorescence Enhancement (ΔF/F0)
0.4
0.3
0.2
0.1
0
0
3
6
9
12
[the Pentasaccharide]/[AT]

c

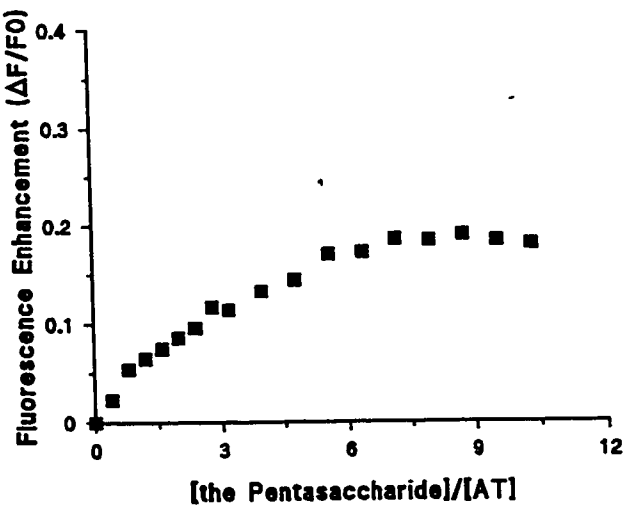
Fluorescence Enhancement (ΔF/F0)
0.4
0.3
0.2
0.1
0
0
3
6
9
12
[the Pentasaccharide]/[AT]

Table 3.1. Dissociation constants for both heparin- and pentasaccharide-complexes of the various AT moieties at I 0.15.

Antithrombin	Dissociation Constant[a] (nM)	
	The Pentasaccharide	Full-length Heparin
Plasma AT	42.1 ± 8.2	11.5 ± 1.4
CHO-derived wt AT	48.8 ± 6.8	13.7 ± 1.4
CHO-derived the Pro397Trp variant	43.2 ± 5.5	10.9 ± 1.1

[a] ± two standard deviations.

the published data of 10-20 nM at physiological pH and ionic strength (Nordenman *et al.*, 1978; Jordan *et al.*, 1979; Olson *et al.*, 1981; Olson *et al.*, 1992). The observed K_d of 13.7±1.4 nM for heparin and recombinant wt AT suggested that CHO-derived wt AT had similar heparin binding properties as the plasma-derived AT. Based on the estimated K_d of 10.9±1.1 nM for heparin and the Pro397Trp variant, the Pro397Trp substitution did not alter the heparin binding activity of AT. The observed K_d values for the pentasaccharide complexes of plasma AT, recombinant wt AT, and the Pro397Trp variant were 42.1±8.2 nM, 48.8±6.8 nM, and 43.2±5.5 nM, respectively. When compared with those for the corresponding heparin-AT complexes, these values were approximately 3- to 4-fold lower, consistent with observations in the literature (Olson *et al.*, 1992). Thus, the substitution of Pro397 with Trp did not change the affinity of AT for the pentasaccharide.

3.2.6. Fluorescence Properties of wt AT and the Pro397Trp Variant

The fluorescence emission spectrum of recombinant AT proteins in comparison with plasma AT is shown in Fig. 3.20. The CHO-derived wt AT, when excited at 280 nm, exhibited a fluorescence emission maximum at 340 nm over the range of 290-400 nm (shown in Fig. 3.20.b). The characteristic 340-nm maximum indicates that the fluorescence of this wt AT is primarily due to the four Trp residues of this molecule. No peak or shoulder was observed at 300-310 nm in

Fig. 3.20. Fluorescence emission spectra of the various AT moieties. The emission spectrum of each AT protein was recorded over the range of 290 to 400 nm at I 0.15 on a luminescence spectrophotometer, with excitation at 280 nm. Panel a shows plasma AT; panel b, the CHO-derived wt AT; and panel c, the CHO-derived Pro397Trp variant.

a

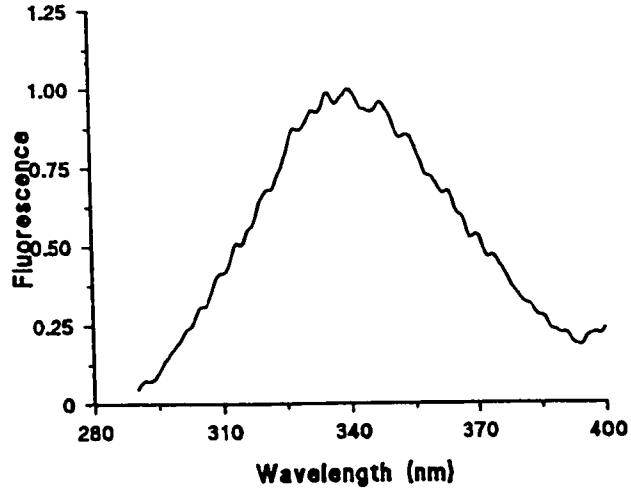
1.25
1.00
0.75
0.50
0.25
0
Flugrescence
280
310
340
370
400
Wavelength (nm)

b

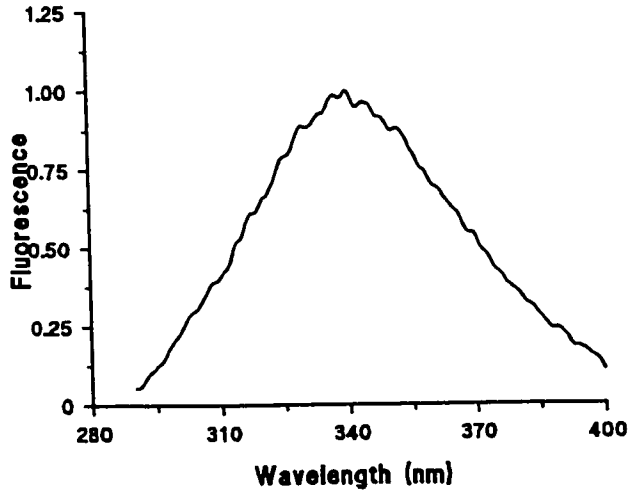
1.25
1.00
0.75
0.50
0.25
0
Flugrescence
280
310
340
370
400
Wavelength (nm)

c

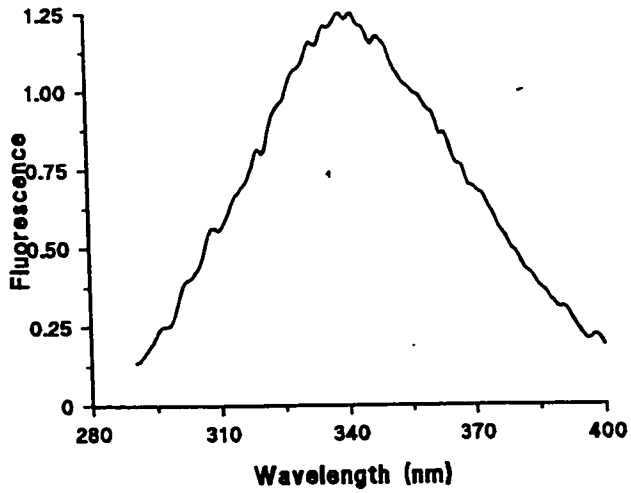
1.25
1.00
0.75
0.50
0.25
0
Flugrescence
280
310
340
370
400
Wavelength (nm)

this 280-nm excited spectrum, suggesting that Tyr emission was minor. In addition, the fluorescence spectrum of this CHO-derived wt AT was identical to that of the plasma AT (shown in Fig. 3.20.a) in terms of the shape of the curve, relative intensity, and the fluorescence emission maximum at 340 nm (compare Fig. 3.20.b to Fig. 3.20.a). The fluorescence emission spectrum of the Pro397Trp variant excited at 280 nm is shown in Fig. 3.20.c. It is obvious that endogenous Trp fluorescence of the Pro397Trp variant is greater than that of wt AT. In fact, the difference between Fig. 3.20.b and Fig. 3.20.c represents the emission spectrum of the novel Trp at position 397. Data from nine individual measurements revealed that there was a 25% enhancement in endogenous Trp fluorescence with the Pro397Trp variant, which is in keeping with the addition of one Trp to the four Trp residues present in the native AT molecule.

3.2.7. The Maximal Fluorescence Enhancements of wt AT and the Pro397Trp Variant

The maximal fluorescence enhancements of wt AT, the Pro397Trp variant, and plasma AT, in the presence of saturating concentration of heparin, are shown in Fig. 3.21. Upon binding, heparin induced a 40% increase in Trp fluorescence in the plasma AT (shown in Fig. 3.21.a), consistent with what has been reported in the literature. A 40% increase in the Trp fluorescence was also seen for both wt AT (shown in Fig. 3.21.b) and the Pro397Trp variant (shown in

Fig. 3.21. Maximal fluorescence changes of the various AT moieties in the presence of saturating concentration of heparin. Panel a shows plasma AT; panel b, the CHO-derived wt AT; and panel c, the CHO-derived Pro397Trp variant.

a

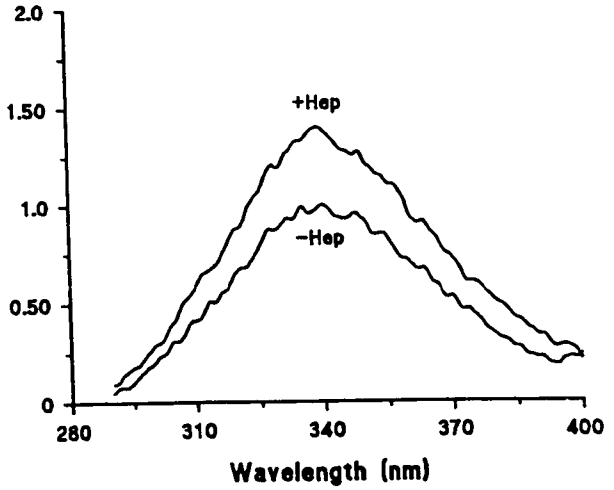
2.0
1.50
1.0
0.50
0
+Hep
−Hep
280
310
340
370
400
Wavelength (nm)

b

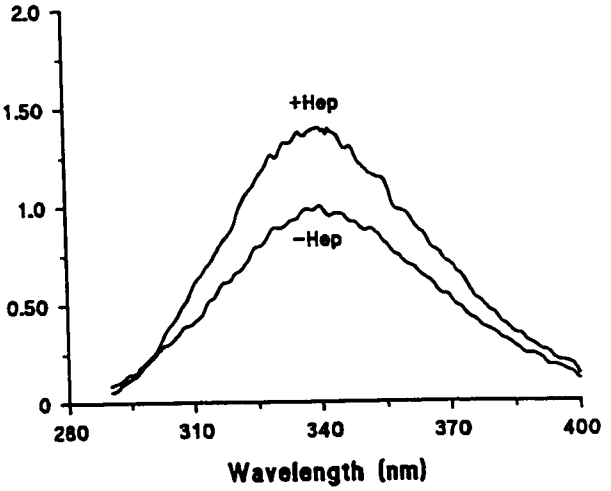
2.0
1.50
1.0
0.50
0
+Hep
−Hep
280
310
340
370
400
Wavelength (nm)

c

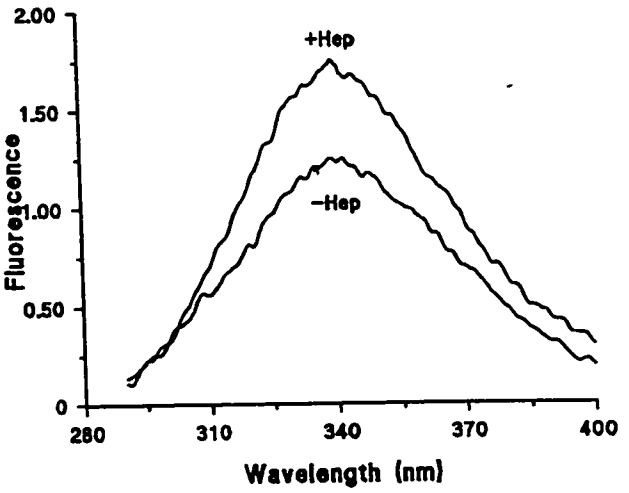
2.00
1.50
1.00
0.50
0
Fluorescence
+Hep
−Hep
280
310
340
370
400
Wavelength (nm)

Fig. 3.21.c). When compared with plasma AT and recombinant wt AT, the same fractional enhancement for the Pro397Trp variant, however, corresponds to a larger absolute enhancement, since the initial fluorescence is increased by the presence of the additional Trp at P4'.

The pentasaccharide induced maximal fluorescence enhancements of these three AT moieties are shown in Fig. 3.22. A 38% increase in Trp fluorescence of plasma AT (shown in Fig. 3.22.a) agrees with previous observations made by Olson *et al.* (1992). The maximal fluorescence enhancement of wt AT in the presence of saturating concentration of the pentasaccharide (shown in Fig. 3.22.b) is similar to that of plasma AT. A 20% increase, however, is seen for the Pro397Trp variant (shown in Fig. 3.22.c). This lower fractional enhancement conforms a smaller absolute enhancement. The heparin-induced AT conformation, thus, is shown to be different from that induced by the pentasaccharide (compare Fig. 3.21.c to Fig. 3.22.c).

Table 3.2 summarizes the fluorescence properties of these three AT moieties in the absence and the presence of the pentasaccharide or heparin. These properties are displayed schematically in Fig. 3.23.a. Fluorescence spectrum differences between the variant Pro397Trp and wt AT exhibit the fluorescence properties of the P4' Trp alone (see Fig. 3.23.b). It appears that the fluorescence of this Trp residue is enhanced 40% by heparin, whereas the

Fig. 3.22. Maximal fluorescence changes of the various AT moieties in the presence of saturating concentration of the pentasaccharide. Panel a shows plasma AT; panel b, the CHO-derived wt AT; and panel c, the CHO-derived Pro397Trp variant.

a

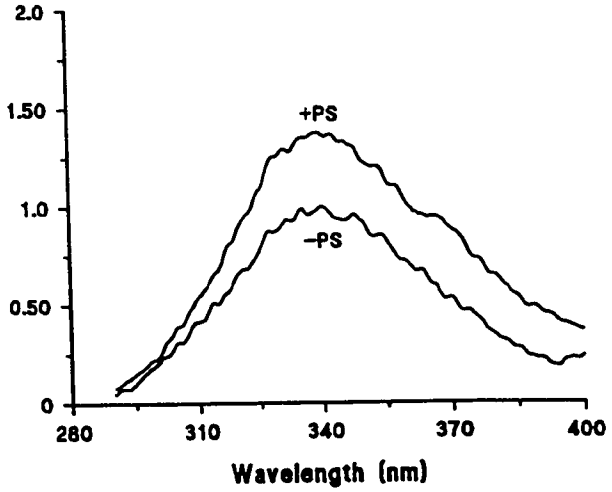
2.0
1.50
1.0
0.50
0
+PS
-PS
280
310
340
370
400
Wavelength (nm)

b

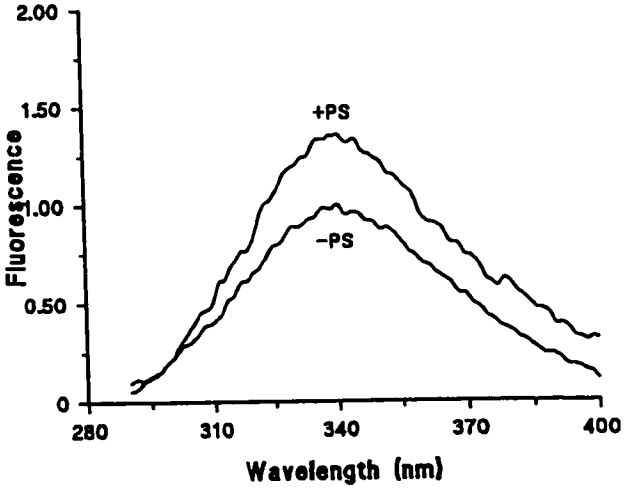
2.00
1.50
1.00
0.50
0
Fluorescence
+PS
-PS
280
310
340
370
400
Wavelength (nm)

c

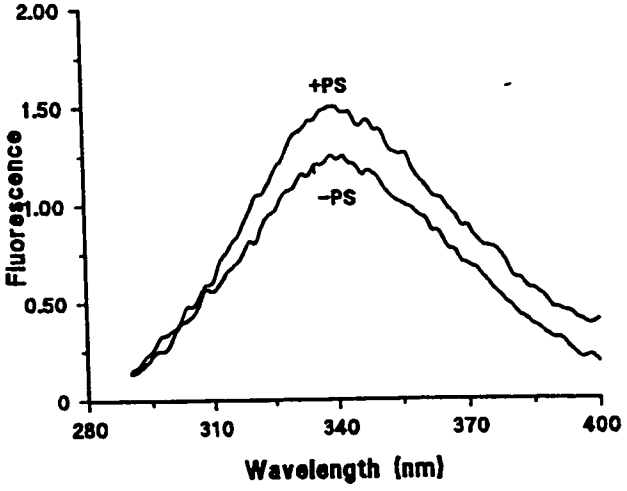
2.00
1.50
1.00
0.50
0
Fluorescence
+PS
-PS
280
310
340
370
400
Wavelength (nm)

Table 3.2. Fluorescence properties of the various AT moieties and their pentasaccharide- and heparin-complexes.

Antithrombin	Fluorescence Intensity	ΔF_{max}[a] (%)	
		The Pentasaccharide	Full-length Heparin
Plasma AT	1.00	38 ± 2	40 ± 2
CHO-derived wt AT	1.00	38 ± 2	40 ± 2
The Pro397Trp variant	1.25	20 ± 2	40 ± 2

[a] ± two standard deviations.

Fig. 3.23. Schematic illustration of the fluorescence properties of the various AT moieties and of the novel P4' Trp residue. Chart a shows plasma AT (labelled as pAT), the CHO-derived wt AT (wt), the CHO-derived Pro397Trp variant (Trp), and their heparin- and pentasaccharide-complexes. Shown in chart b is the fluorescence emission spectra of Trp397, both in the absence and the presence of the pentasaccharide and heparin, respectively. They were obtained by subtracting wt AT fluorescence spectra from those of the corresponding Pro397Trp variant.

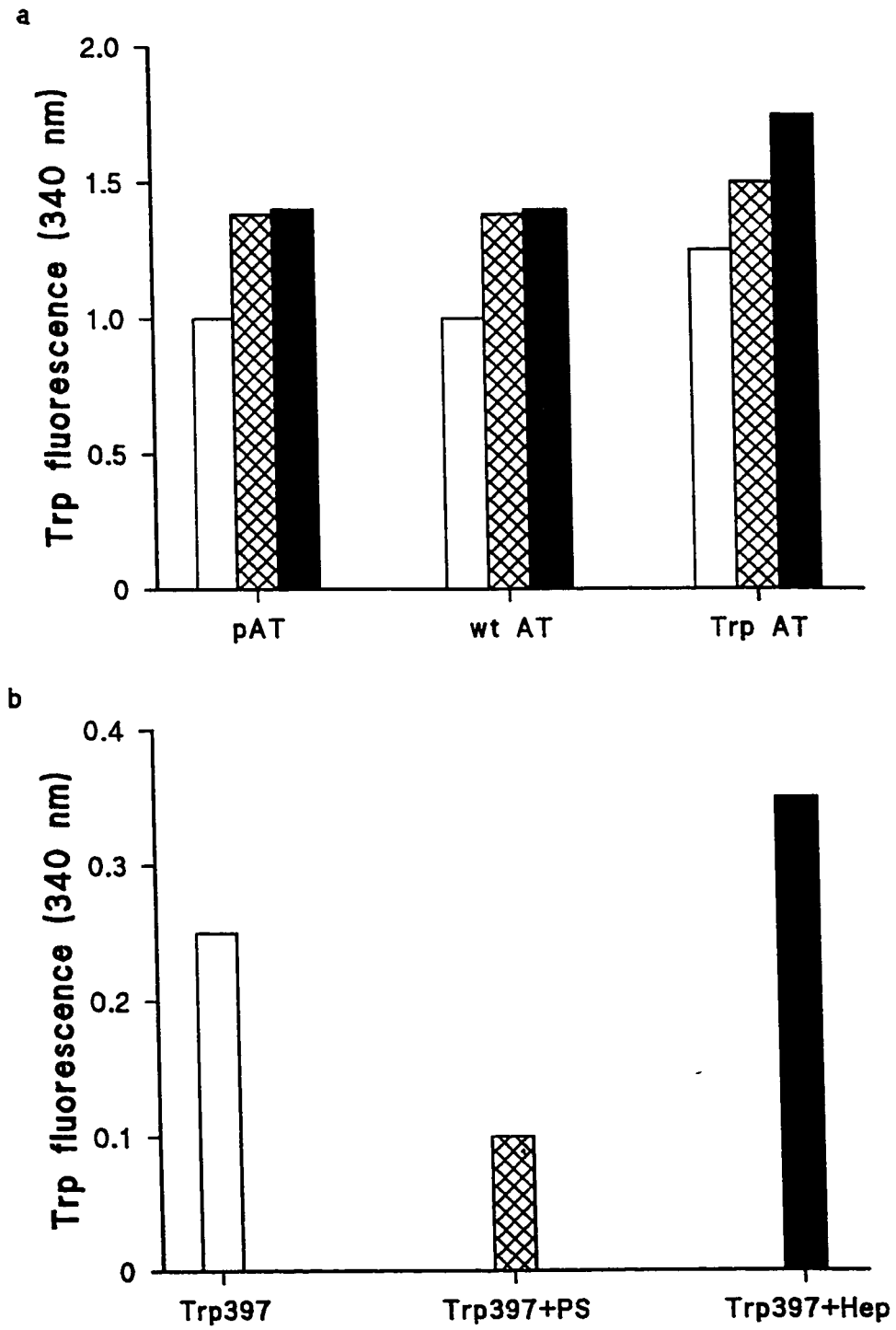
a
2.0
1.5
1.0
0.5
0
Trp fluorescence (340 nm)
pAT
wt AT
Trp AT
b
0.4
0.3
0.2
0.1
0
Trp fluorescence (340 nm)
Trp397
Trp397+PS
Trp397+Hep

pentasaccharide diminishes its fluorescence by 60%. The fluorescence property of Trp is modified by the quenching effects of its environment, and the increased fluorescence of the P4' Trp thus suggests that heparin, upon binding to AT, causes structural perturbation in such a way that the P4' residue is further away from associated fluorescence quenching residues. On the other hand, the pentasaccharide probably transfers the P4' Trp closer to some fluorescence quenching residues. It thus appears that the presence of the novel Trp at P4' of its RCL has allowed us to distinguish and demonstrate different RCL conformations induced by the two different heparin species, i.e. the pentasaccharide and full-length heparin.

3.2.8. Complexes with FXa

To characterize the proteinase inhibitory activity of the Pro397Trp variant, complexation of this variant as well as wt AT and plasma AT to FXa was carried out in the absence and the presence of the pentasaccharide and heparin. In each case, 200 nM AT was incubated with 10 nM FXa. When present in the reaction, the final concentration of the pentasaccharide or heparin was 100 nM. The time-dependent complexation of these AT moieties to FXa are shown in Fig. 3.24 for the pentasaccharide and in Fig. 3.25 for heparin. All three AT moieties complexed with FXa. Both the pentasaccharide (see Fig. 3.24) and heparin (see Fig. 3.25) enhanced the rate of complexation of these AT moieties to FXa. The

Fig. 3.24. Time-dependent complexation of various AT moieties to FXa in the absence (shown by the symbol ◇) and the presence of the pentasaccharide (shown by the symbol ♦). 200 nM AT was incubated with 10 nM FXa in the absence and the presence of 100 nM pentasaccharide. Each reaction was performed in duplicate and shown is the mean of the duplicate with its standard deviation. Panel a shows the results with plasma AT; panel b, with wt AT; and panel c, with the Pro397Trp variant.

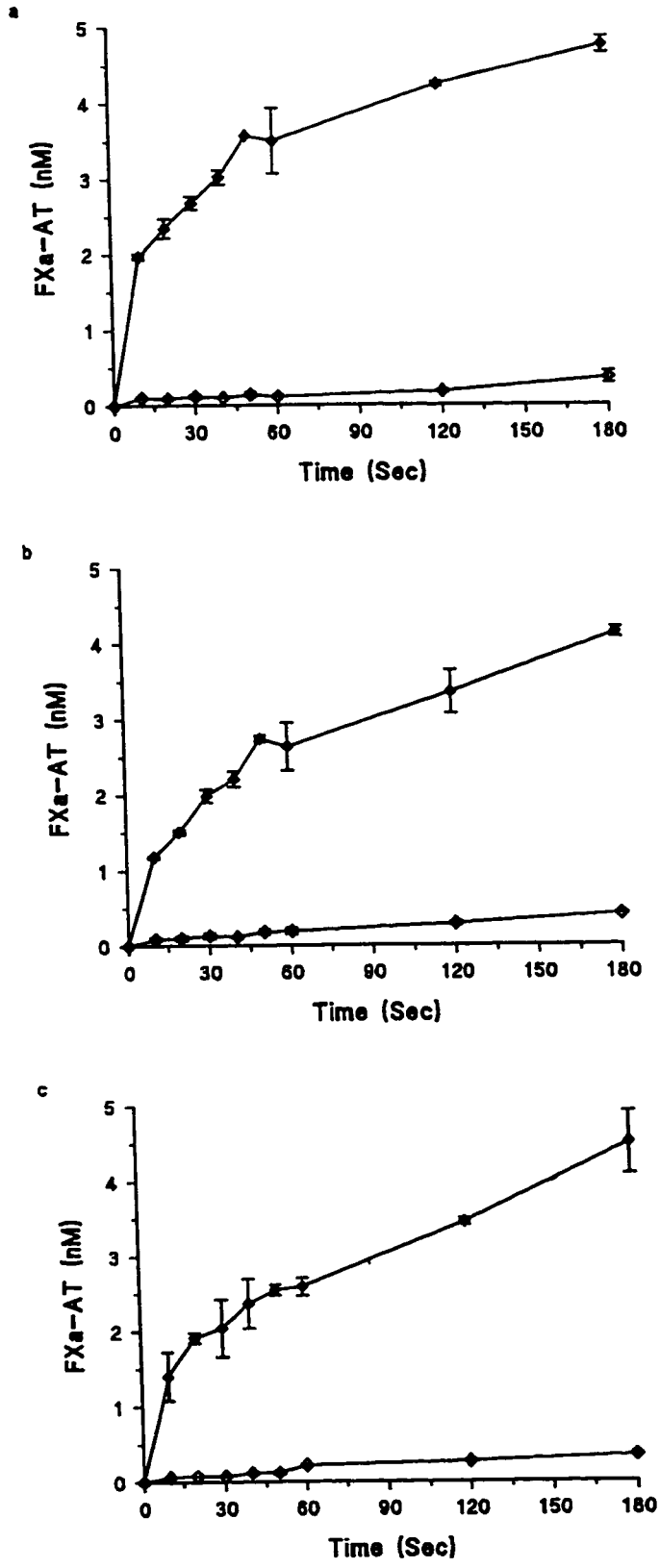
a
FXa-AT (nM)
0
1
2
3
4
5
0
30
60
90
120
150
180
Time (Sec)
b
FXa-AT (nM)
0
1
2
3
4
5
0
30
60
90
120
150
180
Time (Sec)
c
FXa-AT (nM)
0
1
2
3
4
5
0
30
60
90
120
150
180
Time (Sec)

Fig. 3.25. Time-dependent complexation of various AT moieties to FXa in the absence (shown by the symbol ◇) and the presence of heparin (shown by the symbol ♦). 200 nM AT was incubated with 10 nM FXa in the absence and the presence of 100 nM heparin. Each reaction was performed in duplicate and shown is the mean of the duplicate with its standard deviation. Panel a shows the results with plasma AT; panel b, with wt AT; and panel c, with the Pro397Trp variant.

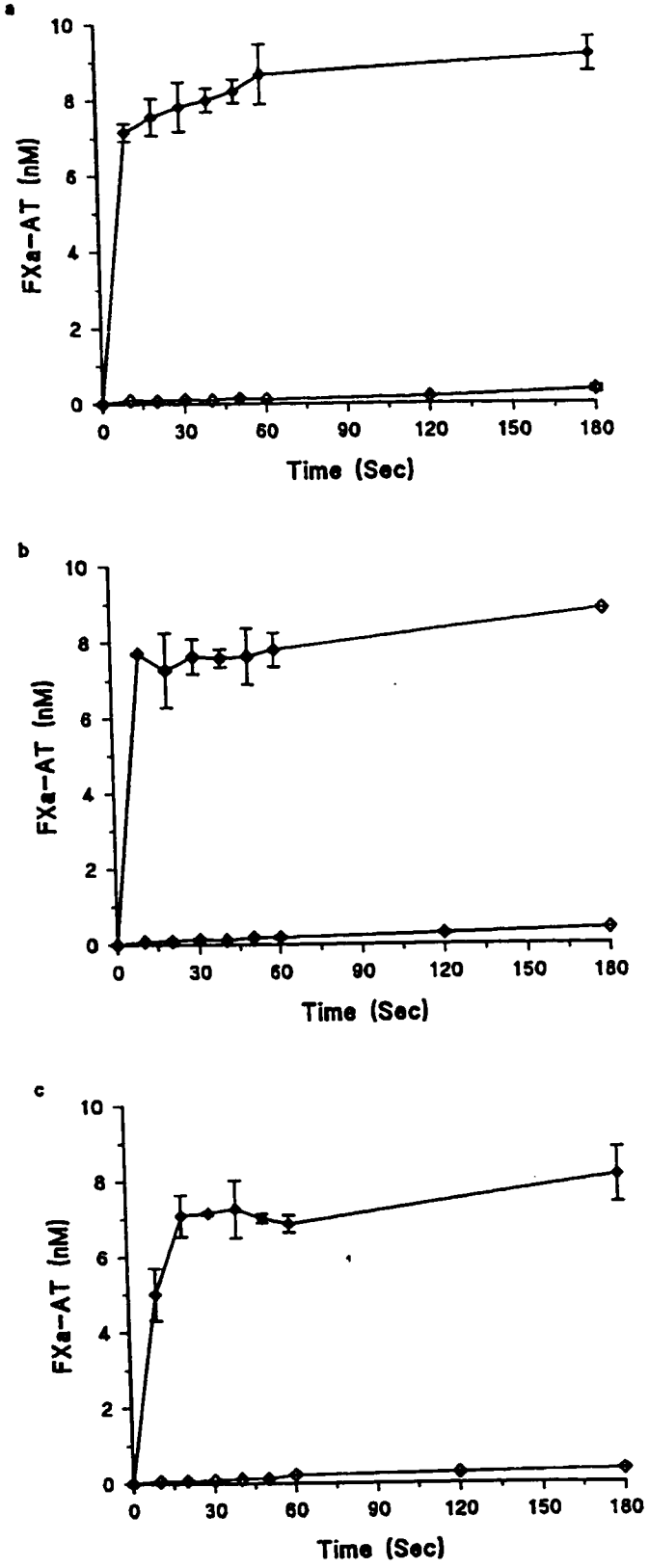
a
FXa-AT (nM)
10
8
6
4
2
0
0
30
60
90
120
150
180
Time (Sec)
b
FXa-AT (nM)
10
8
6
4
2
0
0
30
60
90
120
150
180
Time (Sec)
c
FXa-AT (nM)
10
8
6
4
2
0
0
30
60
90
120
150
180
Time (Sec)

Pro397Trp substitution had no effect on the progressive FXa inhibitory activity of AT and the pentasaccharide and the heparin cofactor activities towards FXa inhibition. Moreover, at the early phase of the reaction, the rate enhancing effect of heparin on FXa inhibition is greater than that of the pentasaccharide (compare Fig. 3.24 and Fig. 3.25). At 10 s, the rate enhancing effects of the pentasaccharide on FXa inhibition by the plasma-derived AT, wt AT, and AT Pro397Trp are 20.4-, 18.6-, and 22.6-fold, respectively. Heparin accelerated complexation of these AT moieties to FXa by 74.5-fold for the plasma-derived AT, 80.3-fold for wt AT, and 80.7-fold for the Pro397Trp variant.

In summary, the CHO-produced wt AT is functionally fully active when compared with the natural plasma-derived protein in terms of heparin binding activity, FXa inhibitory activity, and the pentasaccharide cofactor activity towards FXa inhibition. This recombinant protein also has the same fluorescence properties as the plasma AT in curve shape and relative intensity of the fluorescence spectrum, as well as the fluorescence emission maximum at 340 nm, in both the absence and the presence of the pentasaccharide and heparin. The Pro397Trp substitution does not alter the functional properties of AT. The fluorescence properties of this variant, however, was affected in a number of ways. Firstly, its endogenous Trp fluorescence increased by 25% as a consequence of the extra Trp addition to the four Trp residues in the native AT molecule. Secondly, heparin induced a larger absolute fluorescence enhancement in this variant (0.5

versus 0.4 fluorescence enhancement in wt AT), although the relative percentage of enhancement (40%) was the same as that seen with wt AT. Thirdly, the Trp fluorescence enhancement induced by the pentasaccharide was lesser both in relative and absolute terms, when compared to wt AT. Taken together, the pentasaccharide decreased the emission of P4' Trp at 340 nm by 60%, whereas full-length heparin increased it by 40%. Obviously, the environment of P4' Trp was perturbed by both the pentasaccharide and full-length heparin, and these two different heparin species altered it differently.

4. DISCUSSION

A special property of AT is its ability to bind to, and be activated by two polysulphated glycosaminoglycans, heparin and heparan sulphate, and AT attains its full anti-proteinase activity only upon binding to these specific glycosaminoglycans (Jordan *et al.*, 1979; Olson and Shore, 1981). Four other serpins, namely HC-II, PN-I, PAI-I, and PCI, are also heparin-activatable inhibitors. AT is unique among these serpins in that a sequence-specific pentasaccharide is required for its activation (Lindahl *et al.*, 1980; Casu *et al.*, 1981; Thunberg *et al.*, 1982; Choay *et al.*, 1983; Atha *et al.*, 1984; 1985). The structural specificity of this pentasaccharide implies a well-defined, relatively small complementary site on AT. This pentasaccharide binding site has been mapped biochemically and is defined by basic residues of the D-helix, the N-terminal tip of the A-helix and the extended, flexible N-terminus of the molecule (Carrell *et al.*, 1994). Docking of part of the pentasaccharide at this site provokes a local conformational change in the AT molecule, which, in turn, results in a perfect fit of the other part of the pentasaccharide within this site and therefore a tight binding between the pentasaccharide and the AT (Olson *et al.*, 1981; Grootenhuis and van Boeckel, 1991). In other words, binding of the pentasaccharide to AT transforms AT from its native low affinity state to a high affinity state. As a consequence of this structural rearrangement, the RCL of AT

adopts an optimal inhibitory conformation. To further understand the interaction of the pentasaccharide with AT and its consequences, two specific objectives were set out for this study: (1) to test the consequences of alterations to Arg47 on the binding of the pentasaccharide to AT and the activation of AT by the pentasaccharide and (2) to demonstrate the transmission of structural perturbations to the RCL of AT upon pentasaccharide and heparin binding and to differentiate the pentasaccharide- and heparin-induced conformations of the RCL of AT using an AT variant with a Pro397Trp substitution.

4.1. Association of Arg47 with Activation of AT by the Pentasaccharide

4.1.1. A Role of Arg47 in Binding to Heparin

In native AT, Arg47 is located where the base of the A-helix is in close proximity to the amino end of the D-helix (Delarue *et al.*, 1990; Mourey *et al.*, 1990; 1993; Carrell *et al.*, 1994; Schreuder *et al.*, 1994). Its replacement by Cys (Koide *et al.*, 1984), Ser (Borg *et al.*, 1992), and His (Owen *et al.*, 1987), in naturally occurring variants, impairs binding of heparin to the variants, suggesting a clear role of this basic residue for heparin to interact with AT. To further characterize the role of this Arg in the binding of AT to and activation of AT by the pentasaccharide, AT moieties with substitutions at Arg47 were created by site-

directed mutagenesis (see section 2.2.5) and expressed in transiently transfected COS-1 cells (see section 2.3.1). Recombinant wt AT and the four variants differing only at Arg47, namely AT Arg47Lys, AT Arg47Tyr, AT Arg47Pro, and AT Arg47Glu, were characterized for their heparin binding (see section 2.4.7) and pentasaccharide cofactor properties (see section 2.4.9). The nonconservative substitutions with Tyr, Pro, and Glu, respectively, were expected to cause a loss of cofactor activity of the pentasaccharide, if Arg47 contributed to the pentasaccharide's binding to and activation of AT. The change of Arg to conservative Lys was expected to result in weaker binding and consequently less activation of AT if the positively charged side-chain of Arg47 bonded to negative group(s) of the pentasaccharide and such interaction contributes significantly to the binding energy and the subsequent activation of AT. Alternatively, the replacement of Arg by Lys was predicted would reserve fully the pentasaccharide binding and the pentasaccharide cofactor activities of AT, if this ionic interaction did not make a significant contribution, or the precise bonding of Arg47 to the pentasaccharide was not required.

4.1.2. Expression of the Arg47 Variants in Transiently Transfected COS-1 Cells

To assay the heparin binding property and the pentasaccharide cofactor activity of the Arg47 variants along with wt AT, correctly folded recombinant AT proteins were required. Reduction of the disulphide linkage between Cys8 and

Cys128 of AT impairs the heparin binding ability of the AT (Sun and Chang, 1989). This can be explained readily by the tertiary assembling of the pentasaccharide binding site in light of the crystal structures of AT (Delarue *et al.*, 1990; Mourey *et al.*, 1990; 1993; Carrell *et al.*, 1994). The proteinase inhibitory activity of AT also depends on the overall folding of the molecule. The overall folding of AT, in particular, enables the presentation of its RCL in a conformation that is complementary and thus readily reactive with the active centre of its cognate proteinases. It also ensures the movement of the RCL and related structures necessary for trapping the proteinase and locking it in a covalent complex after its initial encounter with AT. Since bacterial expression systems frequently misfold disulphide-bonded proteins, they were not compatible for this study. In this sense, a mammalian expression system represents a more natural way of producing recombinant AT. In addition, the glycosylation in mammalian cell expressed AT protein shows a close similarity with that of the plasma AT (Bjork *et al.*, 1992c; Fan *et al.*, 1993). The COS cell transient expression system provides an ideal means to generate recombinant AT proteins at μg levels in a relatively rapid and convenient fashion (Stephens *et al.*, 1987; 1988). In the event that the introduced mutations affected the folding of the protein and therefore the passage of the protein through the secretion pathway, this transient expression system would save the time required to establish permanently transfected cell lines. The COS system was thus chosen to produce

the Arg47 variants.

Transfected COS-1 cells expressed and secreted wt AT with an apparent Mr of 58 kDa, similar to that of the plasma-derived AT (see Fig. 3.4 and Fig. 3.5). It thus appears that AT produced in these cells were glycosylated. Ten Arg47 variants, namely AT Arg47Ala, AT Arg47Glu, AT Arg47His, AT Arg47Leu, AT Arg47Lys, AT Arg47Pro, AT Arg47Ser, AT Arg47Thr, AT Arg47Tyr, and AT Arg47Val, were also expressed in transfected COS-1 cells. Except for AT Arg47Ser and AT Arg47Thr, the other eight AT variants co-migrated with the wt AT (see Fig. 3.4 and Fig. 3.5). Moreover, both the α-form and the ß-form were observed for each of these AT moieties (see Fig. 3.5). The placement of Ser or Thr at position 47 introduced a novel N-glycosylation site on AT. Extra glycosylation of AT was suggested for AT Arg47Ser and AT Arg47Thr by their reduced mobility (see Fig. 3.4 and Fig. 3.5).

We report here, for the first time, the observation that COS-1 cells produce endogenous heparin-like species that accelerate the inactivation of FXa by AT (see Fig. 3.6). A heparin adsorbent was used to remove the endogenous heparin-like species from the conditioned medium of COS-1 cells without interfering with the activities of subsequently added the pentasaccharide, and thus enables the experimental examination of the pentasaccharide cofactor activity of these variants (see Fig. 3.7 and Fig. 3.8).

4.1.3. The Heparin Binding and the Anti-FXa Pentasaccharide Cofactor Activities of the Arg47 Variants

The consequences of alterations to the positively charged Arg47 residue were tested in two aspects: the heparin binding property and the anti-FXa pentasaccharide cofactor activity. While the heparin binding property might reveal how important this residue was for the interaction of heparin with AT and why, the anti-FXa pentasaccharide cofactor activity might reveal the role of this residue for the binding of the pentasaccharide to AT and the subsequent activation of AT by the heparin pentasaccharide. Since the pentasaccharide was not large enough for the bridging mechanism to take place, the anti-FXa pentasaccharide cofactor activity would reflect only the activation of AT by the pentasaccharide as a consequence of its binding to the AT molecule. It was the activation of AT by the pentasaccharide that constituted the key issue of this study.

The heparin binding property of wt AT and four Arg47 variants, namely, AT Arg47Lys, AT Arg47Tyr, AT Arg47Pro, and AT Arg47Glu, were examined by affinity chromatography on heparin Sepharose as described in section 2.4.7. The eluting profile of wt AT (see Fig. 3.9.a) served as a positive control for the variants. The heparin binding affinity of the Arg47Lys variant was slightly reduced (see Fig. 3.9.b). The heparin binding affinity of AT Arg47Tyr and AT Arg47Pro was reduced significantly (see Fig. 3.9.c and Fig. 3.9.d). The

substitution of Arg with the negatively charged residue Glu had a profound influence on the interaction of the pentasaccharide with AT. As shown in Fig. 3.9.e, the Arg47Glu variant did not bind to the heparin-Sepharose. It thus appeared that the positively charged residue Arg47 in the wt AT participated in the ionic interaction with the negatively charged group(s) of the pentasaccharide. A positively charged amino acid residue at position 47 of AT, therefore, is essential for binding with high affinity to heparin and the pentasaccharide.

The pentasaccharide cofactor activity of these Arg47 variants, as well as of wt AT, was assayed, as described in section 2.4.9, by determining the acceleration of complexation of the recombinant AT moieties to FXa. The recombinant wt AT complexed with FXa and this reaction was accelerated significantly by the pentasaccharide (compare Fig. 3.10.b to Fig. 3.10.a and Fig. 3.11.b to Fig. 3.11.a). The pentasaccharide also enhanced complexation of the Arg47Lys variant with FXa (see Fig. 3.12 and Fig. 3.13), but to a lesser extent than wt AT. The pentasaccharide, under the same experimental conditions, however, did not alter the rate of complex formation between FXa and the other three variants, namely AT Arg47Tyr, AT Arg47Pro, and AT Arg47Glu (see Fig. 3.14, Fig. 3.15, Fig. 3.16). Thus an amino acid residue with a positively charged side-chain at position 47 is required for the pentasaccharide accelerated FXa-complexing reaction to occur. Between Arg and Lys, Arg at position 47 is more activatable by the pentasaccharide with respect to FXa inhibition. Arg47 thus

appears to fit the pentasaccharide better in terms of binding to and activation of AT by the pentasaccharide, towards optimizing FXa inhibition.

4.1.4. Conclusions Regarding to the Consequences of Alteration to Arg47 in AT

1. A basic amino acid at position 47 of AT is essential for heparin and the pentasaccharide to bind to AT with high affinity.

2. A basic amino acid at position 47 of AT is essential for the pentasaccharide- and heparin-accelerated inactivation of FXa.

3. An AT moiety with an Arg at position 47 is more activatable by the pentasaccharide with respect to FXa inhibition than with a Lys at this position.

4.1.5. Association of Arg47 with Activation of AT by the Pentasaccharide

From the observations made in this study, we concluded that Arg47, in native AT, is a contact residue associated with AT activation by the pentasaccharide. This is in agreement with the proposed pentasaccharide binding site defined by basic residues of the D-helix, the N-terminal tip of the A-helix and the extended N-terminus of the molecule. It also provides experimental evidence for the observed readiness of Arg47 to form ionic interactions with negatively charged group(s) in the crystal structure of a dimeric form of intact AT (Skinner *et al.*, 1997) and for the observed direct bonding of the pentasaccharide with Arg47 in the crystal structure of the pentasaccharide-AT complex (Jin *et al.*,

1997).

4.1.6. Proposed Future Work

A highly selective recognition occurs between heparin pentasaccharide and AT. This recognition, however, is still ill-defined at the molecular level. AT interacts with the pentasaccharide by a two-step mechanism (Olson *et al.*, 1981; 1992). Upon encounter, the two molecules first assemble into a relatively weak complex; the complex then undergoes a highly favourable conformational change resulting in a tight binding. Based on studies on the conformational flexibility of iduronic acid, Terro *et al.* (1986) suggested that the initial weak complex forms between AT and the conformationally rigid DEF-trisaccharide part of the pentasaccharide. Petitou *et al.* (1988), through molecular dynamics simulations, proposed that in the second step an induced fit allows AT to interact with the GH part of the pentasaccharide. Petitou *et al.*, (1997) conducted spectrofluorimetry experiments using synthetic trisaccharides and tetrasaccharide and their data indicated that the unique DEF-trisaccharide sequence plays the key role in the early recognition that precedes the bimolecular complex assembling and the first step of AT activation. The molecular model of Van Boeckel *et al.* (1994), however, is in contradiction, in part, with the hypothesis of Petitou *et al.*. According to Van Boeckel *et al.*, after the initial binding, Arg132, Lys133, and Lys136 which possess a coil-like conformation in the native state of the protein

would move to elongate the D-helix that already accommodates Lys125 and Arg129. The resulting longer helix would establish a new interaction module with the DEF part of the pentasaccharide, accounting for the observed increase in affinity. Meanwhile, a move of the A-sheet frees the RCL to take up an active canonical conformation required to fit the active site of the proteinase. The DEF-trisaccharide sequence is proposed by Van Boeckel *et al.* to be involved in the second step of binding, in sharp contrast to the hypothesis of Petitou *et al.*.

Our Arg47 variants may be used to clarify some of the structural elements involved in the initial recognition. According to Petitou *et al.* (1997), while the pentasaccharide, DEFGH, binds to AT with a K_d of $6.2\pm0.2\times10^{-8}$ M, the tetrasaccharide DEFG has a K_d of $8.3\pm0.5\times10^{-6}$ M. The affinity of the trisaccharide DEF for AT is further reduced (K_d of $1.9\pm0.7\times10^{-4}$ M). On the other hand, there is no binding between the FGH and AT at all. It thus appears that both the G saccharide unit and the H unit contribute to reinforce the initial interaction between the pentasaccharide and AT. Based on the molecular dynamics simulations of Van Boeckel *et al.*, Arg47 only interacts with the H unit, and its adjacent Arg interacts with the H and the G unit as well. If this is the case, the trisaccharide DEF should bind to some of the Arg47 variants, for example, the Arg47Lys, or a variant with a neutral amino acid at this position, with an affinity similar to that of the wt AT. In contrast, the affinity of DEFGH and EFGH for Arg47 variants should be reduced to some extent. Studying the

interactions between the synthetic oligosaccharides and the recombinant Arg47 variants would thus be a very interesting project. The effect of the replacement of Arg47 on the interactions between these oligosaccharides and AT might thus help to orientate the pentasaccharide in the pentasaccharide-AT complex and to identify some of the structural components involved in the initial recognition.

Petitou *et al* (1997) found that the trisaccharide DEF, in contrast to FGH, could provoke the well-documented fluorescence intensity increase that reveals the conformational change of the AT molecule induced by the pentasaccharide upon its binding to AT. In addition, the DEF, but not the FGH, could accelerate the inhibition of FXa by AT (Petitou *et al.*, 1997), although the potency of the DEF was reduced significantly (data was not presented in the paper). In their previous study, Petitou *et al.* (1988) also observed that the EFGH was not able to potentiate AT with respect to FXa inhibition, whereas the DEFG could. It thus appears that while the D saccharide unit is essential for the rate-enhancing effect of the pentasaccharide on the FXa inhibition to occur, sufficient is the trisaccharide DEF. Petitou *et al.*, thus, proposed that initial interaction with the DEF part of the pentasaccharide pushes AT into an active conformation, then the GH part steps in acting as a chock to lock the complex (1997). This hypothesis agrees with the model of Van Boeckel *et al* (1994) on that the DEF is associated with the elongation of the D-helix. The disagreement of the two lies on the timing of the interaction with the DEF. According to Petitou *et al.*, the

interaction with the DEF precedes the docking of the GH part, whereas Van Boeckel *et al.* suggested that GH binding induces D-helix elongation and the interaction with the DEF part occurs as a consequence of this elongation. Thus identifying the structural components involved in initial recognition would help to establish the mechanism for the activation of AT by the pentasaccharide. In this sense, orientating the pentasaccharide in the pentasaccharide-AT complex may also be beneficial. Studying the accelerating effect of the various tri- and tetra-saccharides on the FXa-complexing reaction of the various Arg47 variants, together with an examination of the tri- and tetra-saccharide binding property of these variants, would permit resolution of important questions regarding the mechanism of activation of AT by the pentasaccharide.

4.2. Trp397 as a Probe for the Pentasaccharide- and Heparin-induced Conformations of the RCL of AT

4.2.1. The Conformational Change and the Activation of AT

As discussed in section 1.3.4, serpins inhibit cognate proteinases by a branched pathway and suicide inhibition mechanism, in which the rate-limiting step precedes the branch point and is determined by the efficiency of insertion of the RCL into the main ß-sheet A as an additional strand (Olson, 1985; Rubin *et al.*, 1990; Patston *et al.*, 1991; 1994). Since serpins interacts with target

proteinases primarily through their P1-P1' residues together with flanking binding subsites in the RCL, the rate of serpin-proteinase reaction will be influenced by the conformation of their RCL. For many of these reactions the second-order rate constants are relatively high. AT represents a prominent exception, in that it inhibits FXa and thrombin at much lower rates. This can be explained readily by the non-optimal conformation of the RCL in native AT at least at the P1 residue (Carrell *et al.*, 1994; Schreuder *et al.*, 1994). Heparin enhances these reaction rates to values comparable to those for other serpin-proteinase pairs. Binding of heparin to AT is essential for this rate enhancement and a major conformational change occurs in the AT molecule as a result of this binding (Kress and Catanese, 1981; Olson and Shore, 1981; Olson *et al.*, 1981; Chang, 1989; Bjork *et al.*, 1992b). The heparin-induced AT conformational change has been known to serve two functions: to increase affinity to the pentasaccharide (Olson *et al.*, 1981; Grootenhuis and Van Boeckel, 1991) and to optimize the presentation of the RCL to the target proteinases of AT. The optimal presentation of the RCL by heparin has been identified by the crystal structure of the pentasaccharide-AT complex (Jin *et al.*, 1997) and its significance has been demonstrated naturally by the α_1-PI Pittsburg variant. This variant has been used as a classical example for indicating the importance of the reactive site for proteinase reactivity and specificity, since replacement of the P1 Met by Arg in α_1-PI transforms it from an antielastase to a potent antithrombin (Owen *et al.*,

1983; Schapira *et al.*, 1986; Scott *et al.*, 1986; Wachtfogel *et al.*, 1994). In addition to this dramatic change in the inhibitory profile, the second rate of thrombin inhibition by this α_1-PI variant is comparable to that by AT in the presence of heparin. The RCL conformation of this α_1-PI variant thus appears to represent the conformation of heparin-activated RCL in AT.

The heparin-induced conformational changes in AT coincide with a 40% increase in the endogenous Trp fluorescence (Einarsson and Andersson, 1977; Villanueva and Danishefsky, 1977; Nordenman *et al.*, 1978; Jordan *et al.*, 1979). This 40% fluorescence increase upon binding to heparin is used to demonstrate the conformational changes in AT that result in large rate enhancements of proteinase inhibition. Based on the observations with plasma AT that the pentasaccharide and full-length heparin induce similar conformational changes in AT (Olson *et al.*, 1992), the chain length dependence of heparin's rate enhancement effect for the inhibition of thrombin (Laurent *et al.*, 1978; Andersson *et al.*, 1979; Danielsson and Bjork, 1981) was explained solely by the ability of longer chains to accommodate AT and thrombin simultaneously (Holmer *et al.*, 1979; Olson and Bjork, 1991). Thus, the 4300-fold rate enhancement of thrombin inhibition produced by full-length heparin at I 0.15 versus the 1.7-fold enhancement by the pentasaccharide was attributed solely to the bridging mechanism by longer heparin molecules (Olson *et al.*, 1992).

Based on the fact that thrombin substrate recognition and that of FXa

are different, we proposed the following hypothesis:

(1). The pentasaccharide and full-length heparin, upon binding to AT, induce different RCL conformations.

(2). The differences between RCL conformations induced by the pentasaccharide and full-length heparin contribute to the previously observed difference in the chain-length dependence of the heparin's rate enhancement effect on FXa and thrombin inhibition.

(3). Whereas the pentasaccharide-induced RCL conformation represents an near optimal suicide substrate to FXa, and thus resulting in an increased RCL reactivity towards FXa, this and the native RCL conformations remain poor thrombin substrates. Thus, the 270-fold enhancement of FXa inhibition of the pentasaccharide illustrates near optimal interaction of the pentasaccharide-induced AT RCL for FXa, relative to the 1.7-fold enhancement of the pentasaccharide for thrombin inhibition.

(4). The heparin-induced RCL conformation is required for optimal interaction with FXa and near optimal interaction with thrombin. This explains the 540-fold enhancing effect of heparin on FXa inactivation, i.e. a 2-fold further enhancement compared to the effect of the pentasaccharide. The induced conformation, however, is not sufficient for fully enhanced thrombin inhibition by AT; the bridging mechanism of the longer chain heparin molecules is also required. By these two mechanisms, full-length heparin enhances the rate of

thrombin inhibition by a 4300-fold versus the pentasaccharide's 1.7-fold rate enhancement.

The key issue of this proposal is whether the pentasaccharide and full-length heparin induce different RCL conformational changes in AT. As discussed in 1.4.3, the difference between the pentasaccharide- and the full-length heparin-induced structural rearrangements may not be recognized by the overall 40% increase in endogenous Trp fluorescence of the native AT molecule. In addition, the overall 40% fluorescence increase is not an accurate indicator of changes in RCL conformation with respect to the RCL proteinase reactivity (Atha *et al.*, 1985; Gettins *et al.*, 1992). Fascinated by the apparent different regulation of AT by the pentasaccharide and heparin, we decided to study AT activation in terms of its RCL conformations. Creating an AT moiety that could monitor conformational changes in RCL induced by the pentasaccharide and full-length heparin was thus a major objective of this study.

4.2.2. Creation of an AT moiety with a Trp in its RCL

The specific approach proposed was to insert a Trp near the reactive centre Arg393-Ser394 in a way that would allow one: (1) to demonstrate changes in the RCL conformations induced by the pentasaccharide and heparin; and (2) to differentiate the pentasaccharide- and heparin-induced RCL conformational changes. An appropriate Trp substitution would assure retention of the functional

properties of AT. The appropriateness of substituting Trp for a residue upstream or downstream from P1-P1' could be judged by the following criteria: (1) this residue should not be conserved in AT from different animal species; (2) this residue should be located in a region that does not play a pivotal role in the recognition by cognate proteinases or in the trapping and locking the proteinase-AT in a covalent complex; and (3) the substitution should not disturb significantly the tertiary structure of the AT molecule. A careful search of the RCL and its surrounding region of four AT species, i.e. man, rabbit, cow, and mouse, revealed one poorly conserved region P4-P6 and the P4' residue. Residues in the RCL N-terminal to the reactive centre are known to be involved in trapping and locking of cognate proteinase through their insertion into the main five ß-strand A sheet as the fourth strand. Thus, converting P4' was deemed to be safer than altering P4. Therefore, the P4' residue, Pro397, was chosen to be the site where the novel Trp would be introduced. Displacement of a Trp at position 397 without changing the other four Trp would yield a AT moiety with five Trp and among those only one was in the RCL. The Pro397Trp variant was therefore generated, by site-directed mutagenesis, as outlined in section 2.2.5.

4.2.3. Expression and Purification of wt AT and the Pro397Trp Variant

Two permanent AT-producing CHO cell lines one expressing wt AT and the other the Pro397Trp variant were established and the two AT moieties

produced. Purification of these two AT moieties from the conditioned medium was achieved by affinity chromatography on heparin-Sepharose followed by Q-Sepharose chromatography, and the two ATs were purified to greater than 98% homogeneity. Since the two recombinant proteins lost activity upon storage over weeks, characterization of these recombinant proteins were carried out using fresh samples.

4.2.4. K_ds of the Pentasaccharide- and the Heparin-AT Complexes

The effects of the Pro397Trp substitution on pentasaccharide and heparin binding abilities were assessed by determining the K_ds for the complexes of this variant with both the pentasaccharide and heparin. The estimated K_d values for the heparin-complexes of plasma AT, the CHO-derived wt protein, and the CHO-derived Pro397Trp variant were as expected (Nordenman *et al.*, 1978; Jordan *et al.*, 1979; Olson *et al.*, 1981; Olson *et al.*, 1992). A 3- to 4-fold reduction in affinity was seen for pentasaccharide complexes of these AT moieties, implying that the pentasaccharide accounts for more than 95% of the binding energy associated with heparin-AT interaction. This difference may also account for the difference in the chain-length dependence of the heparin's rate enhancement effect on FXa and thrombin inhibition. Moreover, the values for each the pentasaccharide or heparin complex were very similar for all three, suggesting that the CHO-derived wt AT and the Pro397Trp variant had similar affinities for the

pentasaccharide and heparin as plasma-derived AT.

AT variants with substitution mutations at P14 and P1 of RCL have increased affinity for heparin. The increased heparin affinity of the variant with a replacement of P14 Ser by Trp has been shown to be a manifestation of the partially activated state of this variant (Huntington *et al.*, 1996). Similarly, the increased affinity for heparin of P1 mutations (Bauer *et al.*, 1983; Lane *et al.*, 1987; Wolf *et al.*, 1987; Erdjument *et al.*, 1988; 1989; Owen *et al.*, 1991) could theoretically be the result of breaking the putative salt bridging of the P1 Arg residue with one Glu within the main body of AT molecule. In this study, we have shown that the Pro397Trp variant and wt AT have the same affinity for the pentasaccharide and heparin. Based on the fact that the activated form of AT represents the high heparin affinity state while the native molecule has low affinity for heparin, the unchanged heparin affinity of this variant might suggest that the Pro397Trp substitution does not cause a structural alteration associated with activation of AT.

4.2.5. The Fluorescence Properties of the Pro397Trp Variant

To distinguish the RCL conformations of AT in the presence of the pentasaccharide and full-length heparin, a P4' variant of AT in which the native Pro residue was replaced by the fluorescent amino acid Trp was generated and its fluorescence properties examined. This variant had altered fluorescence

properties as compared to wt AT (see Fig. 3.25). It had a 25% enhancement in endogenous Trp fluorescence, in keeping with the extra Trp addition to the four Trp residues already present in the native AT molecule; and proportionately greater fluorescence enhancement was induced in this variant by full-length heparin. This larger fluorescence enhancement suggests that the quenching effect of the rest of the molecule on this Trp residue was reduced by heparin. In other words, full-length heparin-induced structural perturbations in this AT protein changes the relationship of this Trp residue with associated fluorescence quenching residues in the molecule in such a way that their quenching effect was reduced. Binding of full-length heparin clearly changed the environment of Trp at P4' position. In contrast to this full-length heparin-induced larger fluorescence enhancement, the pentasaccharide induced a lesser fluorescence enhancement. It thus appears that the effect of the associated fluorescence quenching residues in AT molecule on this novel Trp was reinforced by the pentasaccharide. The environmental changes of P4' Trp caused by the pentasaccharide and full-length heparin were more clearly shown by the difference fluorescence emission between this variant and wt AT (see Fig. 3.25.b). Since common features in the two spectra cancelled, the difference emission spectrum can only be interpreted in terms of the known difference between the two AT moieties which was the novel P4' Trp. The fluorescence of this Trp residue is enhanced 40% by full-length heparin, but diminished 60% by the pentasaccharide. These observations clearly

demonstrate that the environment of the P4' Trp residue was perturbed by full-length heparin differently from by the pentasaccharide.

4.2.6. The FXa-Inhibitory Activity of the Pro397Trp Variant

The functional properties of the Pro397Trp variant examined were its FXa inhibitory activity and its pentasaccharide and heparin cofactor activities towards FXa inhibition. This substitution had no effect on FXa inhibition, and the catalytic effect of the pentasaccharide and heparin on FXa inhibition. Thus, the Pro397Trp substitution did not impair the presentation to and recognition of the RCL by FXa nor the subsequent RCL insertion and trapping of FXa. In other words, the structural perturbations of the RCL essential for activations by the pentasaccharide and full-length heparin to take place were not altered by the Pro397Trp substitution. In addition, full-length heparin accelerated FXa inhibition by AT to a greater extent than the pentasaccharide. It appears that the additional interactions between AT and the heparin residues other than the pentasaccharide account for the 3- to 4-fold increase in affinity and this greater rate enhancing effect of heparin.

4.2.7. The Pentasaccharide- and Heparin-induced RCL Conformations of AT

As discussed above, changes in the environment of the P4' Trp as a result of pentasaccharide and heparin binding have been demonstrated directly

in this study. Moreover, it has been shown, for the first time, that the pentasaccharide and full-length heparin induce different conformational changes in the RCL. It thus appears that the adjacent P1-P1' residues and other proteinase interacting subsites are conformationally affected by the pentasaccharide and full-length heparin in different ways. The RCL local structures are apparently rearranged differently by the pentasaccharide and full-length heparin, and thus detectable by the novel P4' Trp, while the sum of the perturbations of the four native Trp residues is almost the same for the two heparin species. Therefore, it is the presence of the novel Trp at the P4' position that allows one to differentiate the two conformations of AT.

Full-length heparin binds AT with an affinity which is 3- to 4- fold higher than that of the pentasaccharide (Atha *et al.*, 1985; Olson *et al*, 1992), suggesting that additional interactions take place between AT and the saccharide residues other than the pentasaccharide. These putative additional interactions achievable by full-length heparin, but not by the pentasaccharide, have been demonstrated using recombinant molecular techniques (Meagher *et al.*, 1996). The functional significance of the additional interactions, however, are not known. Based on our novel observation that the full-length heparin-induced RCL conformation is different from that induced by the pentasaccharide, additional interactions of full-length heparin with AT may serve to facilitate and stabilize a conformational change in AT that may result in an optimal presentation of the

RCL to thrombin and FXa. Therefore, three functional interactions may occur in the tertiary complex consisting of full-length heparin, AT, and thrombin: (1) the core pentasaccharide binds to the pentasaccharide binding site of AT inducing a conformational change in AT that is represented by the RCL being nearly optimally conformed for interaction with FXa; (2) other monosaccharide residues outside of the pentasaccharide interact with AT residues which are not part of the pentasaccharide binding site, and these interactions contribute to additional conformational changes that optimize the presentation of the RCL to FXa but not yet optimized for thrombin; and (3) other heparin monosaccharide residues binds to thrombin simultaneously and serve as a template for optimizing thrombin-AT interaction. Thus, the 4300-fold rate enhancing effect of full-length on thrombin inhibition versus the 1.7-fold enhancement produced by the pentasaccharide may be attributed to two mechanisms: (1) the near optimal presentation of RCL to thrombin; and (2) the bridging mechanism.

4.2.8. Conclusions Relating to the Characterization and Application of the AT Pro397Trp to differentiate relative the Pentasaccharide- and Heparin-induced Conformations of the RCL of AT

1. Recombinant wt AT produced in permanently transfected CHO cells is glycosylated and secreted into the culture medium in its native biologically active form.

2. The Pro397Trp substitution does not alter the functional properties of AT.

3. The Pro397Trp substitution alters fluorescence properties of AT; causing a 25% enhancement of endogenous Trp fluorescence.

4. The pentasaccharide- and full-length heparin-produced structural perturbations in AT are transmitted to the RCL.

5. The pentasaccharide and full-length heparin induce different RCL conformations; whereas the pentasaccharide induces a lesser fluorescence enhancement, full-length heparin induces a larger fluorescence enhancement.

6. It is likely that these different RCL conformations account for the different inhibitory activities of AT produced by the pentasaccharide and full-length heparin.

4.2.9. Future Work Proposed Relating to Mapping the Pentasaccharide- and Heparin-induced Conformations of the RCL of AT

The generation and characterization of the AT Pro397Trp variant in this study has allowed us: (1) to demonstrate the transmission of the structural perturbations in AT, upon binding of the pentasaccharide and heparin, to the RCL of AT; and (2) to differentiate the pentasaccharide- and full-length heparin-induced conformations of the RCL of AT. The following additional experiments should be done to pursue this issue further to shed more light into the mechanism

of activation of AT by the pentasaccharide and full-length heparin:

1. To Study fluorescence changes of the Pro397Trp variant in the presence of the pentasaccharide and low affinity heparin.

2. To monitor fluorescence changes in the Pro397Trp variant induced by different chain-length heparin species, paying particular attentions to those high affinity saccharides which are larger than the pentasaccharide but smaller than 18-mer saccharides.

3. To combine Pro397Trp substitution with mutations in the putative pentasaccharide binding site and/or the residues involved in the interaction with full-length heparin. Hopefully, the structural elements involved in the heparin activation of AT may be identified by characterization of such variants.

5. REFERENCES

Abilgaard, U. (1967) Purification of two progressive antithrombins of human plasma. Scand. J. Clin. Lab. Invest. 19, 190-195.

Abilgaard, U. (1968) Highly purified antithrombin III with heparin cofactor activity prepared by disc electrophoresis. Scand. J. Clin. Lab. Invest. 21, 89-97.

Abilgaard, U. (1969) Binding of thrombin to antithrombin III. Scand. J. Clin. Lab. Invest. 24, 23-27.

Abilgaard, U. (1981) Antithrombin and related inhibitors of coagulation. In Poller, L. (ed): Recent Advances in Blood Coagulation. Edinburgh, Scotland, Churchill Livingstone. pp. 151-173.

Andersson, L.O., Barrowcliffe, T.W., Holmer, E., Johnson, E.A., Sims, G.E.C. (1976) Anticoagulant properties of heparin fractionated by affinity chromatography on matrix-bound antithrombin III and by gel filtration. Thromb. Res. 9, 575-583.

Andersson, L.O., Barrowcliffe, T.W., Holmer, E., Johnson E.A., and Soderstrom, G. (1979) Molecular weight dependency of the heparin potentiated inhibition of thrombin and activated factor X. Effect of heparin neutralization in plasma. Thromb. Res. 15, 531-541.

Anfinsen, C. (1973) Principles that govern the folding of protein chains. Science 181, 223-230.

Atha, D.H., Stephens, A.W., and Rosenberg, R.D. (1984) Evaluation of critical groups required for the binding of heparin to antithrombin. Proc. Natl. Acad. Sci. USA 81, 1030-1034.

Atha, D.H., Favreau, L.V., Braswell, E.H., Rosenberg, R.D., and Choay, J. (1985) Contribution of monosaccharide residues in heparin binding to antithrombin III. Biochemistry 24, 6723-6729.

Aulak, K.S., Pemberton, P.A., Rosen, F.S., Carrell, R.W., Lachmann, P.J., and Harrison, R.A. (1988) Dysfunctional C1-inhibitor (At), isolated from a type II heraditary angio-oedema plasma, contains a P1' reactive centre (Arg^{444}-His)

mutation. Biochem. J. 253, 615-618.

Austin, R.C., Rachubinski, R.A., Fernandez-Rachubinski, F., and Blajchman, M.A. (1990) Expression in a cell-free system of normal and variant forms of human antithrombin III. Ability to bind heparin and react with α-thrombin. Blood 76, 1521-1529.

Baker, D. and Agard, D.A. (1994) Kinetics versus thermodynamics in protein folding. Biochemistry 33, 7505-7509.

Bauer, K.A., Ashenhurst, J.B., Chediak, J., and Rosenberg, R.D. (1983) Antithrombin "Chicago": a functionally abnormal molecule with increased heparin affinity causing familial thrombophilia. Blood 62, 1242-1250.

Bauer, K.A. and Rosenberg, R.D. (1991) Role of antithrombin III as a regulator of in vivo coagulation. Seminars Hematol. 28, 10-18.

Baumann, U., Bode, W., Huber, R., Travis, J., and Potempa, J. (1992) Crystal structure of cleaved equine leucocyte elastase inhibitor determined at 1.95Å resolution. J. Mol. Biol. 226, 1207-1218.

Baumann, U., Huber, R., Bode, W., Grosse, D., Lesjak,, M., and Laurell, C.B. (1991) Crystal structure of cleaved bovine antiththrombin-III at 3.2-Ångstrom resolution. J. Mol. Biol. 218, 595-606.

Beatty, K., Bieth, J., and Travis, J. (1980) Kinetics of association of serpin proteinases with native & oxidized alpha-1-proteinase inhibitor and alpha-1-antichymotrypsin. J. Biol. Chem. 255, 3931-3934.

Biggs, R., Denson, K.W.E., Akman, N., Borrett, R., and Hadden, M. (1970) Antithrombin III, antifactor Xa and heparin. Br. J. Haemotol. 19, 283-305.

Bjork, I. and Fish, W.W. (1982) Production *in vitro* and properties of a modified form of bovine antithrombin, cleaved at the reactive site by thrombin. J. Biol. Chem. 257, 9487-9493.

Bjork, I., Jackson, C.M., Jornvall, H., Lavine, K.K., Nordling, K., and Salsgiver, W.J. (1982) The active site of antithrombin. Release of the same proteolytically cleaved form of the inhibitor from complexes with factor IXa, factor Xa, and thrombin. J. Biol. Chem. 257, 2406-2411.

Bjork, I. and Lindahl, U. (1982) Mechanism of the anticoagulant action of

heparin. Mol. Cell Biochem. **48**, 161-182.

Bjork, I. and Nordenman, B. (1976) Acceleration of the reaction between thrombin and antithrombin III by non-stoichometric amounts of heparin. Eur. J. Biochem. **68**, 507-511.

Bjork, I. and Nordling, K. (1979) Evidence by chemical modification for the involvement of one or more tryptophanyl residues of bovine antithrombin in the binding of high-affinity heparin. Eur. J. Biochem. **102**, 497-502.

Bjork, I., Nordling, K., Larsson, I., and Olson, S.T. (1992a) Kinetic characterization of the substrate reaction between a complex of antithrombin with synthetic reactive-bond-loop tetradecapeptide and four target proteinases of the inhibitor. J. Biol. Chem. **267**, 19047-19050.

Bjork, I., Nordling, K., and Olson, S.T. (1993) Immunologic evidence for insertion of the reactive-bond loop of antithrombin into the A ß-sheet of the inhibitor during trapping of target proteinases. Biochemistry **32**, 6501-6505.

Bjork, I., Olson, S.T., and Shore, J.D. (1989) Molecular mechanism of the accelerating effect of heparin on the reactions between antithrombin and clotting proteinases. In: Lane, D.A. and Lindahl, U. (eds) Heparin: chemical and biological properties, clinical applications. Edward Arnold, London. pp. 229-255.

Bjork, I., Ylinenjarvi, K., Olson, S.T., and Bock, P.E. (1992b) Conversion of antithrombin from an inhibitor of thrombin to a substrate with reduced heparin affinity and enhanced conformational stability by binding of a tetradecapeptide corresponding to the P1 to P14 region of the putative reactive bond loop of the inhibitor. J. Biol. Chem. **267**, 1976-1982.

Bjork, I., Ylinenjarvi, K., Olson, S.T., Hermetin, P., and Conradt, H.S. (1992c) Dereased affinity of recombinant antithrombin for heparin due to increased glycosylation. Biochem. J. **286**, 793-800.

Blajchman, M.A., Austin, R.C., Fernandez-Rachubinski, F., and Sheffield, W.P. (1992) Molecular basis of inherited human antithrombin deficiency. Blood **80**, 2159-2171.

Blackburn, M.N. and Sibley, C.C. (1980) The heparin binding site of antithrombin III. J. Biol. Chem. **255**, 824-826.

Blackburn, M.N., Smith, R.L., Carson, J., and Sibley, C.C. (1984) The heparin-binding site of antithrombin III. J. Biol. Chem. **259**, 939-941.

Bock, S.C., Harris, F.J., Balazs, I., and Trent, J.M. (1985) Assignment of the human antithrombin III structural gene to chromosome 1q23-25. Cytogenet. Cell Genet. **39**, 67-69.

Bock, S.C. and Levitan, D.J. (1983) Characterization of an unusual length polymorphism 5' to the human antithrombin III gene. Nucl. Acids Res. **11**, 8569-8582.

Bock S.C., Marrinan, J.A., and Radziejewska, E. (1988) Antithrombin III Utah: proline-407 to leucine mutation in a highly conserved region near the inhibitor reactive site. Biochemistry **27**, 6171-6178.

Bock, S.C. and Prochownik, E.V. (1987) Molecular genetic survey of sixteen kindreds with hereditary antithrombin III deficiency. Blood **70**, 1273-1278.

Bock, S.C., Wion, K.L., Vehar, G.A., and Lawn, R.M. (1982) Cloning and expression of the cDNA for human antithrombin III. Nucl. Acids Res. **10**, 8113-8125.

Borg, J.-Y., Brennan, S.O., Carrell, R.W., George, P., Perry, D.J., and Shaw, J. (1990) Antithrombin Rouen-IV 24 Arg→Cys. The amino-terminal contribution to heparin binding. FEBS Lett. **266**, 163-166.

Borg, J.-Y., Owen, M.C., Soria, C., Soria, J., Caen, J., and Carrell, R.W. (1988) Proposed heparin binding site in antithrombin based on arginine 47. A new variant Rouen-II, 47 Arg to Ser. J. Clin. Invest. **81**, 1292-1296.

Borsodi, A.D. and Bradshaw, R.A. (1977) Isolation of antithrombin III from normal and α_1-antitrypsin-deficient human plasma. Thromb. Haemostas. **38**, 475-485.

Bray, B., Lane, D.A., Freyssinet, J.-M., Pejler, G., and Lindahl, U. (1989) Anti-thrombin activity of heparin. Effect of saccharide chain length on thrombin inhibition by heparin cofactor II and by antithrombin. Biochem. J. **262**, 225-232.

Brennan, S.O., Borg, J-Y., George, P.M., Soria, C., Soria, J., Caen, J., and Carrell, R.W. (1988) New carbohydrate site in mutant antithrombin (7Ile→Asn) with decreased heparin affinity. FEBS Lett. **237**, 118-122.

Brennan, S.O., George, P.M., and Jordan, R.E. (1987) Physiological variant of antithrombin III lacks carbohydrate side chain at Asn135. FEBS Lett. **219**, 431-436.

Brinkhous, K.M., Smith, H.P., Warner, E.D., and Seegers, W.H. (1939) The inhibition of blood clotting: an unidentified substance which acts in conjunction with heparin to prevent the conversion of prothrombin into thrombin. Am. J. Physiol. **125**, 683-687.

Broker, M., Ragg, H., and Karges, H.E. (1987) Expression of human antithrombin III in *saccharomyces cerevisiae* and *Saccharomyces pombe*. Biochem. Biophys. Res. Commun. 908, 203-213.

Bruch, M. and Bieth, J.G. (1989) Kinetic evidence for a two-step mechanism for the binding of chymotrypsin to alpha 1-proteinase inhibitor. Biochem. J. **259**, 929-930.

Bruch, M., Weiss, V., and Engel, J. (1988) Plasma serine proteinase inhibitors (serpins) exhibit major conformational changes and a large increase in conformational stability upon cleavage at their reactive sites. J. Biol. Chem. **263**, 16626-16630.

Brunel, F., Duchange, N., Fischer, A.M., Cohen, G.N., and Zakin, M.M. (1987) Antithrombin III Alger. A new case of Arg 47-Cys mutation. Am. J. Hematol. **25**, 223-224.

Burnette, W.N. (1981) "Western blotting": Electrophoretic transfer of proteins from sodium dodecyl sulfate-polyacrylamide gels to unmodified nitrocellulose and radiogaphic detection with antibody and radioiodinated protein A. Anal. Biochem. **112**, 195.

Carlson, T.H., Atencio, A.C., and Simon T.L. (1984) *In vivo* behaviour of radioiodinated rabbit antithrombin III. J. Clin. Invest. **74**, 191-199.

Carlson, T.H., Simon T.L., and Atencio, A.C. (1985) *In vivo* behaviour of human radioiodinated antithrombin III. Blood **66**, 13-19.

Carlstrom, A.S., Lieden, K., and Bjork, I. (1977) Decreased binding of heparin to antithrombin following the interaction between antithrombin and thrombin. Throb. Res. **11**, 785-797.

Carrell, R.W. and Evans, D.L.I. (1992) Serpins: mobile conformations in a family of proteinase inhibitors. Current Opnion in Structural Biol., **2**, 438-446.

Carrell, R.W., Evans, D.L.I., and Stein, P.E. (1991) Mobile reactive centre of serpins and the control of thrombosis. Nature, **353**, 576-578.

Carrell, R.W. and Owen, M.C. (1985) Plakalbumin, alpha-1 antitrypsin, antithrombin and the mechanism of inflammatory disease. Nature **317**, 730-732.

Carrell, R.W., Skinner, R., Jin, L., and Abrahams, J.P. (1997) Structural mobility of antithrombin and its modulation by heparin. Thromb. Haemostas. **78**, 516-519.

Carrell, R.W., Stein, P.E., Fermi, G., and Wardell, M.R. (1994) Biological implications of a 3 Å structure of dimeric antithrombin. Structure **2**, 257-270.

Carrell, R.W. and Travis J. (1985) α_1-Antitrypsin and the serpins. Variation and contervariation. Trends Biol. Sci. **10**, 20-24.

Caso, R., Lane, D.A., Thompson, E., Zangouras, D., Panico, M., Morris, H., Olds, R.J., Thein, S.L., and Girolami, A. (1990) Antithrombin Padua I: impaired heparin binding caused by an Arg47 to His (CGT to CAT) substitution. Thrombos. Res. **58**, 185-190.

Casu, B. (1985) Structure and biological activity of heparin. Adv. Carbohydr. Chem. Biochem. **43**, 51-134.

Casu, B., Johnson, E.A., Mantovani, M., Mulloy, B., Oreste, P., Pescador, R., Prino, G., Torri, G., and Zoppetti, G. (1983) Correlation between structure, fat-cleaving and anticoagulant properties of heparins and heparan sulphates. Arzneim.-Forsh./Drug Res. **33**, 135-142.

Casu, B., Oreste, P., Torri, G., Zoppetti, G, Choay, J., Lormeau, J.C., Petitou, M., and Sinay, P. (1981) The structure of heparin oligosaccharide fragments with high anti-(factor Xa) activity containing the minimal antithrombin III-binding sequence. Chemical and ^{13}C nuclear magnetic resonance studies. Biochem. J. **197**, 599-609.

Chan, T.K. and Chan, V. (1981) Antithrombin III, the major modulator of intravascular coagulation is synthesized by human endothelial cells. Thromb. Haemostas. **46**, 504-506.

Chan, V. and Chan, T.K. (1979) antithrombin III in fresh and cultured human

endothelial cell: a natural anticoagulant from the vascular endothelium. Thromb. Res. 15, 209-213.

Chandra, S., Bang, N.U., and Marks, C. (1976) Radiolabelled AT III as a probe for the detection of activation of blood coagulation in vivo. Thromb. Res. 9, 9-23.

Chandra, T., Stackhouse, R., Kidd, V.J., and Woo, S.L. (1983) Isolation and sequence characterization of a cDNA clone of human antithrombin III. Proc. Natl. Acad. Sci. USA 80, 1845-1848.

Chang, J.-Y. (1989) Binding of heparin to human antithrombin III activates selective chemical modification at lysine 236. Lys-107, Lys-125, and Lys-136 are situated within the heparin-binding site of antithrombin III. J. Biol. Chem. 264, 3111-3115.

Chang, J.-Y. and Tran, T.H. (1986) Antithrombin-III Basel. Indentification of a Pro to Leu substitution in a hereditary abnormal antithrombin with impaired heparin cofactor activity. J. Biol. Chem. 261, 1174-1176.

Choay, J., Lormeau, J.C., Sinay, P., Casu, B., and Gatti, G. (1983) Structure-activity relationship in heparin: A synthetic pentasaccharide with high-affinity for antithrombin III and eliciting high anti-factor Xa activity. Biochem. Biophys. Res. Commun. 116, 492-499.

Chowdhury, V., Mille, B., Olds, R.J., Lane, D.A., Watton, J., Barrowcliffe, T.W., Pabinger, I., Woodcock, B.E., and Thein, S.L. (1995) Antithrombins Southpot (Leu 99 to Val) and Vienna (Gln 118 to Pro): two novel antithrombin variants with abnormal heparin binding. British J. Haemat. 89, 602-609.

Cifonelli, J.A. and Korfman, A. (1962) The uronic acid of heparin. Biochem. Biophys. Res. Commun. 7, 41.

Clemmensen, I. (1978) Inhibition of urokinase by complex formation with human antithrombin in the absence and of heparin. Thromb. Haemostas. 39, 616-623.

Collen, D., Schezt, J., DeCock, F., Holmer, E., and Verstraete, M. (1977) Metabolism of antithrombin III (heparin cofactor) in man: effects of venous thrombosis and of heparin administration. Eur. J. Clin. Invest. 7, 27-34.

Craig, P.A., Olson, S.T., and Shore, J.D. (1989) Transient kinetics of heparin-catalyzed protease inactivation by antithrombin III. Characterization of assembly,

product formation, and heparin dissociation steps in the factor Xa reaction. J. Biol. Chem. 264, 5452-5461.

Creighton, T.E. (1992) Up the kinetic pathway. Nature 356, 194-195.

Daly, M., Ball, R., O'Meara, A., and Hallinan, F.M. (1989) Identification and characterisation of an antithrombin III mutant (AT Dublin 2) with marginally decreased heparin reactivity. Thrombos. Res. 56, 503-513.

Daly, M., Bruce, D., Perry, D.J., Price, J., Harper, P.L., O'Meara, A., and Carrell, R.W. (1990) Antithrombin Dublin-3 (Val→Glu): an N-terminal variant which has an aberrant signal peptidase cleavage site. FEBS Lett. 273, 87-90.

Daly, M.E. and Perry, D.J. (1990) Dde 1 polymorphism in intron 5 in the antithrombin III gene. Nucleic Acids Res. 18, 5583.

Damus, P.S., Hicks, M., and Rosenberg, R.D. (1973) Anticoagulant action of heparin. Nature 246, 355-357.

Danielsson, A. and Bjork, I. (1981) Binding to antithrombin of heparin fractions with different molecular weights. Biochem. J. 193, 427-433.

Danielsson, A. and Bjork, I. (1982) Mechanism of inactivation of trypsin by antithrombin III. Biochem. J. 207, 21-28.

Danielsson, A. and Bjork, I. (1983) Properties of antithrombin-thrombin complexes formed in the presence and in the absence of heparin. Biochem. J. 213, 345-353.

Danielsson, A., Raub, E., and Bjork, I. (1986) Role of ternary complexes, in which heparin binds both antithrombin and proteinase, in the acceleration of the reactions between antithrombin and thrombin or factor Xa. J. Biol. Chem. 261, 15467-15473.

Davie, E.W., Fujikawa, K., and Kisiel, W. (1991) The coagulation cascade: initiation, maintenance, and regulation. Biochemistry 30, 10363-10370.

Dawes, J., James, K., and Lane, D.A. (1994) Conformational change in antithrombin induced by heparin, probed with a monoclonal antibody against the 1C/4B region. Biochemistry 33, 4375-4383.

De Agostini, A., Patston, P.A., Marottoli, V., Carrel, S., Harpel, P.C., and Schapira, M. (1988) A common epitope is created when the reactive center of C1 inhibitor is cleaved by plasma kallikrein, activated factor XII, C1 esterase, or neutrophil elastase. J. Clin. Invest. **82**, 700-705.

Delarue, M., Samama, J.-P., Mourey, L., and Moras, D. (1990) Crystal structure of bovine antithrombin III. Acta Crystallogr. (Sect. B) **46**, 550-556.

Deng, W.P. and Nickoloff, J.A. (1992) Site-directed mutagenesis of virtually any plasmid by eliminating a unique site. Anal. Biochem. **200**, 81-88.

Derechin, V.M., Blinder, M.A., and Tollefsen, D.M. (1990) Substitution of arginine for Leu^{444} in the reactive site heparin cofactor II enhances the rate of thrombin inhibition. J. Biol. Chem. **265**, 5623-5628.

deRoux, N., Chadeuf, G., Mohlo-Sabatier, P., Plouin, P.-F., and Aiach, M. (1990) Clinical and biochemical characterization of antithrombin III Franconville, a variant with Pro 41 Leu mutation. Br. J. Haematol. **75**, 222-227.

Dingermann, T., Troidl, E.M., Broker, M., and Nerke, K. (1991) Expression of human antithrombin III in the cellular slime mould *dictyostelium discoideum*. Appl. Microbiol. Biotechnol. **35**, 496-503.

Djie, M.Z., Le Bonniec, B.F., Hopkins, P.C.R., Hipler, K., and Stone, S.R. (1996) Role of the P_2 residue in determining the specificity of serpins. Biochemistry **35**, 11461-11469.

Duchange, N., Chasse, J-F., Cohen, G.N., and Zakin, M.M. (1986) Identification of a mutation leading to cysteine replacement in a silent deficiency. Nucleic Acids Res. **14**, 2408.

Duchange, N., Chasse, J-F., Cohen, G.N., and Zakin, M.M. (1987) Molecular characterization of the antithrombin III Tours deficiency. Thromb. Res. **45**, 115-121.

Egeberg, O. (1965) Inherited antithrombin deficiency causing thrombophilia. Thromb. Diath. Haemorrh. **13**, 516-530.

Einarsson, R. and Andersson, L.O. (1977) Binding of heparin to human antithrombin III as studied by measurements of tryptophan fluorescence. Biochim. Biophys. Acta **490**, 104-111.

Eldering, E., Huijbregts, C.M.M., Lubbers, Y.T.P., Longstaff, C., and Hack, C.E. (1992) Characterization of recombinant C1 inhibitor P1 variants. J. Biol. Chem. **267**, 7013-7020.

Elliott, P.R., Lomas, D.A., Carrell, R.W., and Abrahams, J.P. (1996) Inhibitory conformation of the reactive loop of α_1-antitrypsin. Nature Structural Biol. **3**, 676-681.

Ellis, V., Scully, M.F., and Kakkar, V.V. (1986) The relative molecular mass dependence of the anti-factor Xa properties of heparin. Biochem. J. **238**, 329-333.

Elson, L.A. and Morgan, W.T.J. (1933) A colorimetric method for the determination of glucosamine and chondrosamine. Biochem. J. **27**, 1824.

Engh, R.A., Wright, H.T., and Huber, R. (1990) Modelling the intact form of the alpha 1-proteinase inhibitor. Protein Eng. **3**, 469-477.

Erdjument, H., Lane, D.A., Ireland, H., Panico, M., Dimaizo, V., Blench, I., and Morris, H.R. (1987) Formation of a covalent disulfide-linked antithrombin-albumin complex by an antithrombin variant, antithrombin "Northwick Park". J. Biol. Chem. **262**, 13381-13384.

Erdjument, H., Lane, D.A., Panico, M., DiMarzo, V., and Morris, H.R. (1988) Single amino acid substitutions in the reactive site of antithrombin leading to thrombosis. Congenital substitution of arginine 393 to cysteine in antithrombin Northwick Park and to histidine in antithrombin Glasgow. J. Biol. Chem. **263**, 5589-5593.

Erdjument, H., Lane, D.A., Panico, M., Di Marzo, V., Morris, H.R., Bauer, K., and Rosenberg, R.D. (1989) Antithrombin Chicago, amino acid substitution of arginine 393 to histidine. Thromb. Res. **54**, 613-619.

Evington, J.R.N., Feldman, P.A., Luscombe, M., and Holbrook, J.J. (1986) The catalysis by heparin of the reaction between thrombin and antithrombin. Biochim. Biophys. Acta **870**, 92-101.

Fair, D.S. and Bahnak, B.R. (1984) Human hepatoma cells secrete single chain factor X, prothrombin, and antithrombin III. Blood **64**, 194-204.

Fan, B., Crews, B.C., Turko, I.V., Choay, J., Zettlmeissl, G., and Gettins, P. (1993) Heterogeneity of recombinant human antithrombin III expressed in baby hamster

kidney cells. Effect of glycosylation differences on heparin binding and structure. J. Biol. Chem. **268**, 17588-17596.

Fan, B., Turko, I.V., and Gettins, P.G.W. (1994a) Lysine-heparin interactions in antithrombin. Properties of K125M and K290M, K294M, K297M variants. Biochemistry **33**, 14156-14161.

Fan, B., Turko, I.V., and Gettins, P.G.W. (1994b) Antithrombin histidine variants ^{1}H NMR resonance assignments and functional properties. FEBS Lett. **354**, 84-88.

Fish. W.W. and Bjork, I. (1979) Release of a two-chain form of the human antithrombin from the antithrombin-thrombin complex. Eur. J. Biochem. **101**, 31-38.

Fish, W.W., Danielsson, A., Nordling, K., Miller, S.H., Lam, C.F., and Bjork, I. (1985) Denaturation behaviour of antithrombin in guanidinium chloride. Irreversibility of unfolding caused by aggregation. Biochemistry **24**, 1510-1517.

Fish, W.W., Orre, K., and Bjork I. (1979) The production of an inactive form of antithrombin through limited proteolysis by thrombin. FEBS Lett. **98**, 103-106.

Franzen, L-E., Svensson, S., and Larm, O. (1980) Structural studies on the carbohydrate portion of human antithrombin III. J. Biol. Chem. **255**, 5090-5098.

Fuchs, H.E. and Pizzo, S.V. (1983) Regulation of factor Xa in vitro in human and mouse plasma and in vivo in mouse. Role of the endothelium and plasma proteinase inhibitors. J. Clin. Invest. **72**, 2041-2049.

Fuchs, H.E., Shifman, M.A., Michalopoulos, G., and Pizzo, S.V. (1984a) Hepatocyte receptors for antithrombin III-proteinase complexes. J. Cell. Biochem. **24**, 197-206.

Fuchs, H.E., Shifman, M.A., and Pizzo, S.V. (1982) *In vivo* catabolism of 1-proteinase inhibitor-trypsin, antithrombin III-thrombin and 2-macroglobulin-methylamine. Biochim. Biophys. Acta **716**, 151-157.

Fuchs, H.E., Trapp, H.G., Griffith, M.J., Roberts, H.R., and Pizzo, S.V. (1984b) Regulation of factor IXa in vitro in human and mouse plasma in vivo in the mouse. Role of the endothelium and the plasma proteinase inhibitors. J. Clin. Invest. **73**, 1696-1703.

Furugren, B., Andersson, L.O., and Einarsson, L. (1977) Small-angle X-ray scattering studies on human antithrombin III and its complex with heparin. Arch. Biochem. Biophys. **178**, 419-424.

Gandrille, S., Aiach, M., Lane, D.A., Vidaud, D., Molho-Sabatier, P., Caso, R., deMoerloose, P., Fiessinger, J.-N., and Clauser, E. (1990) Important role of arginine 129 in heparin-binding of antithrombin III. J. Biol. Chem. **265**, 18997-19001.

Gettins, P. (1987) Antithrombin III and its interaction with heparin. Comparison of the human, bovine, and porcine proteins by ^{1}H NMR spectroscopy. Biochemistry **26**, 1391-1398.

Gettins, P., Choay, J., Crews, B.C., and Zettlmeissl, G. (1992) Role of tryptophan 49 in the heparin cofactor activity of human antithrombin III. J. Biol. Chem. **267**, 21946-21953.

Gettins, P., Fan, B., Crews, B.C., Turko, I.V., Olson, S.T., and Streusand, V.J. (1993a) Transmission of conformational change from the heparin binding site to the reactive center of antithrombin. Biochemistry **32**, 8385-8389.

Gettins, P. and Harten, B. (1988) Properties of thrombin- and elastase-modified human antithrombin III. Biochemistry **27**, 3634-3639.

Gettins, P., Patston, P.A., and Schapira, M. (1993b) The role of conformational change in serpin structure and function. Bioessays **15**, 461-467.

Gettins, P., Patston, P.A., and Olson, S.T. (1996) Mechanism of action of serpins as suicide substrate inhibitors. In Serpins: structure, function and biology. R.G. Landes Company. pp. 33-63.

Gettins, P. and Wooten, E.S. (1987) On the domain structure of antithrombin III. Localization of the heparin-binding region using ^{1}H NMR spectroscopy. Biochemistry **26**, 4403-4408.

Gillespie, L.S., Hillesland, K.K., and Knaur, D.J. (1991) Expression of biologically active human antithrombin III by recombinant baculovirus in *Spodoptera frugiperda* cells. J. Biol. Chem. **266**, 3995-4001.

Girot, R., Jaubert, F., Leon, M., Bellon, B., Aiach, M., and Josso, F. (1983) Albumin, fibrinogen, prothrombin and antithrombin III variations in blood, urines

and liver in rat nephrotic syndrome (Heymann nephritis). Thromb. Haemostas. **49**, 13-17.

Gitel, S.N., Medina, V.M., and Wessler, S. (1984) Inhibition of human activated factor X by antithrombin III and α_1-protease inhibitor in human plasma. J. Biol. Chem. **259**, 6890-6895.

Gouin-Thibault, I., Dewar, L., Kulczycky, M., Sternbach, M., and Ofosu, F.A. (1995) Measurement of factor Xa-antithrombin III in plasma: relationship to prothrombin activation *in vivo*. British J. Haematol. **90**, 669-680.

Griffith, M.J. (1982) The heparin-enhanced antithrombin III/thrombin reaction is saturable with respect to both thrombin and antithrombin III. J. Biol. Chem. **257**, 13899-13902.

Griffith, M.J., Noyes, C.M., Tyndall, J.A., and Church, F.C. (1985) Structural evidence for leucine at the reactive site of heparin cofactor II. Biochemistry **24**, 6777-6782.

Grootenhuis, P.D.J. and Van Boeckel, C.A.A. (1991) Constructing a molecular model of the interaction between antithrombin III and a potent heparin analogue. J. Am. Chem. Soc. **113**, 2743-2747.

Hatton, M.W.C., Berry, L.R., and Regoeczi, E. (1978) Inhibition of thrombin by antithrombin III in the presence of certain glycosaminoglycans found in the mammalian aorta. Thrombosis Res. **13**, 655-670.

Hekman, C.M. and Loskutoff, D.J. (1985) Endothelial cells produce a latent inhibitor of plasminogen activators that can be activated by denaturants. J. Biol. Chem. **260**, 11581-11587.

Hermans, J.M., Monard, D., Jones, R., and Stone, S. (1995) Inhibition of acrosin by serpins. A suicide substrate mechanism. Biochemistry **34**, 3678-3685.

Highsmith, R.F. and Rosenberg, R.D. (1974) The inhibition of human antithrombin III in the absence and presence of heparin. Thromb. Haemostas. **39**, 616-623.

Holmer, E., Kurachi, K., and Soderstrom, G. (1981) The molecular-weight dependence of the rate-enhancing effect of heparin on the inhibition of thrombi, factor Xa, factor IXa, factor XIIa and kallikrein by antithrombin. Biochem. J.

193, 395-400.

Holmer, E., Lindahl, U., Backstrom, G., Thunberg, L., Sandberg, H., Soderstrom, G., and Andersson, L.O. (1980) Anticoagulant activities and effects on platelets of heparin fragment with high-affinity for antithrombin. Thromb. Res. **18**, 861-869.

Holmer, E., Soderstrom, G., and Andersson, L.O. (1979) Studies on the mechanism of the rate-enhancing effect of heparin on the thrombin-antithrombin III reaction. Eur. J. Biochem. **93**, 1-5.

Hood, D.B., Huntington, J.A., and Gettins, P.G.W. (1994) α_1-proteinase inhibitor variant T345R. Influence of P14 residue on substrate and inhibitory pathways. Biochemistry **33**, 8538-8547.

Hook, M., Bjork, I., Hopwood, J., and Lindahl, U. (1976) Anticoagulant activity of heparin: Separation of high activity and low activity heparin species by affinity chromatography on immobilized antithrombin. FEBS Lett. **66**, 90-93.

Hopkins, P.C.R., Carrell, R.W., and Stone, S.R. (1993) Effects of mutations in the hinge region of serpins. Biochemistry **32**, 7650-7657.

Hopkins, P.C.R., Chang, W-S.W., Wardell, M.R., and Stone, S.R. (1997) Inhibitory mechanism of serpins. J. Biol. Chem. **272**, 3905-3909.

Hopkins, P.C.R., Crowther, D.C., Carrell, R.W., and Stone, S.R. (1995) Development of a novel recombinant serpin with potential antithrombotic properties. J. Biol. Chem. **270**, 11866-11871.

Horne, A.P. and Gettins, P. (1992) ^{1}H NMR spectroscopic studies on the interactions between human plasma antithrombin III and defined low molecular weight heparin fragments. Biochemistry **31**, 2286-2294.

Howarth, D.J., Samson, D., Stirling, Y., and Seghatchian, M.J. (1985) Antithrombin III Northwick Park: a variant antithrombin with normal affinity for heparin but reduced heparin cofactor activity. Thromb. Haemostas. **53**, 314-319.

Hoylaerts, M., Owen, W.G., and Collen, D. (1984) Involvement of heparin chain-length in the heparin-catalysed inhibition of thrombin by antithrombin III. J. Biol. Chem. **259**, 13979-13982.

Hubbard, S.J., Campbell, S.F., and Thornton, J.M. (1991) Conformational analysis of limited proteolytic sites and serine proteinase protein inhibitors. J. Mol. Biol. **220**, 507-530.

Hunt, L.T. and Dayoff, M.O. (1980) A surprising new protein super-family containing ovalbumin, antithrombin III, and alpha 1-proteinase inhibitor. Biochem. Biophys. Res. Commun. **95**, 864-871.

Huntington, J.A., Olson, S.T., Fan, B., and Gettins, G.W. (1996) Mechanism of heparin activation of antithrombin. Evidence for reactive center loop preinsertion with expulsion upon heparin binding. Biochemistry **35**, 8495-8503..

Jagd, S., Vibe-Pedersen, K., and Magnusson, S. (1985) Location of two of the introns in the antithrombin-III gene. FEBS Lett. **293**, 213-216.

Jallat, S., Carvallo, D., Tessier, H., Roecklin, D., Roitsch, C., Ogushi, F., Crystal, R.G., and Courtney, M. (1986) Altered specificities of genetically engineered α_1-antitrypsin variants. Prot. Eng. **1**, 29-35.

Jesty, J. (1979) The kinetics of formation and dissociation of the bovine thrombin-antithrombin III complex. J. Biol. Chem. **254**, 10044-10050.

Jesty, J. (1986) The kinetics of inhibition of α-thrombin in human plasma. J. Biol. Chem. **261**, 10313-10318.

Jin, L., Abrahams, J., Skinner, R., Petitou, M., Pike, R., and Carrell, R. (1997) 2.9 Å structures indicate mechanism of heparin binding and activation of antithrombin. Thromb. Haemost. Supplement, 189 (abstract).

Johnson, D. and Travis, J. (1979) The oxidative inactivation of human α-1-proteinase inhibitor. Further evidence for methionine at the reactive center. J. Biol. Chem. **254**, 4022-4026.

Jordan, R., Beeler, D., and Rosenberg, R.D. (1979) Fractionation of low molecular weight heparin species and their interaction with antithrombin. J. Biol. Chem. **254**, 2902-2913.

Jordan, R.E, Favreau, L.V., Braswell, E.H., and Rosenberg, R.D. (1982) Heparin with two binding sites for antithrombin or platelet factor 4. J. Biol. Chem. **257**, 400-406.

Jordan, R.E., Oosta, G.M., Gardner, W.T., and Rosenberg, R.D. (1980) The

kinetics of haemostatic enzyme-antithrombin interactions in the presence of low molecular weight heparin. J. Biol. Chem. 255, 10081-10090.

Jornvall, H., Fish, W.W., and Bjork, I. (1979) The thrombin cleavage site in bovine antithrombin. FEBS Lett. 106, 358-362.

Jorpes, E. (1935) The chemistry of heparin. Biochem. J. 29, 1817.

Jorpes, E. and Bergstrom, S. (1936) Der Aminozucker des Heparins. Hoppe-Seyler's Z. Physiol. Chem. 68, 253.

Jorpes, E., Bostrom, H., and Mutt, V. (1950) The linkage of the amino group in heparin. Alleged acetyl content of heparin. J. Biol. Chem. 183, 607.

Kao, F.T., Morse, H.G., Law, M.L., Lidsky, A., Chandra, T., and Woo, S.L. (1984) Genetic mapping of the structural gene for antithrombin III to human chromosome 1. Hum. Genet. 67, 34-36.

Karp, G.I., Marcum, J.A., and Rosenberg, R.D. (1984) The role of tryptophan residues in heparin-antithrombin interactions. Arch. Biochem. Biophys. 233, 712-720.

Katagiri, K., Okada, K., Hattori, H., and Yano, M. (1988) Bovine endothelial cell plasminogen activator inhibitor. Purification and heat activation. Eur. J. Biochem. 176, 81-87.

Kobayashi, N. and Takeda, Y. (1977) Effects of a large dose of oestradiol on antithrombin III metabolism in male and female dogs. Eur. J. Clin. Inv. 7, 373-381.

Koide, T., Odani, S., Takahashi, K., Ono, T., and Sakuragawa, N. (1984) Antithrombin III Toyama: Replacement of arginine-47 by cysteine in hereditary abnormal antithrombin III that lacks heparin-binding ability. Proc. Natl. Acad. Sci. USA 81, 289-293.

Koj, A., Regoeczi, E., Toews, C.J., Leveille, R., and Gauldie, J. (1978) Synthesis of antithrombin III and alpha-1-antitrypsin by the perfused rat liver. Biochim. Biophys. Acta 539, 496-504.

Kress, L.F. and Cataness, J.J. (1981) Identification of the cleavage sites resulting from enzymatic inactivation of human antithrombin III by Crotalus adamanteus

proteinase II in the presence and absence of heparin. Biochemistry **20**, 7432-7438.

Kridel, S.J., Chan, W.W., and Knauer, D.J. (1996) Requirement of lysine residues outside of the proposed pentasaccharide binding region for high affinity heparin binding and activation of human antithrombin III. J. Biol. Chem. **271**, 20935-20941.

Kurachi, K., Schmer, G., Hermodson, M.A., Teller, D.C., and Davie, E.W. (1976a) Characterization of human, bovine and house antithrombin III. Biochemistry **15**, 368-372.

Kurachi, K., Fujikawa, K., Schmer, G., and Davie, E.W. (1976b) Inhibition of bovine factor IXa and factor Xaß by antithrombin III. Biochemistry 15, 373-377.

Laemmli, U.K. (1970) Cleavage of structural proteins during the assembly of the head of bacteriophage. Nature **227**, 680.

Lahiri, B., Rosenberg, R., Talamo, R.C., Mitchell, B., Bagdasarian, A., and Colman, R.W. (1974) Antithrombin III: an inhibitor of human plasma kallikrein. Fed. Proc. **33**, 642 (abstract).

Lam, L.H., Silbert, J.E., and Rosenberg, R.D. (1976) The separation of active and inactive forms of heparin. Biochem. Biophys. Res. Commun. **69**, 570-577.

Lane, D.A., Denton, J., Flynn, A.M., Thunberg, L, and Lindahl, U. (1984) Anticoagulant activities of heparin oligosaccharides and their neutralization by platelet factor 4. Biochem. J. **218**, 725-732.

Lane, D.A., Erdjument, A., Glynn, V., DiMarzo, H., Panic., M., Morris, H.R., Greaves, M., Dolan, G., and Preston, F.E. (1989) Antithrombin Sheffield: amino acid substitution at the reactive site (Arg393 to His) causing thrombosis. Br. J. Haematol. **71**, 91-96.

Lane, D.A., Flynn, A., Ireland, H., Erdjument, H., Samson, D., Howarth, D., and Thompson, E. (1987) Antithrombin III Northwick Park: demonstration of an inactive high MW complex with increased affinity for heparin. Br. J. Heamatol. **65**, 451-456.

Lane, D.A., Ireland, H., Olds, R.J., Thein, S.L., Perry, D.J., and Aiach, M. (1991) Antithrombin III: a database of mutations. Thromb. Haemostas. **66**, 657-661.

Lane, D.A., Olds, R. J., Conard, J., Boisclair, M., Bock, S.C., Hultin, M., Abildgaard, U., Ireland, H., Thompson, E., Sas, G., Horellou, H.M., Tamponi, G., and Thein, S.-L. (1993a) Pleiotropic effects of antithrombin strand 1C substitution mutations. J. Clin. Invest. **90**, 2422-2433.

Lane, D.A., Olds, R.J., Boisclair, M., Chowdhury, V., Thein, S.L., Cooper, D.N., Blajchman, M.A., Perry, D., Emmerich, J., and Aiach, M. (1993b) Antithrombin III mutation database: First update. For the thrombin and its inhibitors subcommittee of the scientific and standardization committee of the international society on thrombosis and Haemostasis. Thrombos. Haemostas. **70**, 361-369.

Laurent, T.C., Tengblad, A., Thunberg, L, Hook, M., and Lindahl, U. (1978) The molecular-weight-dependence of the anti-coagulant activity of heparin. Biochem. J. **175**, 691-701.

Lawrence, D.A., Ginsburg, D., Day, D.E., Berkenpas, M.B., Verhamme, I.M., Kvassman, J.-O., and Shore, J.D. (1995) Serpin-protease complexes are trapped as stable acyl-enzyme intermediates. J. Biol. Chem. **270**, 25309-25312.

Lawrence, D.A., Strandberg, L., Ericson, J., and Ny, T. (1990) Structure-function studies of the SERPIN plasminogen activator inhibitor type I. Analysis of chimeric strained loop mutants. J. Biol. Chem. **265**, 20293-20301.

Lechner, K., Niessner, H., and Thaler, E. (1977) Coagulation abnormalities in liver disease. Semin. Thromb. Haemostas. **4**, 40-56.

Lee, A.K.Y., Chan, V., and Chan, T.K. (1979) The identification and localization of antithrombin III in human tissues. Thromb. Res. **14**, 209-217.

Lellouch, A.C. and Lansbury, P.T. (1992) A peptide model for the heparin binding site of antithrombin III. Biochemistry **31**, 2279-2285.

Leon, M., Aiach, M., Coezy, E., Guennec, J.-Y., and Fiessinger, J.-N. (1983) Antithrombin III synthesis in rat liver parenchymal cells. Thromb. Res. **30**, 369-375.

Leon, M., Aiach, M., Coezy, E., Guennec, J-Y., Jarnet, J., Girot, R., Fiessinger, J.-N., and Jaubert, F. (1982) Antithrombin III in rat hepatocytes. Thromb. Res. **28**, 115-123.

Leonard, B., Bies, R., Carlson, T., and Reeve, E.B. (1983) Further studies of the

turnover of dog antithrombin III. Study of ^{131}I-labelled antithrombin protease complexes. Thromb. Res. **30**, 165-177.

LePaslier, D., Rochu, D., and Lucotte, G. (1985) *Pst*I polymorphism of the antithrombin III gene in a French population. Vox Sang. **49**, 168-170.

Lindahl, U., Backstrom, G., Thunberg, L, and Leder, I.G. (1980) Evidence for a 3-O-sulfated D-glucosamine residue in the antithrombin-binding sequence of heparin. Proc. Natl. Acad. Sci. USA **77**, 6551-6555.

Lindahl, U., Cifonelli, J.A., Lindahl, B., and Roden, L. (1965) The role of serine in the linkage of heparin to protein. J. Biol. Chem. **240**, 571.

Lindahl, U. and Roden, L. (1964) The linkage of heparin to protein. Biochem. Biophys. Res. Commun. **17**, 254.

Lindahl, U. and Roden, L. (1965) The role of galactose and xylose in the linkage of heparin to protein. J. Biol. Chem. **240**, 2821.

Lindahl, U. (1966) Further characterization of the heparin-protein linkage region. Biochim. Biophys. Acta **130**, 368-382.

Lindahl, U., Thunberg, L., Backstrom, G., Riesenfeld, J., Nordling, K., and Bjork, I. (1984) Extension and structural variability of the antithrombin-binding sequence in heparin. J. Biol. Chem. **259**, 12368.

Liu, C.-S. and Chang, J.-Y. (1987) The heparin binding site of human antithrombin III. Selective chemical modification at Lys^{114}, Lys^{125}, and Lys^{287} impairs its heparin cofactor activity. J. Biol. Chem. **262**, 17356-17361.

Lobermann, H., Tokuoka, R., Deisenhofer, J., and Huber, R. (1984) Human α_1-proteinase inhibitor: crystal structure analysis of two crystal modifications, molecular model and preliminary analysis of the implications for function. J. Mol. Biol. **177**, 731-757.

Loeliger, A. and Hers, J.F.Ph. (1957) Chronic antithrombinaemia (antithrombin V) with haemorrhagic diathesis in a case of rheumatoid arthritis with hypergammagloblulinaemia. Thromb. Diath. Haemorrh. 499-528.

Longas, M.O. and Finlay, T.H. (1980) The covalent nature of the human antithrombin III-thrombin bond. Biochem. J. **189**, 481-489.

Longstaff, C. and Gaffney, P.J. (1991) Serpin-serine protease binding kinetics: α_2-antiplasmin as a model inhibitor. Biochemistry **30**, 979-986.

Lormeau, J.C., Herault, J.P., and Herbert, J.M. (1996) Antithrombin-mediated inhibition of factor VIIa-tissue factor complex by the synthetic pentasaccharide representing the heparin binding site to antithrombin. Thromb. Haemostas. **76**, 5-8.

Lovrien, E.W., Magenis, R.E., Rivas, M.L., Goodnight, S., Moreland, R, and Rowe, S. (1978) Linkage study of antithrombin III. Cytogenet. Cell Genet. **22**, 319-323.

Machovich, R., Staub, M., and Patthy, L. (1978) Decreased heparin sensitivity of cyclohexanedione-modified thrombin. Eur. J. Biochem. **83**, 473-477.

Maniatis, T., Fritsch, E.F., and Sambrook, J. (1982) Molecular cloning: a laboratory mannual. Cold Spring Harbor laboratory Press, Cold Spring Harbor, New York. pp. 368-458.

Manson, H.E., Austin, R.C., Fernandez-Rachubiski, F., Rachubinski, R.A., and Blajchman, M.A. (1989) The molecular pathology of inherited human antithrombin III deficiency. Transf. Med. Rev. **3**, 264-281.

Marciniak, E. and Gora-Maslak, G. (1983) High molecular weight forms of antithrombin III complexes in blood. Thromb. Haemostas. **49**, 32-36.

Marcum, J.A., Atha, D.H., Fritze, L.M., Nawroth, P., Stevn, D., and Rosenberg, R.D. (1986a) Cloned bovine aortic endothelial cells synthesize anticoagulantly active heparan sulphate proteoglycan. J. Biol. Chem. **261**, 7507-7517.

Marcum, J.A., Fritze, L., Galli, S.J., Kamp, G., and Rosenberg, R.D. (1983) Microvascular heparinlike species with anticoagulant activity. Am. J. Phys. **245**, H725-H733.

Marcum, J.A., McKenney, J.B., Galli, S.J., Jackman, R.W., and Rosenberg, R.D. (1986b) Anticoagulantly active heparin-like molecules from mast cell deficient mice. Am. J. Physiol. **19**, H879-H888.

Marcum, J.A., McKenney, J.B., and Rosenberg, R.D. (1984) The acceleration of thrombin-antithrombin complex formation in rat hindquarters via heparinlike molecules bound to the endothelium. J. Clin. Invest. **74**, 341-350.

Marcum, J.A. and Rosenberg, R.D. (1984) Anticoagulantly active heparin-like molecules from vascular tissue. Biochemistry **23**, 1730-1737.

Marcum, J.A. and Rosenberg, R.D. (1985) Heparin-like molecules with anticoagulant activity are synthesized by cultured endothelial cells. Biochem. Biophys. Res. Commun. **126**, 365-372.

Mast, A.E., Enghild, J.J., Pizzo, S.V., and Salvesen, G. (1991) Analysis of the plasma elimination kinetics and conformational stabilities of native, proteinase-complexed, and reactive site cleaved serpins: Comparison of α_1-proteinase inhibitor, α_1-antichymotrypsin, antithrombin III, α_2-antiplasmin, angiotensinogen, and ovalbumin. Biochemistry **30**, 1723-1730.

Matheson, N.R., Van Halbeek, H., and Travis, J. (1991) Evidence for a tetrahedral intermediate complex during serpin-proteinase interactions. J. Biol. Chem. **266**, 13489-13491.

Mclean, J. (1916) The thromboplastic action of cephalin. Am. J. Physiol. **41**, 250.

Meagher, J.L., Huntington, J.A., Fan, B., and Gettins, P.G.W. (1996) Role of arginine 132 and lysine 133 in heparin binding to and activation of antithrombin. J. Biol. Chem. **271**, 29353-29358.

Mille, B., Watton, J., Barrowcliffe, T.W., Main, J.-C., and Lane, D.A. (1994) Role of N- and C-terminal amino acids in antithrombin binding to pentasaccharide. J. Biol. Chem. **269**, 29435-29443.

Miller-Andersson, J., Borg, H., and Andersson, L.O. (1974) Purification of antithrombin III by affinity chromatography. Thromb. Res. **5**, 439-452.

Mizuochi, T., Fuji, J., Kurachi, K., and Kobata, A. (1980) Structural studies of the carbohydrate moiety of human antithrombin III. Arch. Biochem. Biophys. **203**, 458-465.

Mohlo-Sabatier, P., Aiach, M., Gaillard, I., Fiessinger, J.N., Fischer, A.M., and Chadeuf, E. (1989) Molecular characterization of antithrombin (AT III) variants using polymerase reaction. Identification of the AT-III Charleville as an Ala384 Pro mutation. J. Clin. Invest. **84**, 1236-1241.

Monkhouse, F.C., France, E.S., and Seegers, W.H. (1955) Studies on the

antithrombin and heparin cofactor activities of a fraction adsorbed from plasma by aluminium hydroxide. Circ. Res. 3, 397.

Morawitz, P. (1905) Die Chemie der Blutgerinnung. Ergeb. Physiol. 4, 307.

Mottonen, J., Strand, A., Symersky, J., Sweet, R.M., Danley, D.E., Goeghegan, K.F., Gerard, R.D., and Goldsmith, E.J. (1992) Structural basis of latency in plsminogen activator inhibitor 1. Nature 355, 270-273.

Mourey, L., Samama, J.P., Delarue, M., Choay, J., Lormeau, J.C., Petitou, M., and Moras, D. (1990) Antithrombin III: Structural and functional aspects. Biochimie 72, 599-608.

Mourey, L., Samama, J.P., Delarue, M., Petitou, M., Choay, J., and Moras, D. (1993) Crystal structure of cleaved bovine antithrombin-III at 3.2-Ångstrom resolution. J. Mol. Biol. 232, 223-241.

Nagy, I. and Lasonczy, H. (1979) Three types of hereditary antithrombin III deficiency. Thromb. Haemostas. 44, 187a.

Najjam, S., Chadeuf, C., Gandrille, S., and Aiach, M. (1994) Arg-129 plays a specific role in the conformation of antithrombin and in the enhancement of factor Xa inhibition by the pentasaccharide sequence of heparin. Biochim. Biophys. Acta. 1225, 135-143.

Nesheim, M.E. (1983) A simple rate law that describes the kinetics for the heparin-catalyzed reaction between antithrombin III and thrombin. J. Biol. Chem. 258, 14708-14717.

Nesheim, M.E., Blackburn, M.N., Lawler, C.M., and Mann, K.G. (1986) Dependence of antithrombin III and thrombin binding stoichiometries and catalytic activity on the molecular weight of affinity-purified heparin. J. Biol. Chem. 261, 3214-3221.

Niewiarowski, S. and Kowalski, E. (1958) Un nouvel anticoagulant derive du fibrinogene. Rev. Hematol. 13, 320.

Nishioka, J. and Suzuki, K. (1992) The role of the COOH-terminal region of antithrombin III. Evidence that the COOH-terminal region of the inhibitor enhances the reactivity of thrombin and factor Xa with the inhibitor. J. Biol. Chem. 267, 22224-22229.

Nordenman, B. and Bjork, I. (1978) Binding of low-affinity and high-affinity heparin to antithrombin. Ultraviolet difference spectroscopy and circular dichroism studies. Biochemistry 17, 3339-3344.

Nordenman, B. and Bjork, I. (1980) Fractionation of heparin by chromatography on immobilized thrombin. Correlation between the anticoagulant activity of the fractions and their content of heparin with high-affinity for antithrombin. Thromb. Res. 19, 711-718.

Nordenman, B. and Bjork, I. (1981) Influence of ionic strength and pH on the interaction between high-affinity heparin and antithrombin. Biochem. Biophys. Acta 672, 227-238.

Nordenman, B., Danielsson, A., and Bjork, I. (1978) The binding of low-affinity and high-affinity heparin to antithrombin. Fluorescence studies. Eur. J. Biochem. 90, 1-6.

Nordenman, B., Nystrom, C., and Bjork, I. (1977) The size and shape of human and bovine antithrombin III. Eur. J. Biochem. 78, 195-203.

Okajima, K., Abe, H., Wagatsuma, M., Okabe, H., and Takatsuki, K. (1995) Antithrombin III Kumamoto II; A single mutation at Arg 393-His increased the affinity of antithrombin III for heparin. Am. J. Haematol. 48, 12-18.

Okajima, K., Abe, H., Maeda, S., Motomura, M., Tsujihata, M., Nagataki, S., Okabe, H., and Takatsuki, K. (1993) Antithrombin III Nagasaki (Ser116-Pro): A Heterozygous variant with defective heparin binding associated with thrombosis. Blood 81, 1300-1305.

Olds, R.J., Lane, D.A., Boisclair, M., Sas, G., Bock, S.C., and Thein, S.L. (1992) Antithrombin Budapest 3. An antithrombin variant with reduced heparin affinity resulting from the substitution L99F. FEBS Lett. 300, 241-246.

Olds, R.J., Lane, D.A., Caso, R., Girolami, A., and Thein, S.L. (1990) Antithrombin III Padua 2. A single base substitution in exon 2 detected with PCR and direct genomic sequencing. Nucleic Acids Res. 18, 1926.

Olds, R.J., Lane, D.A., Chowdhury, V., Stefano, D., Leone, G., and Thein, S.L. (1993) Complete nucleotide sequence of the antithrombin gene: evidence for homologous recombination causing thrombophilia. Biochemistry 32, 4216-4224.

Olsen, S.T. (1985) Heparin and ionic strength-dependent conversion of antithrombin from an inhibitor to a substrate of α-thrombin. J. Biol. Chem. **260**, 10153-10160.

Olsen, S.T. (1988) Transit kinetics of heparin-catalyzed protease inactivation by antithrombin III. Linkage of protease-inhibitor-heparin interactions in the reaction with thrombin. J. Biol. Chem. **263**, 1698-1708.

Olsen, S.T. and Bjork, I. (1991a) Regulation of thrombin by antithrombin and heparin cofactor II. In: Berliner, L.J. (ed) Thrombin: structure and function. Plenum, New York City. pp. 159-217.

Olsen, S.T. and Bjork, I. (1991b) Predominant contribution of surface approximation to the mechanism of heparin acceleration of the antithrombin-thrombin reaction. Elucidation from salt concentration effects. J. Biol. Chem. **266**, 6353-6364.

Olsen, S.T., Bjork, I., Sheffer, R., Craig, P.A., Shore, J.D., and Choay, J. (1992) Role of the antithrombin-binding pentasaccharide in heparin acceleration of antithrombin-proteinase reactions. J. Biol. Chem. **267**, 12528-12538.

Olsen, S.T., Bock, P.E., Kvassman, J., Shore, J.D., Lawrence, D.A., Ginsburg, D., and Bjork, I. (1995a) Role of the catalytic serine in the interactions of serine proteinases with protein inhibitors of the serine family. Contribution of a covalent interaction to the binding energy of serpin-proteinase complexes. J. Biol. Chem. **270**, 30007-30017.

Olson, S.T. and Choay, J. (1989) Mechanism of high molecular weight-kininogen stimulation of the heparin-accelerated antithrombin/kallikrein reaction. Thromb. Haemostas. **62**, 326 (abstract).

Olson, S.T. and Shore, J.D. (1981) Binding of high affinity heparin to antithrombin III. Characterization of the protein fluorescence enhancement. J. Biol. Chem. **256**, 11065-11072.

Olson, S.T. and Shore, J.D. (1982) Demonstration of a two-step reaction mechanism for inhibition of α-thrombin by antithrombin III and identification of the step affected by heparin. J. Biol. Chem. **257**, 14891-14895.

Olson, S.T., Srinivasan, K.R., Bjork, I., and Shore, J.D. (1981) Binding of high affinity heparin to antithrombin III. Stopped flow kinetic studies of the binding

interaction. J. Biol. Chem. **256**, 11073-11079.

Olson, S.T., Stephens, A.W., Hirs, C.H.W., Bock, P.E., and Bjork, I. (1995b) Kinetic characterization of the proteinase binding defect in a reactive site variant of the serpin, antithrombin. Role of the P1' residue in transition-state stabilization of antithrombin-proteinase complex formation. J. Biol. Chem. **270**, 9717-9724.

O'Malley, K.M., Shrikumar, A.N., Rubin, H., and Cooperman, B.S. (1997) The kinetic mechanism of serpin-proteinase complex formation. An intermediate between the Michaelis complex and the inhibited complex. J. Biol. Chem. **272**, 5354-5359.

Oosta, G.M., Gardner, W.T., Beeler, D.L., and Rosenberg, R.D. (1981) Multiple functional domains of the heparin function molecule. Proc. Natl. Acad. Sci. USA **78**, 829-833.

Owen, M.C., Beresford, C.H., and Carrell, R.W. (1988) Antithrombin Glasgow, 393 Arg to His, a P_1 reactive site variant with increased heparin affinity but no thrombin inhibitory activity. FEBS Lett. **231**, 317-320.

Owen, M.C., Borg, J.Y., Soria, C., Siria, J, Caen, J., and Carrell, R.W. (1987) Heparin binding defect in new antithrombin III variant: Rouen, 47 Arg to His. Blood **69**, 1275-1279.

Owen, M.C., Brennan, S.O., Lewis, J.H., and Carrell, R.W. (1983) Mutation of antitrypsin to antithrombin. α_1-Antitrypsin Pittsburgh (358 Met Arg), a fatal bleeding disorder. N. Engl. J. Med. **309**, 694-698.

Owen, M.C., George, P.M., Lane, D.A., and Boswell, R. (1991) P1 variant antithrombins Glasgow (393 Arg to His) and Pescara (393 Arg to Pro) have increased heparin affinity and are resistant to catalytic cleavage by elastase. FEBS Lett. **280**, 216-220.

Owen, M.C., Shaw, G.J., Grau, E., Fontcuberta, J, Carrell, R.W., and Boswell, D.R. (1989) Molecular characterisation of antithrombin Barcelona 2: 47 arginine to cysteine. Thrombos. Res. **55**, 451-457.

Owens, M.R. and Miller L.L. (1980) Net biosynthesis of antithrombin III by the isolated rat liver perfused for 12-24 hours. Compared with rat fibrinogen and α-2 (acute phase) globulin, antithrombin III is not an acute phase protein. Biochim.

Biophys. Acta **627**, 30-39.

Patston, P.A., Gettins, P., Beechem, J., and Schapira, M. (1991) Mechanism of serpin action: Evidence that C1 inhibitor functions as a suicide substrate. Biochemistry **30**, 8876-8882.

Patston, P.A., Gettins, P., and Schapira, M. (1994) Serpins are suicide substrates: Implications for regulation of proteolytic pathways. Sem. Thromb. Haemostas. **20**, 410-416.

Patston, P.A., Roodi, N., Schifferli, J.A., Bischoff, R., Courtney, M., and Schapira, M. (1990) Reactivity of α_1-antitrypsin mutants against proteolytic enzymes of the kallidrein-kinin, complement, and fibrinolytic systems. J. Biol. Chem. **265**, 10786-10791.

Pemberton, P.A., Stein, P.E., Pepys, M.B., Potter, J.M., and Carrell, R.W. (1988) Hormone binding globulins undergo serpin conformational change in inflammation. Nature **336**, 257-258.

Perlin, A.S., Mazurek, M., Jaques, L.B., and Jawabaggm L.W. (1968) A proton magnetic resonance spectral study of heparin. L-Iduronic acid residues in commercial heparins. Carbohydr. Res. **7**, 369-679.

Perlin, A.S. and Sandersson, G.R. (1970) L-Idrronic acid, a major constituent of heparin. Carbohydr. Res. **12**, 183.

Perlin, A.S., Mackey, D.M., and Dietrich, C.P. (1971) Evidence for a (1 leads to 4)-linked 4-O-(-L-idopyranosyluronic acid 2-sulfate)-(2-deoxy-2-sulfoamino-D-glucopyranosyl 6-sulfate) sequence in heparin. Long-range H-H coupling in 4-deoxy-hex-4-enopyranosides. Carbohydr. Res. **18**, 185-194.

Perry, D.J. (1994) Antithrombin and its inherited deficiencies. Blood Rev. **8**, 37-55.

Perry, D.J. and Carrell, R.W. (1989) CpG dinucleotides are "hot-spots" for mutation in the antithrombin III gene. Twelve variants identified using the polymerase chain reaction. Mol. Biol. Med. **6**, 239-243.

Peterson, C.B. and Blackburn, M.N. (1985) Isolation and characterization of a antithrombin-III variant with reduced carbohydrate content and enhanced heparin binding. J. Biol. Chem. **260**, 1723-1729.

Peterson, T.E., Dudek-Wojciechowska, G., Sottrup-Jensen, L. (1979) Primary structure of antithrombin III (heparin cofactor). Partial homology between α_1-antitrypsin and antithrombin III. In: Collen, D., Wiman, B., and Verstraete, M. (eds): The Physiological inhibitors of coagulation and fibrinolysis. Amsterdam, Elsevier/North-Holland. pp. 43-54.

Peterson, C.B. and Jorgensen, M. (1983) Electrostatic interactions in the heparin-enhanced reaction between human thrombin and antithrombin. Biochem. J. 211, 91-97.

Peterson, C.B., Noyes, C.M., Pecon, J.M., Church, F.C., and Blackburn, M.N. (1987) Identification of a lysyl residue in antithrombin which is essential for heparin binding. J. Biol. Chem. 262, 8061-8065.

Petitou, M., Barzu, T., Herault, J.-P., and Herbert, J.-M. (1997) A unique trisaccharide sequences in heparin mediates the early step of antithrombin III activation. Glycobiology 7, 323-327.

Phillips, J.E., Cooper, S.T., Potter, E.E., and Church, F.C. (1994) Mutagenesis of recombinant protein C inhibitor reactive site residues alters target proteinase specificity. J. Biol. Chem. 269, 16696-16700.

Picard, V., Erdsal-Badju, E., and Bock, S.C. (1995) Partial glycosylation of antithrombin III asparagine-135 is caused by the serine in the third position of its N-glycosylation consensus sequence and is responsible for production of the ß-antithrombin III isoform with enhanced heparin affinity. Biochemistry 34, 8433-8440.

Pixley, R.A., Schapira, M., and Colman, R.W. (1985) Effect of heparin on the inactivation rate of human activated Factor XII by antithrombin III. Blood 66, 198-203.

Pletcher, C.H. and Nelsestuen, G.L. (1983) Two-substrate reaction model for the heparin-catalysed bovine antithrombin/protease reaction. J. Biol. Chem. 258, 1086-1091.

Pomeranz, M.W. and Owen, W.G. (1978) A catalytic role for heparin. Evidence for a ternary complex of heparin cofactor, thrombin, and heparin. Biochim. Biophys. Acta. 535, 66-77.

Prochownik, E.V., Antonarakis, S., Bauer, K.A., Rosenberg, R.D., Fearon, E.R.,

and Orkin, S.H. (1983b) Molecular heterogeneity of inherited antithrombin III deficiency. New Engl. J. Med. **308**, 1549-1552.

Prochownik, E.V., Bock, S.C., and Orkin, S.C. (1985) Intron structure of the human antithrombin III gene differs from that of other members of the serine protease inhibitor superfamily. J. Biol. Chem. **260**, 9608-9612.

Prochownik, E.V., Markham, A.F., and Orkin, S.H. (1983a) Isolation of a cDNA clone for human antithrombin III. J. Biol. Chem. **258**, 8389-8394.

Ragg, H. and Preibisch, G. (1988) Structure and expression of the gene coding for the human serpin hLS2. J. Biol. Chem. **263**, 12129-12134.

Rao L.V.M., Rapaport, S.I., and Hoang, A.D. (1993) Binding of factor VIIa to tissue factor permits rapid antithrombin III/heparin inhibition of factor VIIa. Blood **81**, 2600-2607.

Ratnoff, O.D. (1982) Disordered hemostasis in hepatic disease. In: Schiff, L. and Schiff, E.R. (eds): Diseases of the Liver. Philadelphia, J.B. Lippincott. pp. 237-258.

Richer, P.H. and Eigen, M. (1974) Diffusion controlled reaction rates in spheroidal geometry. Application to repressor-operator association and membrane-bound enzymes. Biophys. Chem. **2**, 255-263.

Risenfeld, J., Thunberg, L., Hook, M., and Lindahl, U. (1981) The antithrombin-binding sequence of heparin. Location of essential N-sulfate groups. J. Biol. Chem. **256**, 2389-2394.

Robinson, H.C., Horner, A.A., Hook, M., Ogren, S., and Lindahl, U. (1978) A proteoglycan form of heparin and its degradation to single-chain molecules. J. Biol. Chem. **253**, 6687.

Roden, L. (1989) Highlights in the history of heparin. In: Lane, D.A. and Lindahl, U. (eds): Heparin: chemical and biological properties, clinical applications. CRC Press, Inc., Boca Raton, Florida. pp. 1-23.

Rosenberg, R.D. (1977) Chemistry of the hemostatic mechanism and its relationship to the action of heparin. Fed. Proc. **36**, 10-18.

Rosenberg, R.D. and Damus, P.S. (1973) The purification and mechanism of

action of human antithrombin-heparin cofactor. J. Biol. Chem. **248**, 6490-6505.

Rosenberg, J.S., McKenna, P.W., and Rosenberg, R.D. (1975) Inhibition of human factor IXa by human antithrombin. J. Biol. Chem. **250**, 8883-8888.

Rosenfeld, L. and Danishefsky, I. (1984) Effects of enzymatic deglycosylation on the biological activities of human thrombin and antithrombin. Arch. Biochem. Biophys. **229**, 359-367.

Rosenfeld, L. and Danishefsky, I. (1986) A fragment of antithrombin that binds both heparin and thrombin. Biochem. J. **237**, 639-646.

Rosenfeld, L. and Danishefsky, I. (1988) Location of specific oligosaccharides in heparin in terms of their distance from the protein linkage region in the native proteoglycan. J. Biol. Chem. **263**, 262-266.

Roussel, B., Dieval, J., Delobel, J., Fernandez-Rachubinski, F., Eng, B., Rachubinski, R.A., and Blajchman, M.A. (1991) Antithrombin III-Amiens: A new family with an Arg^{47}-Cys inherited variant of antithrombin III with impaired heparin cofactor activity. Am. J. Hemat. **36**, 25-29.

Rubin, H., Plotnick, M., Wang, Z.M., Liu, X., Zhong, Q., Schechter, N.M., and Cooperman, B.S. (1994) Conversion of α_1-antichymotrypsin into a human neurophil elastase inhibitor: Demonstration of variants with different association rate constants, stoichiometries of inhibition, and complex stabilities. Biochemistry **33**, 7627-7633.

Rubin, H., Wang, Z.M., Nickbarg, E.B., McLarney, S., Naidoo, N., Schoenberger, O.L., Johnson, J.L., and Cooperman, B.S. (1990) Cloning, expression, purification, and biological activity of recombinant native and variant human α-1-antichymotrypsins. J. Biol. Chem. **265**, 1199-1207.

Sambrook, J., fritsch, E.F., and Maniatis T. (1989a) Quantitation of DNA and RNA. In: Nolan, C. (ed): Molecular cloning: a laboratory manual, 2nd ed. Cold Spring Harbor Laboratory Press, Cold Spring Harbor, New York. pp. E.5.

Sambrook, J., fritsch, E.F., and Maniatis T. (1989b) Transfer of proteins from SDS-polyacrylamide gels to sodlid supprots: Immunological detection of immobilized proteins (Western blotting). In: Nolan, C. (ed): Molecular cloning: a laboratory manual, 2nd ed. Cold Spring Harbor Laboratory Press, Cold Spring Harbor, New York. pp. 18.60-18.75.

Sanger, F., Nicklen, S., and Coulson, A.R. (1977) DNA sequencing with chain-terminating inhibitors. Proc. Natl. Acad. Sci. USA 74, 5463.

Sas, G., Blasko, G., Banhegyi, D., Jako, J., and Palos, L.A. (1974) Abnormal antithrombin III (antithrombin III "Budapest") as a cause of familial thrombophilia. Thromb. Diath. Haemorrh. 32, 105-115.

Schapira, M., Ramus, M-A., Jallat, S., Carvallo, D., and Courtney, M. (1986) Recombinant α-antitrypsin Pittsburgh ($Met^{358}\rightarrow Arg$) is a potent inhibitor of plasma kallikrein and activated factor XII fragment. J. Clin. Invest. 77, 635-637.

Schechter, I. and Berger, A. (1967) On the size of the active site of proteases. Biochem. Biophys. Res. Commun. 27, 157-162.

Schechter, N.M., Jordan, L.M., James, A.M., Cooperman, B.S., Wang, Z.M., and Rubin, H. (1993) Reaction ofhuman chymase with rective site variants of alpha-1-antichymotrypsin--modulation ofinhibitor versus substrate properties. J. Biol. Chem. 268, 23626-23633.

Schreuder, H.A., de Boer, B., Dijkema, R., Mulders, J., Theunissen, H.J.M., Grootenhuis, P.D.J., and Hol, W.G. (1994) The intact and cleaved human antithrombin III complex as a model for serpin-proteinase interactions. Nature Struct. Biol. 1, 48-54.

Schulze, A.J., Baumann, U., Knof, S., Jaeger, E., Huber, R., and Laurell, C.B. (1990) Structural transition of α_1-antitrypsin by a peptide sequentially similar to ß-strand s4A. Eur. J. Biochem. 194, 51-56.

Schulze, A.J., Frohnert, P.W., Engh, R.A., and Huber, R. (1992) Evidence for the extent of insertion of the active site loop of intact α_1-proteinase inhibitor in ß-sheet A. Biochemistry 31, 7560-7565.

Scott, C.F., Carrell, R.W., Glaser, C.B. Kueppers, F., Lewis, J.H., and Colman, R.W. (1986) Alpha-1-antitrypsin-Pittsburgh. A potent inhibitor of human plasma factor XIa, kallikrein, and factor XII. J. Clin. Invest. 77, 631-634.

Scott, C.F. and Colman, R.W. (1989) Factors influencing the acceleration of human factor Xa inactivation by antithrombin III. Blood 73, 1873-1879.

Scully, M.F., Shah, N., Ellis, V., and Kaddar, V.V. (1991) Influence of tryptophan modification upon digestion of antithrombin III by elastase. Thromb. Haemostas.

65, 351-354.

Seegers, W.H., Johnson, J.F., and Fall, C. (1954) An antithrombin reaction related to prothrombin activation. Am. J. Physiol. **176**, 97-103.

Shah, N., Scully, M.F., Ellis, V., and Kakkar, V.V. (1990) Influence of chemical modification of tryptophan residues on the properties of human antithrombin III. Thrombos. Res. **57**, 343-352.

Sherman, P.M., Lawrence, D.A., Yang, A.Y., Vandenberg, E.T., Paielli, D., Olson, S.T., Shore, J.D., and Ginsburg, D. (1992) Saturation mutagenesis of the plasminogen activator inhibitor-1 reactive center. J. Biol. Chem. **267**, 7588-7595.

Shifman, M.A. and Pizzo, S.V. (1982) The *in vivo* metabolism of antithrombin III and antithrombin III complexes. J. Biol. Chem. **257**, 3243-3248.

Shore, J.D., Day, D.E., Francis-Chmura, A.M., Verhamme, I., Kvassman, J., Lawrence, D.A., and Ginsburg, D. (1995) A fluorescent probe study of plasminogen activator inhibitor-1. Evidence for reactive center loop insertion and its role in the inhibitory mechanism. J. Biol. Chem. **270**, 5395-5398.

Sinay, P., Jacquinet, J.-C., Petitou, M., Duchaussoy, P., Lederman, I., Choary, J., and Torri, G. (1984) Total synthesis of a heparin pentasaccharide fragment having affinity for antithrombin III. Carbohy. Res. **132**, C5.

Skinner, R., Abrahams, J.-P., Whisstock, J.C., Lesk, A.M., Carrell, R.W., and Wardell, M.R. (1997). The 2.6 Å structure of antithrombin indicates a conformational change at the heparin binding site. J. Mol. Biol. **266**, 601-609.

Skriver, K., Wikoff, W.R., Patston, P.P., Tausk, F., Schapira, M., Kaplan, A.P., and Bock, S.C. (1991) Substrate properties of C1 inhibitor Ma (Alanine 434 → glutamic acid). Genetic and structural evidence suggesting that the P12-region contains critical determinations of serine protease inhibitor inhibitor/substrate status. J. Biol. Chem. **266**, 9216-9221.

Smith, J.W., Dey, N., and Knauer, D.J. (1990) Heparin binding domain of antithrombin III: characterization using a synthetic peptide directed polyclonal antibody. Biochemistry **29**, 8950-8957.

Smith, J.W. and Knauer, D.J. (1987) A heparin binding site in antithrombin III. Identification, purification, and amino acid sequence. J. Biol. Chem. **262**, 11964-11972.

Song, H.K., Lee, K.N., Kwon, K., Yu, M., and Suh, S.W. (1995) Crystal structure of an uncleaved α_1-antitrypsin reveals the conformation of its inhibitory reactive loop. FEBS Lett. **377**, 150-154.

Stackhouse, R., Chandra, T., Robson, K.J.H., and Woo, S.L.C. (1983) Purification of antithrombin III mRNA and cloning of its cDNA. J. Biol. Chem. **258**, 703-706.

Stead, N., Kaplan, A.P., and Rosenberg, R.D. (1976) Inhibition of activated factor XII by antithrombin-heparin cofactor. J. Biol. Chem. **251**, 6481-6488.

Stein, P.E. and Carrell, R.W. (1995) What do dysfunctional serpins tell us about molecular mobility and disease? Structural Biol. **2**, 96-113.

Stein, P.E., Leslie, A.G.W., Finch, J.T., Turnell, W.G., McLaughlin, P.J., and Carrell, R.W. (1990) Crystal structure of ovalbumin as a model for the reactive centre of serpins. Nature **347**, 99-102.

Stephens, A.W., Siddiqui, A., and Hirs, C.H.W. (1987) Expression of functionally active human antithrombin III. Proc. Acad. Sci. USA. **84**, 3886-3890.

Stephens, A.W., Siddiqui, A., and Hirs, C.H.W. (1988) Site-directed mutagenesis of the reactive centre (serine 394) of antithrombin III. J. Biol. Chem. **263**, 15849-15852.

Stone, A.L., Beeler, D., Oosta, G., and Rosenberg, R.D. (1982) Circular dichroism spectroscopy of heparin-antithrombin interactions. Proc. Natl. Acad. Sci. USA **79**, 7190-7194.

Stone, S.R. and Hermans, J.M. (1995) Inhibitory mechanism of serpins. Interaction of thrombin with antithrombin and protease nexin 1. Biochemistry **34**, 5164-5172.

Sun, X.-J. and Chang, J.-Y. (1989) Heparin binding domain of human antithrombin III inferred from the sequential reduction of its three disulfide linkages. J. Biol. Chem. **264**, 11288-11293.

Sun, X.-J. and Chang, J.-Y. (1990) Evidence that arginine-129 and arginine-145 are located within the heparin binding site of human antithrombin III. Biochemistry **29**, 8957-8962.

Tait, R.C., Walker, I.D., Perry, D.J., Islam, S.I., Daly, M.E., McCall, F., Conkie,

J.A., and Carrell, R.W. (1994) Prevalence of antithrombin III deficiency in the healthy population. Br. J. Haemotol. **87**, 106-112.

Taylor, R.L., Shively, J.E., Conrad, H.E., and Cifonelli, A.J. (1973) Uronic acid composition of heparins and heparan sulfates. Biochemistry **12**, 3633-3637.

Thaler, E. and Lechner, K. (1981) Antithrombin III deficiency and thromboembolism. Clin. Haematol. **10**, 369-390.

Theunissen, H.J.M., Dijkema, R., Grootenhuis, D.J., Swinkels, J.C., de Poorter, T.L., Carati, P., and Visser, A. (1993) Dissociation of heparin-dependent thrombin and factor Xa inhibitory activities of antithrombin-III by mutations in the reactive site. J. Biol. Chem. **268**, 9035-9040.

Thunberg, L., Backstrom, G., and Lindahl, U. (1982) Further characterization of the antithrombin-binding sequence in heparin. Carbohydr. Res. **100**, 393-410.

Thunberg, L., Lindahl, U., Tengblad, Laurent, T.C., and Jackson, C.M. (1979) On the molecular-weight dependence of the anticoagulant activity of heparin. Biochem. J. **181**, 241-243.

Towbin, H., Staehelin, T., and Gordon, J. (1979) Eletrophoretic transfer of proteins from polyacrylamide gels to nitrocellulose sheets: Procedure and some applications. Proc. Natl. Acad. Sci. **76**, 4350-4354.

Travis, J., Matheson, N.R., George, P.M., and Carrell, R.W. (1986) Kinetic studies on the interaction of α_1-proteinase inhibitor (Pittsburgh) with trypsin-like serine proteinases. Biol. Chem. Hoppe-Seyler. **367**, 853-859.

Tyler-Cross, R., Sobel, M., Marques, D., and Harris, R.B. (1994) Heparin binding domain peptides of antithrombin III: Analysis by isothermal titration calorimetry and circular dichroism spectroscopy. Protein Science **3**, 620-627.

Tyler-Cross, R., Sobel, M., McAdory, L.E., and Harris, R.B. (1996) Structure-function relations of antithrombin III-heparin interactions as assessed by biophysical and biological assays and molecular modelling of peptide-pentasaccharide-docked complexes. Arch. Biochem. Biophys. **334**, 206-213.

Ueyama, H., Murakami, T., Nishiguchi, S. Maeda, S., Hashimoto, Y., Okajima, K., Shimada, K., adn Araki, S. (1990) Antithrombin III Kumamoto. Identification of a point mutation and genotype analysis of the family. Thromb. Haemostas. **63**,

231-234.

Van Boeckel, C.A.A., Grooperman, B.S., and Christianson, D.W. (1994) A mechanism for heparin-induced potentiation of antithrombin III. Nature Struct. Biol. 1, 423-425.

Vidaud, D., Sireix, M.E., Ahlenc-Gelas, M., Chadeuf, G., Aillaud, M.F., Juhan-Vague, I., and Aiach, M. (1991) A double heterozygosity in 2 brothers with antithrombin (ATIII) deficiency due to the association of an Arg 47 to His mutation with a 9 base pair (bp) deletion in exon VI. Thromb. Haemostas. 65, 838-845.

Villanueva, G.B. (1984) Predictions of the secondary structure of antithrombin III and the location of the heparin-binding site. J. Biol. Chem. 259, 2531-2536.

Villanueva, G.B. and Allen, N. (1983) Refolding properties of antithrombin III. Mechanism of binding to heparin. J. Biol. Chem. 258, 14048-14053.

Villanueva, G.B. and Danishefsky, I. (1977) Evidence for a heparin-induced conformational change on antithrombin III. Biochem. Biophys. Res. Commun. 74, 803-809.

Villanueva, G.B., Perret, V., and Danishefsky, I. (1980) Tryptophan residue at the heparin binding site in antithrombin III. Arch. Biochem. Biophys. 203, 453-457.

Vogel, C.N., Kingdon, H.S., and Lundblad, R.L. (1979) Correlation of *in vivo* and *in vitro* inhibition of thrombin by plasma inhibitors. J. Lab. Clin. Med. 93, 661-673.

Wachtfogel, Y.T., Bischoff, R., Bauer, R., Hack, C.E., Nuijens, J.H., Kucich, U., Niewiarowski, S., Edmunds, L.H.Jr., and Colman, R.V. (1994) α_1-Antitrypsin Pittsburgh ($Met^{358} \rightarrow Arg$) inhibits the contact pathway of intrinsic coagulation and alters the release of human neutrophil elastase during simulated extracorporeal circulation. Thromb. Haemostas. 72, 843-847.

Wasley, L.C., Atha, D.H., Bauer, K.A., and Kaufman, R.J. (1987) Expression and characterization of human antithrombin III synthesized in mammalian cells. J. Biol. Chem. 262, 14766-14772.

Watada, M., Nagakawa, M., Kitani, T., Okajima, Y., Maeda, Y., Urano, S., and Ijichi, H. (1981) Identification of the AT III synthesizing hepatocytes by

immunofluorescent technique. Thromb. Haemostas. **46**, 284 (abstract).

Watton, J., Longstaff, C., Lane, D.A., and Barrowcliffe, T.W. (1993) Heparin binding affinity of normal and genetically modified antithrombin III measured using a monoclonal antibody to the heparin binding site of antithrombin III. Biochemistry **32**, 7286-7293.

Waugh, D.F. and Fitzgerald, M.A. (1956) Quantitative aspects of antithrombin and heparin in plasma. Am. J. Physiol. **184**, 627.

Wei, A., Rubin, H., Cooperman, B.S., and Chnistianson, D.W. (1994) Crystal structure of an uncleaved serpin reveals the conformation of an inhibitory reactive loop. Nature Struct. Biol. **1**, 251-258.

Wells, P.S., Blajchman, M.A., Henderson, P., Wells, M.J., Demers, C., Bourque, R., and McAvoy, A. (1994) Prevalence of antithrombin deficiency in healthy blood donors: a cross-sectional study. Am. J. Hematol. **45**, 321-324.

Whisstock, J., Lesk, A.M., and Carrell, R. (1996) Modelling of serpin-proteinase complexes: antithrombin-thrombin, α_1-antitrypsin (358Met$\rightarrow$Arg)-thrombin, α_1-antitrypsin (358Met$\rightarrow$Arg)-trypsin, and antitrypsin-elastase. Proteins: structure, function, and genetics, **26**, 288-303.

Wiman, B. and Collen, D. (1978) On the kinetics of the reaction between human antiplasmin and plasmin. Eur. J. Biochem. **84**, 573-578.

Winter, R.B., Berg, O.G., and von Heppel, P.H. (1981) Diffusion-driven mechanism of protein translocation on nucleic acids. 3. The *Escherischia coli* lac repressor-operator interaction. Kinetic measurements and conclusions. Biochemistry **20**, 6961-6977.

Winter, J.H., Fenech, A., Ridley, W., Bennett, B., Cumming, A.M., Mackie, M., and Douglas, A.S. (1982) Familial antithrombin III deficiency. Quart. J. Med. **204**, 373-395.

Wolf, M., Boyer-Newmann, C., Meyer, D., Tripodi, A., Mannuci, P.M., and Larrieu, M.J. (1987) Purification and further characterization of antithrombin III Milano: lack of reactivity with thrombin. Thromb. Haemostas. **58**, 888-895.

Wolf, M., Boyer-Neumann, C., Molho-Sabatier, P., Nermann, C., Meyer, D., and Larrieu, M.J. (1990) Familial variant of antithrombin III (AT III Bligny, 47 Arg

to his) associated with protein C deficiency. Thromb. Haemostas. **63**, 215-219.

Wolfrom, M.L. and Rice, F.A.H. (1946) The uronic acid component of heparin. J. Am. Chem. Soc. **68**, 532.

Wright, H.T., Qian, H.X., and Huber, R. (1990) Crystal structure of plakalbumin, a proteolytically nicked form of ovalbumin. Its relationship to the structure of cleaved α-1-proteinase inhibitor. J. Mol. Biol. **213**, 513-528.

Wu, Y.I., Sheffield, W.P., Austin, R.C., and Blajchman, M.A. (1992) Mapping the heparin binding domain of human antithrombin III. Blood **80** (Suppl): 312 (abstract).

Wu, Y.I., Sheffield, W.P., Austin, R.C., and Blajchman, M.A. (1993) Use of antithrombin recombinant derivatives and fusion products to map its heparin binding domains. Thromb. Haemostas. **69**, 760a (abstract).

Wu, Y.I., Sheffield, W.P., and Blajchman, M.A. (1994) Defining the heparin-binding domain of antithrombin. Blood Coag. Fibrinolysis **5**, 83-95.

York, J.D., Li, P., and Gardell, S.J. (1991) Combinatorial mutagenesis of the reactive site region in plasminogen activator inhibitor I. J. Biol. Chem. **266**, 8495-8500.

Zettlmeissl, G., Conradt, H.S., Nimtz, M., and Karges, H.E. (1989) Characterization of recombinant human antithrombin III synthesized in Chinese hamster ovary cells. J. Biol. Chem. **264**, 21153-21159.

Zhou, C., Yang, Y., and Jong, A.Y. (1990) Mini-prep in ten minutes. BioTechniques **8**, 172-173.